Supernova mechanisms

H. A. Bethe

Newman Laboratory of Nuclear Studies, Cornell University, Ithaca, New York 14853

Supernovae of Type II occur at the end of the evolution of massive stars. The phenomenon begins when the iron core of the star exceeds a Chandrasekhar mass. The collapse of that core under gravity is well understood and takes a fraction of a second. To understand the phenomenon, a detailed knowledge of the equation of state at the relevant densities and temperatures is required. After collapse, the shock wave moves outward, but probably does not succeed in expelling the mass of the star. The most likely mechanism to do so is the absorption of neutrinos from the core by the material at medium distances. Observations and theory connected with SN 1987A are discussed, as are the conditions just before collapse and the emission of neutrinos by the collapsed core.

CONTENTS

I. HISTORICAL AND GENERAL

A. Historical supernovae[1]

At least as early as the second century A.D., Chinese asronomers observed and recorded "guest stars," i.e., stars that suddenly appeared in the sky, were visible for a certain length of time, and then faded away. The "guest stars" that were visible for a year or longer were probably supernovae, the shorter guests common novae. One of the more prominent supernovae reported was seen in 185 A.D.; its remnant gives a strong x-ray image now.

[1]Sections I.A and I.B are largely based on the popular book by Laurence A. Marschall, *The Supernova Story,* 1988. For more scientific accounts, see Clark and Stephenson (1977) and Murdin and Murdin (1985).

The most brilliant supernova ever appeared on 1 May 1006. It was observed extensively in China and also in several places in the Middle East and Europe. It was "bright enough to cast shadows on the ground at night, brighter than the quarter moon" (Marschall, 1988). Its remnant can be observed now as a radio image. Marschall recounts amusing astrological predictions in connection with the supernova of 1006, as well as that of 185.

The most famous old supernova is that of 1054, also recorded by the Chinese, but not reported anywhere in Europe. Its remnant is the Crab Nebula, a tangle of brilliant filaments easily visible. It differs fundamentally from the remnants of 185 and 1006, which show only as radiant shells, representing the shock wave that these suprnovae have sent out into space. In the Crab Nebula, a whole volume is luminous. This is connected with the fact that at the center of the Crab there is a neutron star, a pulsar, which emits electromagnetic radiation of all frequencies at regular intervals, about 30 pulses per second. The pulsar probably also emits electrons, and it is these which irradiate material throughout the remnant and make it, in turn, emit visible (and polarized) light. The remnants of 185 and 1006 have no pulsars in the center.

Supernovae remnants that have a neutron star at their center are certainly Type II (see Sec. I.B); those that do not are predominantly, but perhaps not exclusively, Type I.

In 1572, on November 17, the Danish astronomer Tycho Brahe discovered a "new star" in Cassiopeia, brighter than Venus. He was only 26 years old at the time. He determined its exact position every clear night during the several months the star was visible and found that it did not change relative to the fixed stars; thereby he meant to refute the idea of Aristotle that nothing ever changes beyond the moon: here was a star, appearing and disappearing again, which was certainly much farther away than the moon. The remnant of the Tycho supernova gives a beautiful x-ray picture, but has no pulsar in it.

Kepler, in October 1604, saw another supernova, less bright than Tycho's but remaining visible for a whole year. It was seen by trained astronomers before maximum light so that we can, to some extent, reconstruct its light curve. Its position in the sky was accurately described by the astronomers of the time, and the x-ray emission from its remnant has been measured.

Another supernova exploded in our galaxy between 1650 and 1680, known as Cas A (Cas for Cassiopeia). Its remnant is a very strong radio source, but it was not reported by contemporary observers; it is described in detail by Marschall (1988). Some supernovae in other galaxies were observed between 1885 and 1930; see Marschall.

B. Systematic observations

Zwicky and Baade began a systematic study of supernovae. Zwicky was a Swiss physicist with a fertile imagination, Baade a particularly careful German astronomer; both worked at Caltech and collaborated closely for many years. In 1934, they wrote a paper wondering about the rare but spectacular phenomenon of the supernova. They concluded that it should be possible to find many more supernovae by a systematic survey of galaxies: a supernova would easily stand out over the background of ordinary stars in the galaxy.

Zwicky obtained one of the newly developed Schmidt telescopes, which can photograph a fairly large area of the sky. His first Schmidt had a diameter of 18 inches. Within a year, he discovered three supernovae; in five years, he and his assistant, J. J. Johnson, found nearly 20. They are detected by comparing the picture of a galaxy at two different times: if the later picture shows a bright spot where the earlier one had none, this is likely to be a supernova (SN). Minkowski, also of Caltech, measured the spectra of the discovered SN's. Together, the astronomers found that there are at least two types of SN's: Type II has strong lines of hydrogen, Type I has none. The first 12 of Zwicky's SN's were all Type I, but number 13, discovered by Johnson, was Type II. Zwicky actually distinguished five types, but it is now customary to distinguish only two, recognizing some subclasses within each type. Since then astronomers at various observatories have discovered between 10 and 30 supernovae each year, the total now being about 700. They are designated by the year of discovery and a capital letter.

The light curve, i.e., the optical luminosity as a function of time, has been measured for many supernovae. Typical light curves for Type I and Type II both start with a rise in luminosity, extending over a week or two, which is due to the expansion of the luminous surface. Type I has a fairly narrow peak, while the peak of Type II is broad, of the order of 100 days. Then the intensity declines over a period of about a year. The light curve will be discussed in more detail in Sec. VII, in connection with SN 1987A. Not all SN's of each type have the characteristic light curve, but in Type I about 80% do; they are designated Type Ia.

Zwicky and Baade, already in their 1934 paper, suggested that supernovae derive their tremendous energy from gravitational collapse, in particular that the inner part of the star collapses to a neutron star. The concept of a neutron star had been proposed by Landau in 1932, and such a star was expected to have a radius of about 10 km (still the accepted figure). This idea of collapse to a neturon star is the accepted model for Type II.

Type I SN's are believed to derive their energy from thermonuclear reactions. This mechanism was suggested by Hoyle and Fowler (1960) and by Fowler and Hoyle (1964) for all supernovae. They, on one side, and Baade and Zwicky (1934) on the other, between them suggested the mechanisms that now are believed to power the two types of supernovae.

C. Supernovae of Type I

The mechanism of Type I supernovae is less well understood than that of Type II. The various theories and

the observational evidence are discussed in the review article by Woosley and Weaver (1986), and I shall here give only a brief summary.

While several models were proposed in the past, there now appears to be agreement that Type I (or at least the subtype Ia, which comprises about 80% of Type I) is due to the thermonuclear disruption of white dwarfs. This model was first proposed by Hoyle and Fowler (1960) in their fundamental paper on supernovae. A white dwarf, consisting mainly of C and O, accretes material from a companion star and thereby grows to a Chandrasekhar mass, as proposed by Whelan and Iben (1973) and others. In this process, carbon (or possibly helium) is ignited under highly degenerate conditions, and a substantial fraction of the star is burned to nuclear statistical equilibrium.

The end product of this nuclear burn is Fe, which is very abundant in the optical spectrum of Type I SN's. The nuclide initially formed in the nuclear burn is ^{56}Ni (see Sec. VII.E), which decays to ^{56}Co, which in turn decays to ^{56}Fe with a half-life of 77 days. Co has been observed in the spectra of some SN's. The velocity of the exploding material agrees well with the energy liberated when C and O burn to nuclear statistical equilibrium. The total optical energy observed can be calculated from the assumption that most of the light is generated by the decay of ^{56}Co and ^{56}Ni (Colgate and McKee, 1969, and others) and that essentially all the mass of the star burns to these end products, the mass being that of a white dwarf at the Chandrasekhar limit, 1.4 $M_\odot$ ($M_\odot$ = mass of the sun). In fact, SN's of Type I have been proposed as "standard candles" for determining the absolute magnitudes of galaxies, and hence their distance. The model explains why the light curves of all Type Ia SN's are similar. The absence of hydrogen lines is to be expected from white dwarfs (the hydrogen accreted from the companion is quickly converted into helium, before the supernova explosion). In short, the white dwarf nuclear burn fits the observations.

However, the decay of the light intensity with time for some of the best observed supernovae corresponds to a half-life of 56 days, rather than 77. This is usually explained by the escape of the γ rays emitted by ^{56}Co, due to the increasing transparency of the material.

The mechanism of the burn is still unclear. The original calculations of Arnett (1968b, 1969, 1971) postulated a detonation, i.e., a supersonic wave, going through carbon. Much later work has followed; see Woosley and Weaver (1986) for references. Some of the calculations assumed a subsonic flame front (deflagration) going through the star, some a deflagration turning into a detonation. The process seems to depend on the rate of accretion of material from the companion star, which may range from 10^{-10} to 10^{-5} $M_\odot$ per year.

Also undecided is the nature of the companion: it could be a supergiant, a main-sequence star, or a second white dwarf. One problem is whether the material accreted onto the white dwarf will actually stick to it or be reemitted. Another problem is to get a sufficient frequency of type I SN.

Many of the historical supernovae have been shown to be Type I. The absence of a pulsar is one piece of evidence supporting this designation; this makes the SN of 1006, as well as Tycho's and Kepler's SN's Type I. This evidence is confirmed by the observation of x rays from the remnant, as investigated by Helfand and collaborators using the Einstein x-ray satellite; see Helfand and Becker (1984). The remnants of the SN's mentioned show x rays from a shell, which is interpreted as the shock wave from the SN propagating into the interstellar gas. The remnant of the 1054 SN, the Crab, also shows x rays from the center of the shell, presumably the observed pulsar or the gas immediately surrounding it, thus indicating a Type II.

Some Type I's, i.e., SN's without hydrogen lines, behave differently from Ia. A dimmer subclass, called Ib by Elias *et al.* (1985) and Branch (1986), and comprising about 10% of all Type I's, might possibly be massive stars that have lost their hydrogen during the supergiant stage, but might also be white dwarfs that do not fully burn up. The other subclass, Ip, called "peculiar," have many different spectral and photometric properties and are not explained.

D. Theories before 1975

In the 1960s, Colgate and collaborators outlined the two mechanisms that are still considered important for Type II supernova explosions. By 1960, it was generally accepted that the core of a massive star collapses at the end of its lifetime to something like a neutron star.

Colgate and Johnson (1960) postulated that, after collapse, the core would bounce back part of the way and start a shock, which would then propagate into the mantle and propel most of the star's mass to infinity. This idea is still very actively used in the prompt-shock model (Sec. V of this review). The main difference is that Colgate and Johnson assumed that the bounce would occur at a density of about 3×10^{13} g cm^{-3}, while present theories put the bounce at densities greater than normal nuclear density, $\rho > 3\times10^{14}$ cm^{-3}.

Because of difficulties with the bounce model, Colgate and White (1966) proposed the neutrino transport model. The collapsed core still contains most of the energy released by the gravitational collapse, in the form of heat, with temperatures of several times 10^{11} K, equivalent to tens of MeV. This heat energy is then emitted in a few seconds in the form of neutrinos (see Sec. IX). If some modest fraction (of the order of one percent) of the neutrino energy could be converted back into material energy, this could drive the explosion.

Arnett (1966, 1967, 1968a) and Wilson (1971) criticized this model because it would not give enough energy. But in 1982, Wilson revived it (Bowers and Wilson, 1982; Wilson, 1985) and then developed it further; it is now the delayed-shock model; see Sec. VI of this review.

Further discussion of the theories of the 1960s and early 1970s is given in the review by Woosley and Weaver (1986). One trouble with this early work was the neglect of neutrino scattering by heavy nuclei. This was remedied by Freedman (1974), who pointed out that, due to the weak neutral current, the nucleons in a heavy nucleus scatter neutrinos coherently, giving a cross section proportional to A^2; see Sec. II.E. Due to this large cross section, neutrinos are trapped in the core of a collapsing supernova once the density surpasses about 10^{12} g cm^{-3}; this helps the subsequent explosion.

The main trouble with the old calculations was that the computers available on the 1960s were not big enough and fast enough for the kind of calculation that has been found necessary in modern theories.

E. Needed information

For a successful theory of Type II supernovae, the first requirement is a good equation of state, both at densities below normal nuclear density (see Sec. III) and above that density (Sec. IV). Next, the interaction of neutrinos must be treated, namely, (1) emission and capture by nuclei, (2) scattering by nuclei and nucleons, (3) scattering by electrons, and (4) production of neutrino pairs from electron pairs, and its inverse, neutrino pair annihilation (Secs. II and VI.I).

Accurate account must be taken of the entropy of each matter element as a function of time. The initial entropy, left over from the presupernova evolution, is important, as are the density and composition resulting from that evolution (Sec. VIII). With this information, one calculates the dynamics of the star (Secs. II, V, and VI). Comparison with the observations on Supernova 1987A is essential (Sec. VII). Neutrino diffusion is important both for the theory and for neutrino observations (Sec. IX).

II. THE COLLAPSE

A. Initial conditions and general features

The conditions of the star before its collapse are determined by its prior evolution; this problem will be discussed in Sec. VIII of this review. Many calculations have been made, but the theory is still not final. However, the main features of the collapse of the star under gravity are insensitive to the initial conditions.

We therefore give here a fairly arbitrary initial condition, namely that published by Arnett (1977a), Fig. 1. The star has several shells in which energy is produced by nuclear reactions. With increasing atomic number of the reacting nuclei, the temperature increases; T_9 means the temperature in units of 10^9 K. The density also increases and is near 10^8 in the shell in which Si reacts. At the center of the star, the density is about $10^{9.5}$. The material inside the Si shell is mainly Fe and neighboring elements (called the iron core), and its mass is about

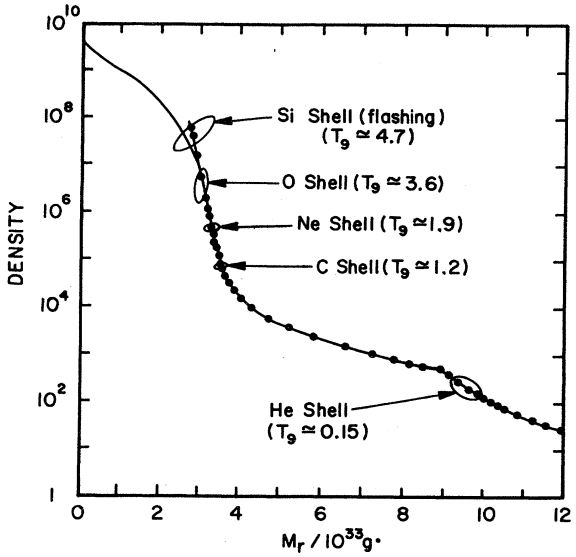

FIG. 1. Density distribution of a star before supernova collapse, according to Arnett (1977a). The enclosed mass is given in units of 10^{33} grams; the Sun's mass is 2×10^{33} g. The location of shells is indicated in which various nuclear reactions take place, together with the temperature in units of 10^9 K.

2.8×10^{33} g $=1.4\,M_\odot$, where $M_\odot$ is the mass of the sun.

Once the initial conditions are given, the calculation of collapse is rather straightforward. Each mass element retains essentially its initial entropy, except for a small correction due to electron capture, which will be discussed in Sec. II.D. Energy transport is negligible, due to the very short time scale of the collapse, less than one second. The transport of electromagnetic radiation is very slow, due to the high densities involved; the same holds for electronic heat conduction. For neutrinos, the opposite is true: They move essentially without resistance. Once emitted, they escape from the star and will not be absorbed again, hence they cannot transport energy from one material element to another. (This becomes different at very high density, above about 10^{11} g cm^{-3}, as will be discussed in Sec. II.E.)

The most important requirement for a calculation of the collapse is the equation of state of the material, i.e., the pressure as a function of density and entropy. The dominant contribution to the pressure comes from the electrons; these are degenerate and relativistic, so that the electron pressure p_e is given by

$$p_e/\rho \simeq \tfrac{1}{4} Y_e \mu_e \tag{2.1}$$

where ρ is the material density in g cm^{-3}, Y_e is the number of electrons per nucleon, and μ_e is the chemical potential of the electrons,

$$\mu_e \simeq 1.11(\rho_7 Y_e)^{1/3}\ \text{MeV}\ . \tag{2.2}$$

Here ρ_7 is the density in units of 10^7 g cm^{-3}. Equation (2.1) gives p_e/ρ in MeV, and

$$1 \text{ MeV} = 0.96 \times 10^{18} \text{ ergs/g} . \tag{2.3}$$

In addition to p_e, there is pressure from the nuclei. This arises mostly from the electrostatic interaction between nuclei and electrons and is therefore generally negative. Its calculation is a fairly involved problem, which will be treated in Sec. III, but the nuclear pressure is small compared to the electron pressure, typically 5–10 %.

It is well known that a gas of relativistic electrons, of mass greater than the Chandraskhar mass,

$$M_{\text{Ch}} \simeq 5.8 Y_e^2 M_\odot , \tag{2.4}$$

has no stable configuration, so it will collapse indefinitely. This process is accelerated by the negative nuclear pressure. It can be stopped only when the nuclear pressure becomes positive, which happens only when the nuclei touch and fuse together, forming nuclear matter, i.e., at densities above normal nuclear density. Thus the collapse can stop only above nuclear density. This was first pointed out by Bethe, Brown, Applegate, and Lattimer (1979), hereafter referred to as BBAL.

B. Numerical computations

Essentially all computations so far have employed spherical symmetry because any more complicated assumption would be beyond the capacity of even the big modern computers. Most of them have used Newtonian gravity, but in some calculations general relativity has been used (see Sec. V.G). In Newtonian approximation, the equation of motion is

$$\frac{d^2R}{dt^2} = -\frac{GM_r}{R^2} - \frac{1}{\rho}\frac{\partial P}{\partial R} , \tag{2.5}$$

where R is the position of a given mass element, M_r the mass enclosed by it, ρ its density, and G the gravitational constant. The pressure is given by the equation of state

$$P = P(\rho, T, Y_e) , \tag{2.6}$$

which depends on the electron fraction Y_e; it will be discussed in Sec. III. It is often convenient to use the entropy S instead of the temperature because it remains essentially constant with time for any given mass element; we define S as the entropy per nucleon in units of the Boltzmann constant, so S is a pure number, usually of order 1.

The computation is done in Lagrangian coordinates, labeled conveniently by the enclosed mass M_r. The iron core, and some region around it, is divided into mass elements, often called zones, typically about 100 of them. These may be of equal mass, but often the zones are chosen wider near the center of the star where not much happens and narrower near the surface of the iron core. James Wilson, who has the most experience with these calculations, often subdivides the zones in some regions whenever conditions (density, temperature) change rapidly.

The time step in integrating the equation of motion must be chosen small enough to fulfill the Courant condition, i.e., a sound wave must not be able to traverse a full zone in one time step. This makes the time steps of the order of a microsecond or less in the most critical period, i.e., near collapse. Since this critical period lasts several milliseconds, usually of the order of 10 000 or more time steps are required, and only very fast computers are able to carry out these calculations.

The computation is further complicated by the behavior of neutrinos (see Secs. II.E–II.G). In the beginning of the collapse, neutrinos that are produced by electron capture stream out freely, but as the density increases beyond 10^{11}, neutrinos are trapped, and their behavior depends on their energy. In most calculations, the neutrinos are divided into energy bins; e.g., in the work of Wilson and collaborators, a given bin contains neutrinos of energy from E to $E\sqrt{2}$. About 12 bins are needed to cover the spectrum. Cooperstein *et al.* (1986), in order to save computer time, use instead a Fermi distribution of neutrinos, with temperature T_ν and chemical potential μ_ν different from those of electrons (Sec. II.F).

The method of computing stellar collapse and subsequent explosion was developed first by Arnett (1968a, 1968b, 1969, 1971, 1972, 1977a, 1977b) and Colgate (1960, 1966), and then further refined (especially by including neutrino diffusion) and extensively applied by James Wilson of the Lawrence Livermore National Laboratory. He has used the presupernova distributions of density and temperature calculated by Weaver and Woosley at the same laboratory (see Sec. VIII.A). He and his collaborators have used various equations of state. In most of their computations, the prompt shock following collapse gets stuck in the iron core.

However, in one of his computations, Wilson discovered that the shock can be revived by absorption of the neutrinos emitted by the hot star that is formed at the center, the proto–neutron star. This delayed shock (Sec. VI) starts about one-half second after collapse and has been the main subject of investigation of the Wilson group since about 1983.

Cooperstein and Baron, working mostly at the State University of New York at Stony Brook and at Brookhaven National Laboratory, have been able to find conditions for which the prompt shock succeeds in getting out of the iron core. They also use the presupernova distributions of Woosley and Weaver, and in some cases that calculated by Nomoto and his group. They are very careful in designing good equations of state, for densities both below and above nuclear density (Secs. III and IV). In most of their work, they include the effect of general relativity.

Bruenn (1985, 1988) and Myra *et al.* (1987), pay great attention to neutrino transport including neutrino-electron scattering (Sec. II.G). They concluded that,

with the latter effect included, the prompt shock stagnates and thus is not successful in causing an explosion, at least for an iron core of mass 1.3 $M_\odot$. Bruenn (1988), in a very thorough paper, concludes that the prompt shock can only be successful if the iron-core mass is 1.1 $M_\odot$ or less.

There are numerous other computations of collapse and subsequent shock. I apologize to their authors for not mentioning them.

C. The similarity solution

Goldreich and Weber (1980) discovered that the inner part of the star collapses similar to itself, i.e., the distribution of density and temperature remains similar, and only the scale changes with time; the collapse is homologous.

Yahil and Lattimer (1982) and Yahil (1983) then made this theory more general and more quantitative. They assumed an equation of state

$$P=K\rho^{\gamma} , \tag{2.7}$$

where γ is the adiabatic index and K is a constant, both in space and time, depending only on the entropy. Time is counted from the moment of complete collapse, and the process of collapse is at negative time. They then show that all hydrodynamic quantities are functions of the similarity variable

$$X=K^{-1/2}G^{(\gamma-1)/2}r(-t)^{\gamma-2} , \tag{2.8}$$

where G is the gravitational constant. The interesting range of γ is

$$1.20<\gamma<4/3 . \tag{2.9}$$

Some hydrodynamic quantities are then

$$\rho=G^{-1}(-t)^{-2}D(X) , \tag{2.10}$$

$$v=B(-t)^{1-\gamma}V(X) , \tag{2.11}$$

$$m(r)=C(-t)^{4-3\gamma}M(X) , \tag{2.12}$$

where $m(r)$ is the mass enclosed by r, while B and C are constants that can be expressed in terms of G and K. The functions D, V, and M obey ordinary differential equations and have been calculated by numerical integration for values of γ in the range of Eq. (2.9). The asymptotic behavior for large X is determined by the condition that the hydrodynamic quantities must remain finite for $t=0$, e.g.,

$$D(X)\rightarrow X^{-2/(2-\gamma)} . \tag{2.13}$$

Note that for $\gamma=4/3$, i.e., for a pure relativistic gas, the time factor in Eq. (2.12) is equal to one, so that a given mass m corresponds to a definite X. In this case, Eqs. (2.13) and (2.10) show that, for large r,

$$\rho=Hr^{-3} , \tag{2.14}$$

with H another constant. Numerical computations show that, for most stars,

$$H=3\times10^{31} \tag{2.14a}$$

within a factor of three.

Figure 2 shows the dimensionless infall velocity $V(X)$

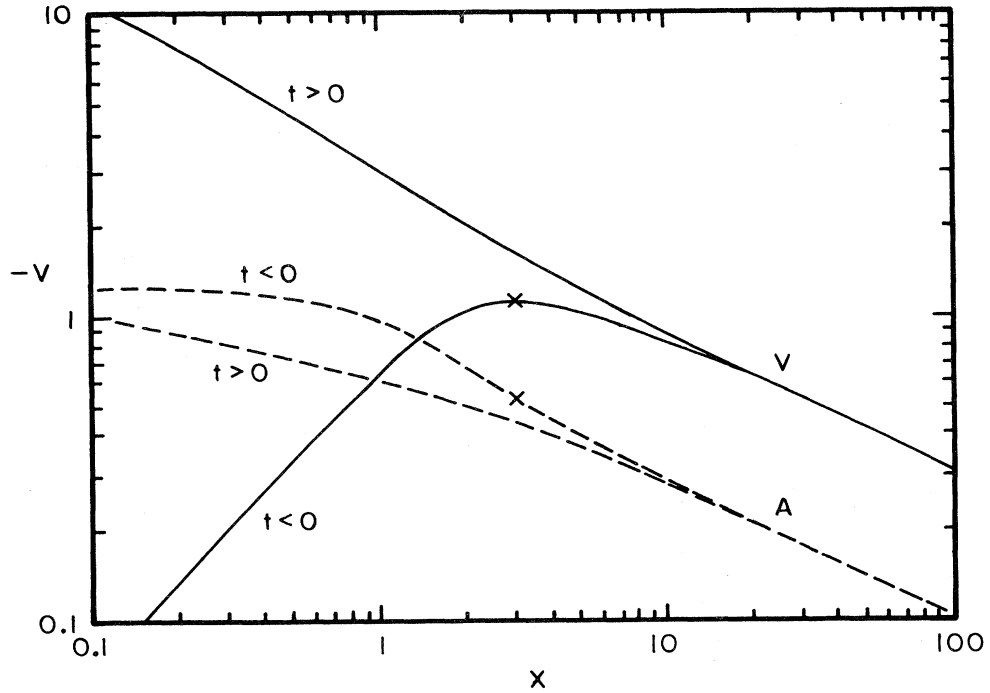

FIG. 2. Quantities in Yahil's theory of self-similar collapse (Yahil and Lattimer, 1982). For definitions, see Sec. II.C. The abscissa x is proportional to the position of the mass element, V is proportional to the infall velocity, and A is proportional to the local sound velocity.

for $\gamma=1.30$. The curve $t<0$ should be used. It shows that, for small X, in the "inner core," the velocity is proportional to the radius (to X), which means that the infall is indeed homologous. V reaches a maximum at a certain X (denoted by a cross in the figure) and then declines. At large X, V falls off as $X^{-1/2}$. This is the same behavior as for free fall. Yahil and Lattimer calculated that at the maximum, V is just slightly over one-half of the free-fall velocity, for $\gamma<1.32$.

These features are reproduced very well by the numerical calculations of Sec. II.B; see also Sec. II.H. In particular, there is a large homologous core, of mass somewhat larger than the Chandrasekhar mass for the given K. Moreover, an infall velocity of about one-half of free fall is a good approximation outside the homologous core.

Figure 2 also shows the local sound velocity A on the same scale (dotted curve). The homologous core moves at less than sound speed, as is essential for all its parts to move in unison. The outer part of the star moves at supersonic speed. These results are also in accord with numerical computations, but the Mach number V/A in the computations (cf. Fig. 4 below) is generally not as high as in Fig 2, viz., about 1.7 rather than about 3.

Figure 2 also gives results from the similarity solution for $t>0$, i.e., after collapse. [For a real star, of course, complete collapse is prevented by the nuclear pressure, and after collapse a shock moves out (Sec. V); the $t>0$ similarity solution is only valid outside the shock, where the material still moves in.] The sound velocity for $t>0$ is not very different from $t=0$, but the material infall velocity at small X becomes very large and approaches the full free-fall velocity.

The density factor,

$$C(X)=D(X)X^{2/(2-\gamma)} , \tag{2.15}$$

was also computed by Yahil and Lattimer. It approaches a constant for large X. But for small X and $t>0$, i.e., long after collapse, $C(X)$ becomes very small and

$$D(X)\sim X^{-3/2} . \tag{2.16}$$

D. Electron capture

The behavior of the supernova after collapse is very sensitive to the mass of the homologous core, and hence to the final electron fraction Y_e. Therefore the capture of electrons by nuclei is very important. (In addition, it affects the entropy.)

The theory of electron capture has gone a full circle and a half. In early theories, it was assumed that capture takes place on free protons. In 1978, BBAL showed that the concentration of free protons is very low, and therefore assumed that the capture takes place on complex nuclei of atomic weight from 60 to 80. In these nuclei, protons are in the $f_{7/2}$ shell, and BBAL assumed that, on electron capture, they become neutrons in the $f_{5/2}$ shell, by an allowed Gamow-Teller transition. However, Fuller (1982) pointed out that the $f_{5/2}$ neutron shell is full at $N=38$, a condition that may be reached even before collapse begins, after which capture on free protons dominates.

Cooperstein and Wambach (1984) carried out a very thorough investigation of electron capture. They found that, in addition to capture on free protons, forbidden transitions in complex nuclei are important.

It is possible (see Sec. VIII) that the SN collapse begins at a lower temperature than was hitherto supposed. This would further reduce the concentration of free protons and would again make capture by complex nuclei dominant, probably favoring forbidden transitions. A thorough investigation has yet to be made.

The cross section for electron capture by a free proton at rest is

$$\sigma=4.5\times10^{-44}\varepsilon_\nu^2 \text{ cm}^2 , \tag{2.17}$$

where ε_ν is the energy of the emitted neutrino in MeV. The rate of electron capture is then

$$\alpha=\sigma_c N_A Y_p=160\rho_{11}\varepsilon_\nu^2 Y_p \text{ sec}^{-1} , \tag{2.18}$$

where N_A is Avogadro's number and Y_p is the number of free protons divided by the total number of nucleons. The density changes typically [see, for example, BBAL Eq. (10)] as

$$\frac{d\ln\rho}{dt}=200(\rho_{11}^m)^{1/2} , \tag{2.19}$$

where ρ_{11}^m is the density at some mean point in the star, e.g., at half the mass of the homologous core (see Sec. II.C), in units of 10^{11} g cm^{-3}. Combining Eqs. (2.18) and (2.19), we have

$$-\frac{d\ln Y_e}{d\ln\rho}=0.8(\rho_{11}^m)^{1/2}\varepsilon_\nu^2 Y_p . \tag{2.20}$$

Assuming $\varepsilon_\nu=10$ MeV and $\rho_{11}^m=1$, we find that electron capture on free protons will be significant [i.e., Eq. (2.20) of the order of 0.01] if

$$Y_p\simeq10^{-4} . \tag{2.21}$$

The density 10^{11} was chosen because at lower density ε_ν, as well as the factors $\rho_{11}^{1/2}$ and Y_p, are likely to be too small. A proton fraction of 10^{-4} is possible with the entropies and temperatures believed in 1984 (see Cooperstein and Wambach, 1984), but it may actually be smaller.

When an electron is captured, the change of entropy is given by Eq. (3) of BBAL, viz.,

$$T\,dS=dQ-\sum\mu_i\,dN_i , \tag{2.22}$$

where μ_i is the chemical potential of the ith particle species, dN_i the change of the number of particles of species i, and dQ the change of total energy of the medium. Assuming that the neutrinos escape freely, the particle species are electrons, protons, and neutrons, and in the capture of one electron,

$$dN_e=dN_p=-dN_n=-1 . \tag{2.23}$$

TABLE I. Properties of matter during collapse, as a function of density. T, $\hat{\mu}$, and μ_e are in MeV; ρ is in g cm^{-3}; S is in units of k_B. Z and A are average values. The Ejiri factor on the Gamow-Teller matrix element is assumed to be 1/3. From Cooperstein and Wambach (1984).

logρ	Y_e	T	$\hat{\mu}$	μ_e	S	$10^4 X_p$	$1-X_H$ (%)	Z	A
10	0.420	0.885	3.1	8.1	1.00	2.7	3.6	28	68
10.5	0.418	1.04	3.3	11.9	0.99	5.4	4.8		
11	0.410	1.21	4.5	17.5	0.97	5.3	4.7		
11.5	0.389	1.37	7.4	25	0.93	1.6	4.2		
12	0.358	1.49	12.1	36	0.91	0.16	5.9	37	97

Thus

$$T\,dS = dQ + \mu_e - \hat{\mu} \tag{2.24}$$

where

$$\hat{\mu} = \mu_n - \mu_p \ . \tag{2.25}$$

This latter quantity is derivable from the equation of state of nuclear matter; see Sec. III.A. Of course, electron capture generally occcurs only if

$$\mu_e - \hat{\mu} > 0 \ . \tag{2.25a}$$

Further, $-dQ$ is the average energy carried off by the escaping neutrino. In the particular case of capture by a proton, essentially *all* the electron energy goes to the neutrino, and the entire energy spectrum of the electrons participates. Then

$$-dQ = \frac{\int_0^{\mu_e} \varepsilon\varepsilon^2\varepsilon^2 d\varepsilon}{\int_0^{\mu_e} \varepsilon^2\varepsilon^2 d\varepsilon} = \frac{5}{6}\mu_e \ . \tag{2.26}$$

Here $\varepsilon^2 d\varepsilon$ is the momentum space volume, and the extra factor ε^2 comes from the cross section of electron capture, Eq. (2.17). Inserting into Eq. (2.24), we have

$$T\,dS = \tfrac{1}{6}\mu_e - \hat{\mu} \ , \tag{2.27}$$

which is nearly always negative; electron capture on protons cools the star. Of course, once the neutrinos get trapped (Sec. II.E), $T\,dS$ becomes positive.

Cooperstein and Wambach (1984) have considered capture by nuclei for densities of 10^{10}–10^{12}. They chose as typical nuclei ^{82}Ge ($Z=32$, $N=50$) and ^{90}Zr ($Z=40$, $N=50$). They showed that, around $\rho=10^{11}$, first forbidden transitions dominate, but near 10^{12}, allowed transitions become important again, chiefly

$$(1g_{9/2})_{\text{proton}} \rightarrow (1g_{7/2})_{\text{neutron}} \ . \tag{2.28}$$

This, like the BBAL transition

$$(1f_{7/2})_p \rightarrow (1f_{5/2})_n \ , \tag{2.28a}$$

is a Gamow-Teller transition and is therefore strongly suppressed (compared to allowed Fermi transitions), as was shown by Ejiri (1982). At ρ from 10^{10} to 10^{11}, proton capture dominates.

Most of the captures in complex nuclei occur only because the temperature is appreciable, of the order of 1 MeV. Then either a proton may be excited above the Fermi energy, or a neutron level below the Fermi energy may be empty, due to temperature. Because the capture starts from thermally excited states, the energy content in the nuclei usually decreases in the capture process, and the nucleus is left with reduced excitation energy. Therefore, in capture by nuclei, the entropy usually decreases also.

Table I gives some of the results of Cooperstein and Wambach for densities of 10^{10}–10^{12}. Temperatures are generally of the order of 1 MeV, increasing slowly with density, about as $\rho^{0.11}$. We believe that $\hat{\mu}$ should be about 3 MeV higher than is shown in Table I. Therefore the free-proton fraction X_p is likely to be less than that given in the table. Other entries are likely to remain about the same, including the average Z and A as a function of density.

Table II gives the average energy of emitted neutrons, E_ν and the average nuclear excitation energy ε^*, for electron capture at $\rho=10^{12}$, for different capture processes. The "average" is weighted, allowed and forbidden capture being about equally probable, and capture by free

TABLE II. Average energies of outgoing neutrinos E_ν and of nuclear excitation ε^* (in MeV) and final electron fraction Y_{ef} from electron capture process, for two densities. From Cooperstein and Wambach (1984).

			Electron capture process		
Quantity	logρ	Free protons	Allowed	Forbidden	Average
E_ν	10	7	6	5	6
E_ν	12	30	24	19	22
ε^*	10		−1.5	0	
ε^*	12		−5	+1	
Y_{ef}		0.38			0.36

protons one-third as probable. The estimated resulting electron fraction after capture is given, assuming that all neutrinos escape. This Y_{ef} is rather low.

The main electron capture takes place at $\rho=10^{11.5}-10^{12}$ (at still higher ρ the neutrinos will be trapped; see Sec. II.E). The corresponding μ_e are 26 and 37 MeV, respectively, and the most likely A are 83 and 92 [see Baym *et al.* 1971, Eq. (5)]. Assuming $Y_e=0.40$, the likely neutron numbers are 50 or 55, and $Z=33$ or 37. Thus good candidates for electron capture may be the nuclear transitions

$$2p_{3/2,\,1/2}(\text{proton})\rightarrow 2d_{5/2,\,3/2}(\text{neutron}) ,$$

$$1f_{5/2}(\text{proton})\rightarrow 1g_{7/2}(\text{neutron}) .$$

In each case, considerable energy (beyond $\hat{\mu}$) will be given to the nucleus. All these transitions are first forbidden, but this diminishes the transition probability only by a factor of about

$$(qR)^2/5, \quad \langle q^2\rangle = k_e^2+k_\nu^2 , \tag{2.29}$$

where R is the nuclear radius. Because the electron momentum k_e and the nuclear radius are large, this factor is about 0.1, i.e., the forbidden transitions are not very weak compared to the allowed ones.

E. Neutrino trapping

Electron capture would continue indefinitely, and the final electron fraction Y_{ef} at collapse would be extremely small, were it not for the trapping of neutrinos at high density. A small Y_{ef} would make the mass of the homologous core, Eq. (2.4), very small, and a supernova would be impossible; see Sec. V.

Neutrino trapping was discovered by Freedman (1974), Mazurek (1975), and Sato (1975). It is due to the neutral weak current between neutrinos and neutrons (and, to a lesser extent, protons), which gives rise to substantial elastic scattering of neutrinos by nuclei. A detailed theory of this and other neutrino interactions was worked out by Tubbs and Schramm (1975). A simplified theory was published by Lamb and Pethick (1976) and further modified by BBAL (1979). In the latter form, the mean free path of neutrinos for elastic scattering is

$$\lambda_\nu=1.0\times 10^8\rho_{12}^{-1}[(N^2/6A)X_h+X_n]^{-1}\varepsilon_\nu^{-2}\ \text{cm} . \tag{2.30}$$

Here ρ_{12} is the density of matter in units of 10^{12} g cm^{-3}, ε_ν is the neutrino energy in MeV, N and A are the number of neutrons and of nucleons in an average nucleus, and X_h and X_n are the fractions (by mass) of the stellar material in heavy nuclei and nucleons, respectively. In deriving Eq. (2.30), BBAL took the Weinberg (1967) angle to be $\sin^2\theta_W=0.25$. The best experimental determination is about 0.23, which would replace N in Eq. (2.30) by

$$N-0.08Z . \tag{2.30a}$$

During the infall, nearly all matter is in heavy nuclei (see Sec. III.A), so $X_h=1$, $X_n=0$.

For density 10^{12}, we have $N\simeq 50$, $N/A=0.6$, so

$$\lambda_\nu=2\ \text{km}\ (10/\varepsilon_\nu)^2 . \tag{2.31}$$

If we take the average neutrino energy to be 22 MeV (see Table II), then

$$\lambda_\nu=0.4\ \text{km} . \tag{2.31a}$$

In a time t the neutrons diffuse a distance L given by

$$L^2=\tfrac{1}{3}c\lambda t . \tag{2.32}$$

If for t we take the dynamic time, the reciprocal of Eq. (2.19), i.e.,

$$t_d\simeq 1.6\ \text{ms (milliseconds)} , \tag{2.32a}$$

then

$$L\simeq 8\ \text{km} . \tag{2.33}$$

The radius corresponding to $\rho=10^{12}$ is about

$$R\simeq 30\ \text{km} . \tag{2.34}$$

In diffusion theory, the distribution settles down to

$$\sin\pi r/R . \tag{2.34a}$$

Therefore we should consider

$$\Lambda=\pi L/R . \tag{2.35}$$

With the numbers given above, this is about equal to 1. This indicates that the neutrinos are just about unable to diffuse out of the core in one dynamic time; they are trapped.

Cooperstein (1988) has discussed neutrino diffusion and trapping in great detail, and the reader is referred to his paper for further information. As he points out, one may define trapping as occurring when the neutrinos cannot escape from the star and are dragged in with the collapsing matter. In this definition, which was used by BBAL, trapping occurs at 6×10^{11} g cm^{-3}. A more useful definition requires that neutrinos cease to diffuse appreciably with respect to the matter; this occurs at $\rho\simeq 10^{12}$.

An important concept is the optical depth,

$$\tau=\int dr/\lambda_\nu . \tag{2.36}$$

Inserting Eq. (2.30) with $X_h=1$, $X_n=0$, we have

$$\tau(R)=10^{-8}(N^2/6A)\varepsilon_\nu^2\int_R^\infty \rho_{12}dr . \tag{2.37}$$

Using Eq. (2.14), we find

$$\int_R^\infty \rho_{12}dr=\tfrac{1}{2}\rho_{12}(R)R=\tfrac{1}{2}\times 10^{-4}H^{1/3}\rho_{12}^{2/3} . \tag{2.38}$$

Inserting Eq. (2.14a), we get from Eq. (2.37)

$$\tau(R)=\frac{N^2}{6A}\frac{\varepsilon_\nu^2}{60}\rho_{12}^{2/3} . \tag{2.39}$$

Using, as before, $N^2/A=30$, we get

$$\tau(R)=(\varepsilon_\nu^2/12)\rho_{12}^{2/3} . \tag{2.39a}$$

Thus, for $\varepsilon_\nu=22$ MeV (as above) and $\rho_{12}=1$, we obtain

$$\tau(R)=40 . \tag{2.39b}$$

The neutrino sphere is the place from which neutrinos can escape essentially freely to infinity. Wilson has defined this as

$$\tau(R_\nu)=2/3 . \tag{2.40}$$

The value 2/3 is chosen rather than 1 to take into account that the neutrinos do not emerge radially but at an angle. Inserting Eq. (2.39a) we find

$$\rho_{12}(R_\nu)=23\varepsilon_\nu^{-3} . \tag{2.41}$$

Thus the density at the neutrino sphere depends very strongly on the neutrino energy; for $\varepsilon_\nu=10$ MeV, it is about 2×10^{10}. Using once more Eqs. (2.14) and (2.14a), we find that the radius of the neutrino sphere is

$$R_\nu=11\varepsilon_\nu \text{ km} . \tag{2.42}$$

Thus the neutrino sphere is far outside the trapping sphere; the neutrinos escaping from the trap diffuse for a long time (distance) before they are actually emitted. This is important especially for neutrino-electron scattering (Sec. II.F).

We have considered only elastic scattering of neutrinos, not absorption and reemission. This is justified during the infall because the matter is nearly all in complex nuclei, for which $\nu\rightarrow e$ and $e\rightarrow\nu$ processes are reduced by about a factor of 1000 compared with free nucleons. The formulas given here are only valid for the infall.

F. Neutrino-electron scattering

Bruenn and Bludman have often emphasized the importance of scattering of neutrinos by electrons (see, for example, Bruenn, 1985, 1988; Myra *et al.*, 1987). Bethe, Brown, Applegate, and Lattimer (1979) calculated, for one particular set of parameters, that

$$\sigma_{e\nu}/\sigma_{\rm sc}\simeq 1/600 ,$$

where $\sigma_{\rm sc}$ is the cross section for scattering by nuclei, and concluded that *νe* scattering is negligible. This, however, is erroneous because a neutrino suffers many elastic scatterings by nuclei before it escapes from the star, and therefore a few *νe* scatterings are also likely to occur. In scattering by electrons, the neutrino generally loses energy, because the electrons are highly degenerate and therefore can only gain energy. With lower energy, the neutrino can escape more easily; therefore *νe* scattering will cause a loss of leptons from the star, which is important.

The most thorough investigation of *νe* scattering has been carried out by Bruenn (1988; see therein also earlier references). He starts from the *νe* cross section of Tubbs and Schramm (1975).

$$\sigma_{\nu e}=\sigma_1\varepsilon_\nu^3/\mu_e , \tag{2.43}$$

where $\sigma_1=0.64\times10^{-44}$ cm^2 and ε_ν and μ_e are in MeV. This formula assumes that $\varepsilon_\nu\ll\mu_e$ and that the electrons are highly degenerate, which is generally true. (If T is not very small compared to ε_ν, the cross section is reported to be larger by terms of order T/ε_ν, but then there are also scatterings in which the neutrinos gain energy that partly compensate for this.) We may assume that the neutrinos are scattered roughly uniformly into any state inside the sphere of momentum ε_ν/c, so the average energy loss of a neutrino is

$$\Delta\varepsilon_\nu=\varepsilon_\nu/4 . \tag{2.44}$$

The rate of energy loss is then

$$-\frac{d\varepsilon_\nu}{dt}=\frac{N_A c}{4}\rho Y_e\sigma_1\frac{\varepsilon_\nu^4}{\mu_e}$$
$$=29\rho_{12}Y_e\varepsilon_\nu^4/\mu_e , \tag{2.45}$$

where N_A is Avogadro's number. Using $Y_e=0.4$ and $\mu_e=38\rho_{12}^{1/3}$ MeV, we can integrate Eq. (2.45) to give

$$\varepsilon_\nu^{-3}=0.9\rho_{12}^{2/3}t+\varepsilon_0^{-3} \tag{2.46}$$

where ε_0 is the energy at which the neutrino was emitted. Using $\varepsilon_0=22$ MeV, as in Table II, we find $\varepsilon_0^{-3}=0.10\times10^{-3}$, which is usually unimportant.

We may take for t the dynamic time,

$$t_d=1.7\times10^{-3}\rho_{12}^{-1/2} , \tag{2.47}$$

from which Eq. (2.46) yields

$$\varepsilon_{\nu f}=6.5\rho_{12}^{-1/18} \text{ MeV} . \tag{2.48}$$

This is rather low. But as the neutrinos become degenerate, their energy cannot be reduced much below their chemical potential,

$$\mu_\nu=11.1(\rho_{10}2Y_\nu)^{1/3}$$
$$=14(\rho_{12}100Y_\nu)^{1/3} . \tag{2.49}$$

Even with a neutrino fraction as low as $Y_\nu=0.01$, this is 14 MeV, considerably higher than Eq. (2.48). The energy of 14 MeV is reached by *νe* scattering after only 0.3 ms.

Thus *νe* collisions are a rapid mechanism for establishing equilibrium between neutrinos and matter. This is accompanied by a substantial increase of entropy: Bruenn gives the resultant entropy change corresponding to a capture of $-\Delta Y_e$ electrons as

$$T\Delta S=-\Delta Y_e(\mu_e-\hat{\mu}-\varepsilon_{\nu f}) , \tag{2.50}$$

where $\varepsilon_{\nu f}$ is the final neutrino energy after *νe* scattering, in contrast to the emission energy ε_0. The parentheses in Eq. (2.50) may easily be 15 MeV, and T could be as low as 1 MeV, which means $\Delta S=0.15$ for $\Delta Y_e=-0.01$. The total electron capture $-\Delta Y_e$ may be 0.04–0.06, corresponding to an entropy change $\Delta S=0.6$–0.9. It is interesting that, according to Eq. (2.50), the entropy

change is greater the lower the initial entropy. Thus *ve* scattering makes the final entropy, at the end of collapse, largely independent of the initial entropy; we estimate the final value to be about 1.5.

As neutrinos diffuse out through the wide diffusion region between trapping sphere and neutrino sphere (see Sec. II.E), they are likely to suffer further *ve* collisions, which reduce their energy further. This will facilitate their escape. The diffusion distance,

$$L=(\tfrac{1}{3}ct\lambda)^{1/2}\ , \tag{2.51}$$

is roughly inversely proportional to the neutrino energy and may increase due to *ve* scattering by a factor of 1.5–2. Reliable answers on the final Y_L in the core can only be obtained by a complete numerical computation, such as Bruenn has performed, using 20 energy bins for the neutrinos. He finds that Y_L is decreased due to *ve* scattering by about 0.02, which, unfortunately, has a bad effect on the outgoing shock; see Sec. V.

These results depend, of course, on the initial conditions of the star. Bruenn uses a star of 12 $M_\odot$ whose evolution was calculated by Woosley and Weaver (1986) and which has an Fe core of 1.39 $M_\odot$. Recent evolution calculations, which give smaller Fe cores, may lead to different results for the effect of *ve* scattering.

Those neutrinos that do not escape assemble at low energy and build up Y_ν, thereby impeding further *ve* scattering [see Eq. (2.49)]. They gradually form a Fermi distribution, and ultimately equilibrium is established between neutrinos and matter, such that

$$\mu_\nu=\mu_e-\hat{\mu}\ . \tag{2.52}$$

According to Bruenn, this happens at a density

$$\rho_{\rm eq}\simeq 2\times 10^{12}\ , \tag{2.53}$$

which defines completion of trapping. Thereafter, there are just as many $\nu\rightarrow e$ as $e\rightarrow\nu$ processes; there is no (appreciable) further decrease of Y_L.

This conclusion is limited by the fact that there is still some loss of neutrinos through the "window" at very low energy, $\varepsilon_\nu<5$ MeV (Mazurek, 1976). By *ve* scattering, a neutrino of average energy, say of order μ_ν, may be scattered into the window; then, due to its long mean free path for elastic scattering, it may escape. This loss in Y_L is estimated to be less than 0.005.

G. Getting into equilibrium

After neutrinos are trapped, they fill the available phase space. It is illuminating to describe them by a Fermi distribution with a temperature T_ν and chemical potential μ_ν, different from those of the electrons. This description was introduced and discussed in detail by Cooperstein, van den Horn, and Baron (1986, 1987) and reported more concisely by Cooperstein (1988); it is, of course, only approximate because neutrinos cannot establish equilibrium by themselves but only by interacting with other particles, but it is very convenient.

The rate of generation of total entropy is then

$$\dot{S}=\dot{S}_{\rm neq}+\dot{S}_{\rm diff} \tag{2.54}$$

where $\dot{S}_{\rm diff}$ is the contribution from the diffusion of neutrinos. The other part, $\dot{S}_{\rm neq}$, arises from the fact that neutrinos are not in thermal equibrium with electrons and matter in general. According to Cooperstein, van den Horn, and Baron,

$$\dot{S}_{\rm neq}=\Delta_\beta q-\Delta_T y/T_m\ , \tag{2.55}$$

where q and y are the rates at which lepton number and energy, respectively, are transferred from the matter to the neutrinos. The Δ's measure the deviation from equilibrium, viz.,

$$\Delta_T=\frac{T_\nu-T_m}{T_\nu},\quad \Delta_\beta=\frac{\mu_e-\hat{\mu}}{T_m}-\frac{\mu_\nu}{T_\nu}\ , \tag{2.56}$$

where T_m is the temperature of the matter, for both electrons and nuclei.

Using these concepts, Baron and Cooperstein (1988) have carried out calculations for a 15-$M_\odot$ star whose presupernova evolution was calculated by Woosley and Weaver (1986, 1988); the result is shown in Fig. 3, which refer to a mass element at 0.5 $M_\odot$. The lepton number begins at 0.435, goes down to 0.405 at the nominal trapping density $\rho_{12}=1$, and finally levels off at about 0.385 at $\rho\sim 3\times 10^{12}$. This density of complete trapping is close to that derived by Bruenn, Eq. (2.53). This is interesting because Baron and Cooperstein, in these calculations, relied on β interactions to establish equilibrium, while Bruenn uses the (probably more powerful) *ve* scattering. The two calculations also agree quite well on the increase of entropy. The final Y_L with *ve* scattering also agrees well with Bruenn's calculation.

For the Baron-Cooperstein method, Fig. 3 also shows the approach to equilibrium of both the temperature Δ_T and the chemical potential of the neutrinos. As Cooperstein (1988) points out, the β interactions mediate both energy and lepton exchange between neutrinos and "matter;" therefore Δ_T and Δ_β go essentially in parallel. Most of the drop in these two quantities occurs between $\rho_{12}=0.7$ and 3.

H. Result of the infall

Figure 4 gives the distribution of velocity of the infalling material, about 0.2 milliseconds before collapse, according to Arnett (1977). The inner part of the star, out to about 40 km, has velocity proportional to the radius, as expected for homologous collapse (Sec. II.C). The outer part, from 40 km on out, falls in with a velocity proportional to $1/\sqrt{R}$, slightly over half of free-fall velocity (see Sec. II.C). Very far out, the velocity is smaller because these parts of the star have not yet received the signal that the core is falling in.

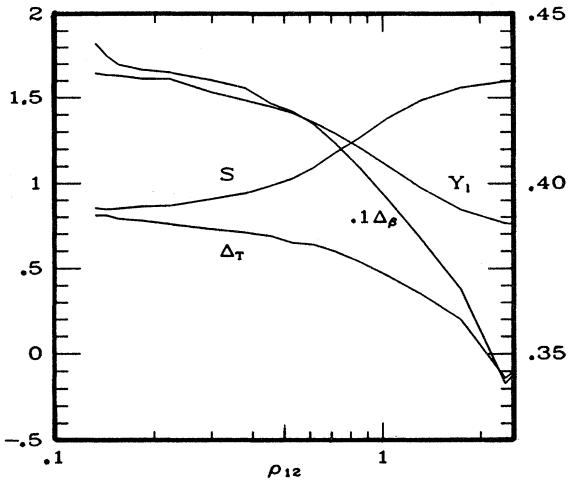

FIG. 3. Approach to equilibrium, in the infall, according to the theory of Cooperstein *et al.* ΔT is related to the difference in temperature of neutrinos and matter, Δ_β to the difference in chemical potential. Both of these decrease as the matter density increases. The lepton fraction Y_l and the entropy S are shown. From Baron and Cooperstein (1990). Right-hand scale for Y_l, left scale for all others.

The figure also shows the local sound velocity a. The inner core falls in with less than sound velocity; this is necessary in order to have the good communication that leads to homologous collapse. The outer core moves at supersonic velocity. The Mach number,

$$M = v/a \ , \tag{2.57}$$

is about 1.7, somewhat less than in the theory of Yahil and Lattimer (Sec. II.C). At $R = 24$ km, $M = 1$; this is the sonic point. A sound signal coming from the inside cannot get beyond this point because it moves with velocity a relative to the material, which itself moves with velocity $-v$ relative to the center of the star.

Somewhat farther out than the sonic point, the velocity reaches a maximum, in this case 4.0×10^9 cm/sec, about one-eighth the velocity of light. This will increse somewhat further as the collapse is completed. General relativity has been used by Cooperstein; with Newtonian gravitation, the maximum velocities are somewhat lower.

Collapse continues until the central density becomes substantially greater than nuclear density. Then nuclear pressure slows down the infall and finally stops it; the inner core reaches a maximum density. Cooperstein has called this the time of "maximum scrunch." The central density at this time is about 3–4 times nuclear density in most models (see Table VII below); in one model it goes to 12 times. After maximum scrunch, the core rebounds and a shock starts (see Sec. V).

I. Final Y_L and inner-core mass

The extensive calculations of Baron and Cooperstein (Baron, Cooperstein, and Kahana, 1985a, 1985b; Baron and Cooperstein, 1988) find a final value of about $Y_L = 0.38$. The effect of neutrino-electron collisions (Bruenn, 1985; Myra *et al.*, 1987; Baron and Cooperstein, 1990) lowers this to about $Y_L = 0.36$.

This difference appears small but seems to be very important. The mass of the inner core, i.e., inside the point of maximum infall velocity is (Bruenn, 1988)

$$\begin{aligned} M_{\rm IC} &= 0.75\ M_\odot \ \text{(without } \nu e \text{ scattering)} \ , \\ M_{\rm IC} &= 0.64\ M_\odot \ \text{(with } \nu e \text{ scattering)} \ . \end{aligned} \tag{2.58}$$

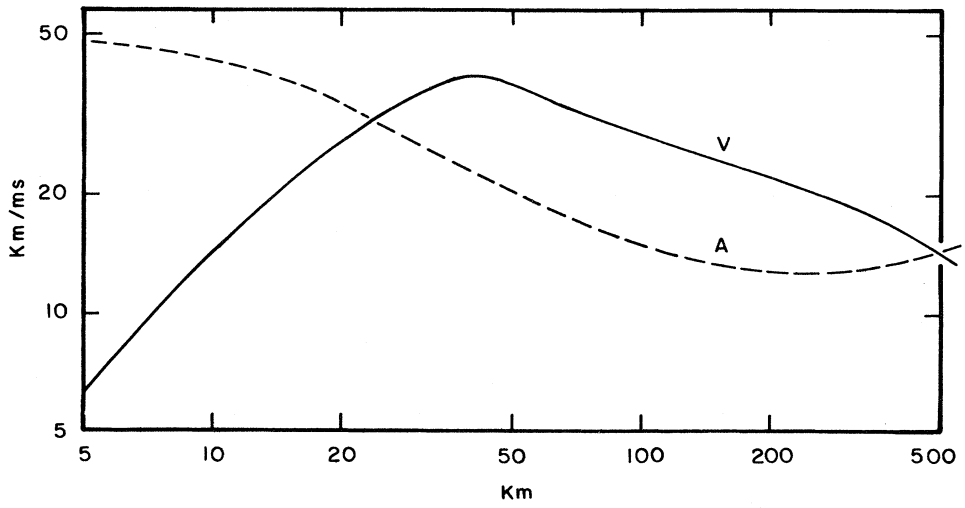

FIG. 4. Infall velocity V and local sound velocity A about a millisecond before collapse, according to a calculation by Arnett (1977). Note the sonic point, i.e., the crossing of curves V and A, at a radius of about 25 km, and the maximum infall velocity at about 40 km.

We shall find in Sec. V that the success of the prompt shock depends on the *difference* between the initial Fe core mass, of 1.1–1.3 $M_\odot$, and the final inner-core mass, Eq. (2.64). It is understandable that the difference of 0.11 $M_\odot$ between the two results for Eq. (2.64) can be important.

Numerical computations with Newtonian gravity give for the mass of the core up to the sonic point 0.7–0.8 $M_\odot$, in accord with Eq. (2.64). When general relativity is used, the masses are about 0.1 $M_\odot$ smaller.

III. EQUATION OF STATE BELOW NUCLEAR DENSITY[2]

A. Basic equation of state

The basic equation of state (EOS) has been derived by Lamb *et al.* (1978, 1981) and Lattimer *et al.* (1985). Matter consists of a nuclear and an electron component. Neutrinos have negligible interaction and can be disregarded as long as they escape from the star, i.e., for densities $\rho < 5\times10^{11}$ g cm^{-3}. The state of matter is described by the density ρ, the temperature T, and the number of electrons per nucleon Y_e. (Strictly speaking, Y_e is the difference between the number of electrons and that of positrons.) For the temperature, we generally give kT in MeV; 1 MeV $=1.16\times10^{10}$ K.

The forces are nuclear and electromagnetic; statistical mechanics is used to derive the EOS. Because of the attractive nuclear forces, the nuclear component condenses into nuclei. Outside of these, we have a lower-density "gas" of nucleons and alpha particles. Thus we have a two-phase system; the chemical potential μ must be continuous at the boundary between the two phases, both for neutrons and protons.

The electrons are essentially uniformly distributed in space, both inside and outside the nuclei. In equilibrium, we must have

$$\mu_e=\mu_n-\mu_p=\hat{\mu}\ . \tag{3.1}$$

Especially at the higher temperature, positrons are present; their chemical potential is $\mu_+=-\mu_-\ (=-\mu_e)$;

$$\hat{\mu}=250(0.46-Y_e)\ . \tag{3.1a}$$

The size of the nuclei is determined by the combined action of surface and Coulomb energy. The surface energy was derived by Ravenhall, Bennett, and Pethick (1972) and can be written as

$$W_{\rm surf}=A^{2/3}290x^2(1-x)^2\ , \tag{3.2}$$

where x is the fraction of protons inside the nucleus. In most cases when there are not many nucleons outside the nuclei, $x=Y_e$. All nuclei are assumed to have the same A and Z; to assume a statistical distribution does not make much difference.

At high temperature, the nuclei evaporate into a gas of nucleons, as described in detail by Lamb *et al.* (1978, 1981, 1985). There is a critical point at $T\approx15$ MeV.

As the density increases to about one-half of the saturation nuclear density, we no longer have nuclei, but instead all of space is filled by nuclear matter of uniform density with empty bubbles distributed in it. This phase is commonly called "Swiss cheese." Ultimately, these empty bubbles disappear and we get nuclear matter filling space uniformly. This is discussed in more detail in Sec. III.C. The saturation density of symmetric nuclear matter we take to be

$$\rho_s=0.16\ {\rm fm}^{-3}\ . \tag{3.3}$$

Because of their Coulomb repulsion, the nuclei form a lattice, and we assume the same for the bubbles. It is often convenient to use a Wigner-Seitz cell, which contains one nucleus. For calculations, that cell is usually assumed to be spherical.

For definiteness, Lamb *et al.* (1978, 1981, 1985) use a specific nuclear force, namely the Skyrme force *I*. This is somewhat too stiff, having a compression modulus $K=370$ instead of 210 ± 30 MeV, the "experimental" value. However, a definite nuclear force is useful for calculating unique values of several physical quantities: the entropy S, measured in units of k_B per nucleon; the chemical potentials μ_n and μ_p of neutrons and protons; the fraction X_H of nucleons that are in nuclei; the pressure P in MeV fm^{-3} (one of these units is 1.6×10^{33} dyne cm^{-2}); the energy per nucleon in MeV; and the free energy $F=E-TS$.

Using such calculations, Fig. 5 shows the adiabats

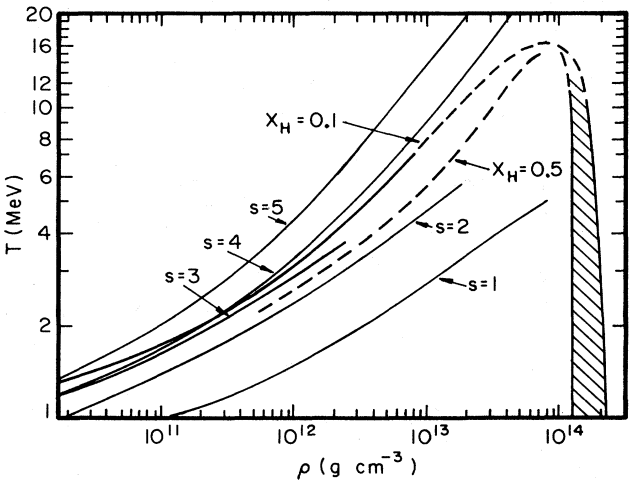

FIG. 5. Equation of state for nuclear matter, as a function of density ρ and temperature T, according to Lamb, Lattimer, Pethick, and Ravenhall (1978). Shown are the adiabats $S=1$–5; a collapsing supernova has S close to 1. Dashed are the lines at which 10% or 50% of the matter is in heavy nuclei. In the shaded area, we have nuclear matter with empty "bubbles" in it; to the right of the shaded area is uniform nuclear matter.

[2]Reproduced (adapted) with permission from the *Annual Review of Nuclear and Particle Science,* Volume 38, ©1988 by Annual Reviews Inc.

$S=1$ to $S=5$ for $Y_e=0.35$, which is close to the Y_e relevant in calculations of supernova collapse. Also shown are the curves for $X_H=0.5$ and 0.1; X_H depends chiefly on μ_n and ρ. From calculations of the evolution of stars before supernova collapse, one finds that S is about 1 or less. Figure 5 shows, then, that generally X_H is near 1, i.e., only a small fraction of the nuclear material is in the "gas."

The pressure from the nuclear phase is calculated. It is often negative because the Coulomb energy per nucleon is smaller than it is for free nuclei. This in turn is due to the fact that some of the electrons are inside nuclei. The total pressure is therefore mostly due to electrons. When the material has overall density $\rho_s=0.16$ fm^{-3} and $Y_e=0.3$, the electron contribution is

$$P_e/\rho=20 \text{ MeV} . \tag{3.4}$$

By comparison, the nuclear P/ρ is of the order of 1 MeV.

For many problems having to do with the dynamics of the supernova, the adiabatic index plays an important role,

$$\Gamma=(\partial \log P/\partial \log\rho)_S . \tag{3.5}$$

Figure 6 shows Γ as a function of ρ. There is no resistance to the gravitational collapse of the star as long as $\Gamma<4/3$. Γ has a minimum at about $(2/3)\rho_S$; it then rises quickly because at ρ_S the nuclear pressure has to become zero. The homology of the collapse (see Sec. II.C) stops effectively at $(2/3)\rho_s$ (Cooperstein, private communication). Beyond ρ_S, Γ becomes large (see Sec. III.E).

The fact that $\Gamma<4/3$ for a material with $S\sim 1$ shows that the collapse of a supernova cannot be stopped until the material reaches nuclear density. This was recognized by Lamb *et al.* (1978) and also elaborated by Bethe *et al.* (1979). It was contrary to the belief held by astrophysicists before 1978.

The energy in nuclei increases with T. This is due to excitation of the higher energy levels of the nucleus. The density of the energy levels increases exponentially with the entropy S in nuclei. Lamb *et al.* (1978, 1981, 1985) desribed this effect in terms of a Fermi gas of nucleons inside the nucleus. Experimentally, it is known (Bohr and Mottelson, 1969) that the level density of excited levels of nuclei is greater than the Fermi-gas approximation. It is as if the entropy inside nuclei were multiplied by a factor

$$m^*/m>1 . \tag{3.6}$$

Some part of this increased level density is a surface effect. The energy in excitation of nuclei does not contribute to the pressure.

The difference $\hat{\mu}=\mu_n-\mu_p$ is positive because all the nuclei concerned have an excess of neutrons. The value of $\hat{\mu}$ depends on the nuclear symmetry energy (see Secs. III.D and III.F). The quantity $\hat{\mu}$ is important for the fraction of protons, which is

$$Y_p=Y_n e^{-\hat{\mu}/T} . \tag{3.7}$$

Y_p gives the number of protons in the gas phase as a fraction of the total number of nucleons in gas plus nuclei. Because of the exponent, Y_p is generally very small, $<5\times10^{-4}$.

Lamb *et al.* (1985) discuss the phase transitions, from nuclei to bubbles, and then from bubbles to uniform nuclear matter. The change of properties at the phase transitions is generally small. The transition from bubbles to nuclear matter would in principle be first order, but is in practice second order, the latent heat is only the lattice Coulomb energy, which is very small, especially because the empty bubbles are quite small before they disappear (see Sec. III.C).

Lattimer *et al.* (1985) give a large number of useful tables and figures. They also discuss the case of high densities, $\rho>10^{12}$ g cm^{-3}, when neutrinos are trapped in the stellar material because of the weak neutral interaction. In this case, the total number of leptons per nucleon, Y_e+Y_ν, not Y_e, is given *a priori*. The condition of chemical equilibrium then determines Y_e. Curves are given by Lattimer *et al.* (1985) for given values of Y_L.

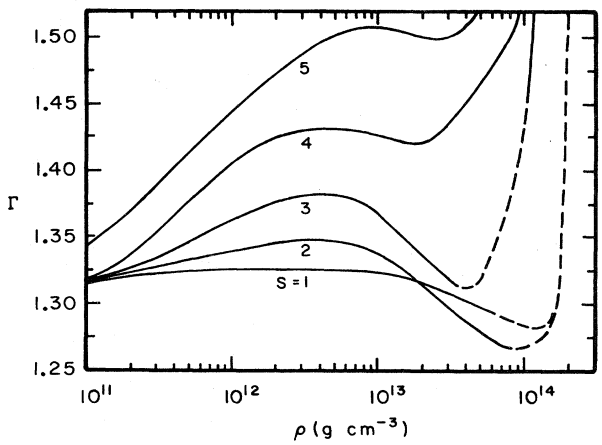

FIG. 6. The adiabatic index $\Gamma=(\partial \log p/\partial \log\rho)_S$ for different values of the entropy, according to Cooperstein (1985).

B. More elaborate equations of state

Ravenhall, Pethick, and Wilson (1983) discussed the shape of the nuclei and bubbles. At low overall density, the nuclei are spherical. At higher density, however, energy is minimized by choosing different shapes. At first, the spheres deform into prolate ellipsoids, arranged parallel to each other. Next, these change into long cylinders. After some intermediate steps, the most favorable configuration is flat plates. At this stage, there is no difference between plates of nuclear matter in a dilute gas of nucleons, or plates of gas between uniform nuclear matter. With further increasing density, they become spaghettilike gas spaces embedded in uniform nuclear matter, and finally spherical bubbles of gas in nuclear matter. Cooperstein and Baron (1990) have coined the phrase "nuclear pasta" to describe all these funny

geometries.

With these assumptions, Ravenhall *et al.* (1983) get a rather smooth EOS; in particular, the total nuclear energy per unit volume becomes nearly smooth as a function of density. In reality, they argue, the spheres should be deformed, and likewise the cylinders and plates should have bulges. This would make the EOS even smoother.

The maximum nuclear energy per unit volume turns out to be

$$0.015 \text{ MeV fm}^{-3} . \tag{3.8}$$

For comparison, the nuclear energy of nuclear matter at normal density is 2.5 MeV fm^{-3}. So the entire energy in the subnuclear density regime is quite small, about 0.6%. Ravenhall *et al.* used the same Skyrme interaction as Lamb *et al.* (1981).

An alternative Skyrme interaction was used by Bonche and Vautherin (1981, 1982). Their interaction gives the correct equilibrium density and the observed compression modulus, as well as other quantities in agreement with observation. The interaction is taken from Bohigas *et al.* (1980). The characteristic quantities at nuclear density are as follows:

$$k_F = 1.33, \quad K = 213, \quad m^*/m = 0.79 ,$$
$$\text{symmetry energy} = 30.6 \text{ MeV} . \tag{3.9}$$

Bonche and Vautherin solved the Hartree-Fock equation in a Wigner-Seitz cell. Like Lamb *et al.* (1981), they assumed spherical nulei plus a low-density nucleon gas at low overall density, and empty bubbles in nuclear matter for high-density ρ. The calculations were done at various temperatures. Curves were given for P/ρ, the energy per particle, and the equilibrium atomic weight A as functions of the density for $T = 1$ and 4 MeV. In a table, they give T, P, and A along the adiabat $S = 1$ for $\rho = 0.02$–0.07 fm^{-3}; A goes from 300 to 1000.

Cooperstein and Baron (1990) have discussed the EOS in more detail, including some minor improvements.

C. A simplified, analytical equation of state

Cooperstein (1985) constructed a simple EOS whose components can be understood physically. He had three reasons for constructing this EOS, namely, (a) to get analytical formulas, (b) to get a smooth EOS that goes from low density to normal nuclear saturation density ρ_s without discontinuities, and (c) to use observed nuclear parameters, rather than some nucleon interaction, such as Skyrme, that may not give good agreement with experimental data.

Requirement (b) is essential to obtain stability in hydrodynamic calculations of the implosion of the supernova. Ravenhall *et al.* (1983) have showed that a smooth EOS is actually obtained if the change of shape of the nucleus with increasing density is properly considered. Cooperstein obtained similar smoothness by finding a correct formula for spherical nuclei at low density and for spherical bubbles at high density, then interpolating sensibly between them. The result is Eq. (3.18) below; it agrees almost precisely with Ravenhall *et al.*

We define the fraction of space occupied by nuclei,

$$u = \rho/\rho_0 , \tag{3.10}$$

where ρ is the overall average density and ρ_0 the density of the nuclei. We assume that the nuclei are compressible, as in Lattimer (1985), and write

$$\rho_0 = \rho_s \theta , \tag{3.11}$$

where ρ_s is the saturation density. The latter is taken to depend on $x = Z/A$, the fraction of protons inside the nuclei, and is assumed to be

$$\rho_s(x) = (0.16 \text{ fm}^{-3})\phi(x) , \tag{3.12}$$

$$\phi(x) = [1 - \tfrac{3}{4}(1-2x)^2] . \tag{3.13}$$

This equation says that the saturation density becomes smaller for unsymmetric matter. Probably this effect is underestimated because Eq. (3.13) gives $\phi(s) = 1/4$ for pure neutron matter, while in reality such matter is not bound at all; Eq. (3.13) is appropriate only for x near 1/2. At the boundary between nuclei and gas, the pressure is continuous, and so are the chemical potentials of neutrons and protons.

The energy per nucleon of bulk nuclear matter (in MeV) is given by

$$W_{\text{bulk}} = -16 + 29.3(1-2x)^2 + \tfrac{1}{18}K(1-\theta)^2 , \tag{3.14}$$

where K is the compression modulus and is assumed to be independent of x. The coefficients are chosen to give the best possible agreement with Bonche and Vautherin (1982), $K = 220$ MeV. This value was obtained experimentally by Blaizot *et al.* (1976). The volume and bulk symmetry coefficient of -16 and 29.3 MeV are not important for the ensuing analysis (but the symmetry energy is important in Sec. III.D). For finite nuclei, one has to add to W_{bulk} another term, W_{size} (Cooperstein, 1985), which includes all surface and Coulomb effects; it is

$$W_{\text{size}} = \beta(x)\theta^{-1/3}G(u) , \tag{3.15}$$

$$\beta(x) = 75x^2(1-x)^{4/3}\phi^{-1/3} . \tag{3.16}$$

The factor $\beta(x)$ is the characteristic surface and Coulomb energy of an isolated nucleus. W_{size} depends on the density of the nucleus as $\rho_0^{-1/3}$, hence $(\theta\phi)^{-1/3}$.

When the nucleus is at the center of a Wigner-Seitz cell, the Coulomb energy is diminished, as compared with a free nucleus, by a factor

$$g(u) = 1 - \tfrac{3}{2}u^{1/3} + \tfrac{1}{2}u . \tag{3.17}$$

When the sum of surface and Coulomb energy is mini-

mized, it becomes proportional to $g^{1/3}$. Numerical values are shown in Table III. For u near 1, nuclei are replaced by empty bubbles in nuclear matter, and a somewhat different formula is obtained. Cooperstein now interpolates between these two cases with the formula

$$G(u)=(1-u)[g^{1/3}(u)+g^{1/3}(1-u)] . \tag{3.18}$$

This formula is correct for u near 0 and near 1, and reproduces very well the more elaborate calculations in Bonche and Vautherin (1982).

The same calculation gives for the mass of the average nucleus

$$A=192(1-x)^2(\theta\phi)^{-1}g^{-1}(u) . \tag{3.19}$$

At $x=1/3$, which is standard for nuclei in a collapsing supernova, $A=85$ for $u=0$; it increases to 225 for $u=1/3$ and to 1100 for $u=1/2$.

The energy

$$W=W_{\rm bulk}+W_{\rm size} \tag{3.20}$$

depends on the density through both u and θ. The pressure, by general thermodynamics, is given by

$$\frac{P}{\rho}=\frac{dW}{d\ln\rho}=\frac{\partial W}{(\partial\ln\theta)_u}=\left[\frac{\partial W}{\partial\ln u}\right]_\theta . \tag{3.21}$$

This equation gives the pressure and, in addition, gives a relation between θ and u, namely,

$$\theta^{4/3}(1-\theta)+\varepsilon_{\rm size}\tfrac{1}{3}(G+G')=0 , \tag{3.22}$$

where the prime denotes $d/d\ln u$. This equation insures pressure balance at the surface, and

$$\varepsilon_{\rm size}=9\beta/K \tag{3.23}$$

can be calculated as a function of x.

This procedure gives perfectly reasonable values for θ as long as $x<1/3$. But for nearly symmetric nuclear matter and u near 1, there is no solution: in this case a bubble in nuclear matter would collapse.

This problem is resolved if we consider matter at nonzero temperature, the only case of physical interest. For finite temperature we write the free energy

$$F=E-TS=W_{\rm bulk}+W_{\rm size}-\frac{a}{A}\frac{m^*}{m}T^2 . \tag{3.24}$$

In the thermal term, Cooperstein separates the dependence on the simple Fermi-gas level-density parameter

$$\frac{a}{A}=\frac{\pi^2}{4\varepsilon_F}=[(\theta\phi)^{2/3}\times 14.9\ \text{MeV}]^{-1} \tag{3.25}$$

TABLE III. $G=g^{1/3}(u)$.

u	G
1/8	0.721
1/4	0.565
1/2	0.406

from an effective mass m^*/m. The entropy is given by

$$S=-\frac{\partial F}{\partial T}=2\frac{a}{A}\frac{m^*}{m}T . \tag{3.26}$$

This entropy is closely related to the level density of excited states of the nucleu, which is e^S. With $m^*/m=1$, we recover the level density for the simple Fermi gas.

It is well known from measurements (Bohr and Mottelson, 1969) that the level density in actual nuclei is greater than that given by the Fermi gas. In fact, for nuclei in the Fe region, $m^*/m=m_0\approx 2$. This large number, and hence large level density is at least partly due to the surface of the nucleus. On the other hand, in a saturated uniform medium, the surface effects disappear and

$$m^*/m=m_s\approx 0.7 , \tag{3.27}$$

where the last number is derived from Brueckner theory. Cooperstein (1985) now adopts an interpolation

$$\frac{m^*}{m}=m_s+\frac{(m_0-m_s)}{(1+T/T^*)^2}\frac{W_{\rm size}}{W_{\rm size}(\rm Fe)} . \tag{3.28}$$

This is reasonable because m^*/m is an effect of the surface of the nucleus. However, the actual calculation of m^*/m is a rather difficult task. Bonche and Vautherin (1982) have considered this problem in a finite-temperature Hartree-Fock theory for ^{208}Pb and ^{56}Fe

The entropy, Eq. (3.26), as mentioned, is related to the level density and thus to nuclear excitation. Similarly, the energy and free energy here considered are those in nuclear excitation.

After some algebra, Cooperstein finds that θ is made smoother by the inclusion of finite temperature. At $u=0$ and $x=0.4$, $\theta\sim 1.05$ for any value of the entropy. Near $u=1$, at $S=0$, θ becomes very low and the bubble (recall that for $u>1/2$ we have bubbles in nuclear matter) would collapse. However, for $S\geq 1$, this is not true; the bubbles are saved by finite temperature. If the entropy in nuclear matter is $S=1$, the expression for θ is very smooth and is approximately

$$\theta=0.7+0.02T . \tag{3.29}$$

The EOS of the gas in the low-density phase is relatively simple. The pressure of the gas further compresses the nuclei, i.e., increases θ somewhat. More important, since the low-density phase consists mostly of neutrons, its existence makes the high-density phase less neutron rich. Both effects were taken into account in the actual calculations.

The transition from nuclei to "Swiss cheese" is completely smooth, by the definitions of the theory. The transition from "Swiss cheese" to uniform nuclear matter is also very smooth, as Ravenhall *et al.* (1983) pointed out. If the Coulomb interaction between bubbles is neglected, this transition is second order. In fact, the Coulomb interaction is very small because near the transition the bubbles are small and fairly widely separated.

To make this transition smooth, Cooperstein uses a shortcut: he continues the bubble solution up to $u=1$,

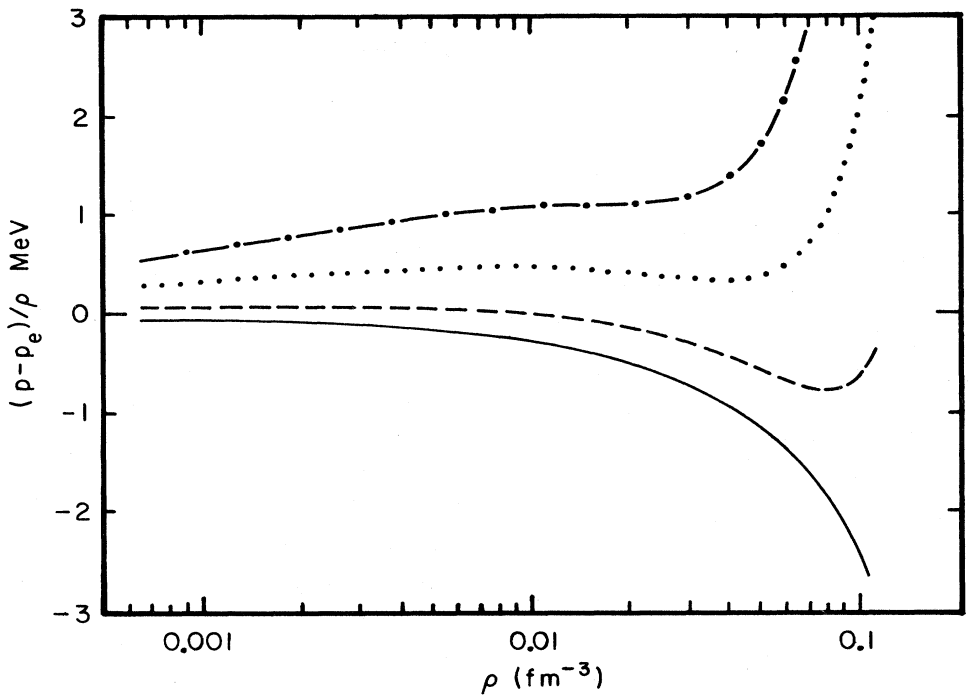

FIG. 7. The nuclear contribution to p/ρ, as a function of density (nucleons per fm^3), according to the theory of Cooperstein (1985): Solid curve, $S=0.5$; dashed curve $S=1$; dotted curve, $S=1.5$; dot-dashed curve, $S=2$. p_e is the pressure due to degenerate electrons. Note the small value of the nuclear pressure. The electrons give p_e/ρ about 20 at $\rho=0.1$.

and then uses uniform matter at higher ρ. This makes the transition exactly second order. At $u=1$ and $Y_e=0.3$,

$$\frac{P-P_{\rm lep}}{\rho}\approx -0.7\ \text{MeV}\ . \tag{3.30}$$

For $S=1$, the transition to uniform nuclear matter is at about $T=5$ MeV; hence from Eq. (3.29) we find $\theta=0.8$.

This last result indicates that, after the elimination of bubbles, the uniform nuclear matter does not have saturation density but is actually stretched to 80% of that density. This means that, at this point, the nuclear pressure is negative. According to Eq. (3.30), at the transition point the nuclear P/ρ is -0.7 MeV, which compares with a pressure in the degenerate electron gas of

$$P_{\rm lep}/\rho\sim 20\ \text{MeV}\ . \tag{3.31}$$

If the entropy is higher than 1, the nuclear pressure remains positive all the time. Collapsing supernovae have about $S=1$, but $S\sim 1.5$ near $u=1$.

Together with the nuclear pressure, shown in Fig. 7 as a function of density for different entropies, the adiabatic index behaves very smoothly. While it goes down to about 1.27 in the work of Lamb *et al.*, its minimum in Cooperstein's theory is 1.29 for $S=1$ or 2; for $S=1.5$ it is about 1.30. Table IV gives the variation of various important quantities for $\rho=0.001-0.1$ nucleon per fm^3 corresponding to $1.7\times10^{12}-1.7\times10^{14}$ g cm^{-3}.

The most important quantity for supernova collapse is P/ρ. It is remarkable that, after all the effort to construct a nuclear equation of state, the nuclear contribution to P/ρ is very small compared to that of the degenerate electrons; this ensures the smoothness of P vs ρ. The fraction of nuclear material in the gas phase, $1-X_H$, is small and actually decreases with increasing density, from 15 to 2 %—somewhat against intuition. The density of the nuclei, ρ_0, varies appreciably, from 0.157 to 0.127 fm^{-3}, which shows that one could not obtain a valid EOS by assuming the nuclei to be incompressible. The temperature, at constant $S=1$, rises substantially with density, from $T=1$ to 6 MeV; T is important for electron capture (see Sec. II.D).

TABLE IV. Physical quantities as functions of density, for entropy $S=1$ and $Y_e=0.3$. From Cooperstein (1985).

ρ (fm^{-3})	Γ	$\frac{P-P_e}{\rho}$ (MeV)	ρ_0 (fm^{-3})	T (MeV)	$1-X_H$
0.001	1.332	0.1	0.157	1.3	0.13
0.003	1.327	0.1	0.154	1.7	0.13
0.01	1.311	0.0	0.149	2.6	0.12
0.03	1.293	−0.3	0.140[a]	3.7	0.07
0.1	1.46	−0.6[a]	0.141	6.2	0.01

[a]Minimum values.

IV. EQUATION OF STATE AT DENSITIES ABOVE NUCLEAR

A. Theories before 1982

Obtaining an equation of state above nuclear density is far more difficult and controversial than at lower density. There are essentially no experimental data; heavy-ion collisions, on which many hopes were pinned, turned out to be irrelevant because the temperature in these is much higher than in supernovae (see Sec. IV.F). Therefore we are completely dependent on theory.

Bethe and Johnson (1974) calculated neutron matter at high density assuming the Reid potential (1968) to act between nucleons, with certain modifications dictated by physical considerations. They used an early, and rather simple, version of Pandharipande's hypernetted chain (HNC) method. They paid special attention to the appearance of hyperons (Λ, Σ, and Δ) in the neutron matter, and they found large concentrations of Σ^- and Δ^-, which serve to compensate the charge of protons that are also mixed with the neutrons. In this way, the concentration of electrons is minimized, which reduces the total energy at high density because the Fermi kinetic energy is particularly high for the (essentially massless) electrons. Bethe and Johnson treated the baryons nonrelativistically; Pandharipande (1973) used relativity and found fewer hyperons.

Bethe and Johnson used five different models of the interaction, model I being closest to the original Reid interaction and being stiffest, i.e., having the highest pressure for given density, which asymptotically (for large ρ) behaves as

$$p = 364\rho^{2.54}\ \text{MeV/fm}^3\ , \tag{4.1}$$

where the density is in units of nucleons per fm^3. The energy (excluding rest mass) per baryon is

$$E = 236\rho^{1.54}\ \text{MeV}\ . \tag{4.1a}$$

Normal nuclear density is 0.16 nucleons/fm^3. Model V is somewhat softer, especially when hyperons are included.

Table V gives the pressure as a function of density for model I and for model V with hyperons (H) and with neutrons only (N). It is seen that the pressure is much reduced when hyperons are included. Pressure is given in MeV fm^{-3},

$$1\ \text{MeV fm}^{-3} = 1.6\times10^{33}\ \text{dyne/cm}^2\ . \tag{4.2}$$

Friedman and Pandharipande (1981) carried out the most elaborate calculation of this type. They took a very sophisticated interaction between two nucleons, consisting of 14 terms of different dependence on spin, including tensor and spin-orbit interaction, all of them adjusted to give correct scattering phase shifts for the two-nucleon problem. They added a three-body interaction chosen to give correct properties for nuclear matter near normal density. Then they used a variational method to calculate energies, pressures, etc., and added to this the three-body interaction for which they assumed a special dependence on density.

TABLE V. Energy per baryon, in MeV, vs density (in baryons per fm^3).

Density	Model I H	V H^*	V N^*
0.5	89	64	64
1.0	245	185	191
2.4	680	480	570
4	1900	1200	1650
10	7100	4000	6000

*N=only nucleons considered; H=all types of hyperons included.

Friedman and Pandharipande obtained results for symmetric nuclear matter (equal numbers of neutrons and protons) and for pure neutron matter, as functions of density as well as of temperature (the latter from 0 to 20 MeV). At any given density and temperature, they found lower pressure and sound velocity than did Lamb *et al.* (1981), which might be expected because Lamb *et al.* used a Skyrme force that was too stiff. Even for Friedman and Pandharipande, the sound velocity a becomes greater than the velocity of light, going up to $1.3c$, at very high densities. But for neutron stars of the commonly observed mass, 1.4 $M_\odot$, a never exceeds c. The density at the center of such a star is 1.3×10^{15} g cm$^{-3}\simeq5\rho_0$, and the radius is 10.3 km, close to the (not very accurate) observation.

The compression modulus of symmetric nuclear matter,

$$K_{\text{th}} = 9\left[\frac{dp}{d\rho}\right]_{\rho_0}\ , \tag{4.3}$$

is calculated to be

$$K_{\text{th}} \simeq 240\ \text{MeV}\ , \tag{4.4}$$

somewhat larger than the observed value of Blaizot *et al.* (1976),

$$K_{\text{exp}} = 210\pm30\ \text{MeV}\ ; \tag{4.5}$$

see Sec. IV.D.

B. The formula of Baron, Cooperstein, and Kahana

Baron, Cooperstein, and Kahana (1985a, 1985b) have introduced a schematic formula for the equation of state of nuclear matter at high density, viz.,

$$p = \frac{K_0\rho_0}{9\gamma}[(\rho/\rho_0)^\gamma - 1]\ , \tag{4.6}$$

where K_0 is the compression modulus that will be discussed in Sec. IV.C, ρ_0 is the normal density of nuclear matter, and γ is a parameter. This formula is very convenient for computation of supernova behavior.

The formula does not have any theoretical basis, but it

represents the qualitative features of any reasonable theory; the pressure increases more than linearly with density at high density and is zero at $\rho=\rho_0$. The compression modulus K_0 should be determined from the properties of nuclear matter, but the exponent γ can only be estimated from theory. The coefficient 9 in the denominator of Eq. (4.6) is needed to conform with the standard definition of K_0, Eq. (4.3).

For detailed computation, K_0 and ρ_0 are assumed to depend on $x=Z/A$; specifically,

$$\rho_0(x)=0.16[1-0.75(1-2x)^2]\ \text{fm}^{-3}\ , \tag{4.7}$$

$$K_0(x)=K_{0,0}[1-2(1-2x)^2]\ , \tag{4.8}$$

where $K_{0,0}$ is the value for symmetric nuclear matter. Both expressions are suggested by theoretical considerations and hold only for small values of $1-2x$, i.e., for matter nearly symmetrical in neutrons and protons.

Equation (4.6) holds only for $\rho>\rho_0$; for lower density, see Eq. (3.14). The energy of compression is obtained by integration:

$$E(u)=\frac{K_0}{9\gamma(\gamma-1)}[u^{\gamma-1}+(\gamma-1)u^{-1}-\gamma]\ , \tag{4.9}$$

where $u=\rho/\rho_0$ and $E=0$ for $u=1$. Both Eqs. (4.6) and (4.9) hold for "cold" nuclear matter, at temperature $T=0$.

At nonzero temperature, one has to add to Eq. (4.6) the thermal pressure,

$$P_{\text{therm}}=\frac{\pi^2T^2}{6\varepsilon_f}\frac{m^*}{m}\rho u^{-2/3}\ , \tag{4.10}$$

where $\varepsilon_f=34$ MeV is the Fermi energy at saturation, and m^* is an effective mass of the nucleon for which usually the Brueckner theory value is taken, $m^*/m=0.7$.

C. The compression modulus K_0

The compression modulus of symmetrical nuclear matter was determined by Blaizot, Gogny, and Grammaticos (1976; Blaizot, 1980) from the energy of the breathing mode of doubly magic nuclei. This had been measured by Marty *et al.* for ^{40}Ca, ^{50}Zr, and ^{208}Pb (as quoted by Blaizot *et al.*, 1976). Blaizot *et al.* extrapolated these results, using a theory of nuclear matter by Gogny (1975). For example, for Pb, the compression modulus for infinite nuclear matter contributes 228 MeV, and the surface correction -53 MeV. The result of Blaizot *et al.* is

$$K_0=210\pm30\ \text{MeV}\ . \tag{4.11}$$

This standard value has been widely used.

However, G. E. Brown, in a number of papers (e.g., 1988a, 1988b, 1988c), has given strong reasons for lower value of K_0. Generally, his arguments are based on the Fermi-liquid theory introduced by Landau (1956–1958) and Migdal (1967); see also Brown (1971). Landau pointed out that interactions in liquids (and nuclei) are very complicated, but have one simplifying feature: quasiparticles move only on the surface of the Fermi sphere. Therefore it is reasonable to write the basic interaction between two quasiparticles as a function of only one variable, the scattering angle in mometum space. In nuclear matter, the interaction is

$$\mathcal{F}=F+G\boldsymbol{\sigma}_1\cdot\boldsymbol{\sigma}_2+F'\boldsymbol{\tau}_1\cdot\boldsymbol{\tau}_2+G'\boldsymbol{\sigma}_1\cdot\boldsymbol{\sigma}_2\boldsymbol{\tau}_1\cdot\boldsymbol{\tau}_2\ , \tag{4.12}$$

where F, G, F', and G' are functions of the Landau scattering angle θ_L. These are now expanded in Legendre polynomials, and it is expected (and in some cases verified by explicit calculations) that the expansion coefficients F_l, etc. for $l>2$ are small. For $l=0$ and 1, they are related to important parameters in the theory, viz.,

$$m_n^*/m_n=1+\tfrac{1}{3}F_1\ , \tag{4.13}$$

$$K_0=3(k_f^2/m_n^*)(1+F_0)\ , \tag{4.14}$$

where m_n^* is the effective mass of the nucleon in nuclear matter, m_n the mass of a free nucleon, and k_f the Fermi momentum.

There are two sum rules between the F_l, due to the antisymmetry of the overall wave function. The useful one in our context is (Friman and Dhar, 1979)

$$\sum\frac{F_l}{1+F_l/(2l+1)}=-3\sum\frac{G_l'}{1+G_l'/(2l+1)}+\delta_t\ , \tag{4.15}$$

where δ_t is a small correction for tensor forces which Brown (1988b) takes to be

$$\delta_t=0.1\ . \tag{4.16}$$

Brown now neglects all terms with $l\geq2$. F_1 can be obtained from the fact that, for nuclear matter,

$$m_n^*/m_n=1\pm0.1\ , \tag{4.17}$$

hence from (4.13), $F_1\sim0$. The G' comes entirely from forces of very short range, hence even G_1' should be small. Thus the sum rule (4.15) becomes simply

$$\frac{F_0}{1+F_0}=-3\frac{G_0'}{1+G_0'}+\delta_t\ . \tag{4.18}$$

G_0' can be determined from the position of the giant Gamow-Teller resonance (Brown and Rho, 1981), giving

$$G_0'=1.6\ . \tag{4.19}$$

Inserting this, and $\delta_t=0.1$, into Eq. (4.18) gives

$$F_0=-0.64 \tag{4.20}$$

and, from Eq. (4.14),

$$K_0=84\ \text{MeV}\ . \tag{4.21}$$

This compression modulus, obtained by Brown and

Osnes (1985), is "startlingly low, perhaps unbelievably low," according to Brown (1988b). How can it be reconciled with the "empirical" value, Eq. (4.11)?

The reason, according to Brown (1988b), is the difference between nuclear matter and doubly magic nuclei. He argues first that F_0 should be essentially the same for both cases, and he shows that for nuclear matter it is nearly independent of the energy of the nucleon.

On the other hand, for a doubly magic nucleus like ^{208}Pb, the effective mass is different from that in nuclear matter and is in fact strongly energy dependent. The effective mass is given by

$$\frac{m_n^*}{m_n}=\frac{1-\mathrm{Re}(\partial\Sigma/\partial\omega)}{1+\mathrm{Re}(\partial\Sigma/\partial T_k)}\ , \tag{4.22}$$

where Σ is the self-energy and ω the energy of the quasiparticle; T_k is its kinetic energy. The real part of Σ can be obtained from the imaginary part by using the dispersion integral

$$\mathrm{Re}\Sigma(\omega)=\int_{-\infty}^{\infty}\frac{\mathrm{Im}\Sigma(\omega')}{\omega-\omega'}d\omega'\ . \tag{4.23}$$

In nuclear matter, $\mathrm{Im}\Sigma$ is a smooth function of the energy ω, and $\mathrm{Re}(\partial\Sigma/\partial\omega)$ is then also a smooth function.

In a doubly magic nucleus, on the other hand, there are gaps in the energy spectrum (the Fermi energy lies in the middle of such a gap). Therefore $\mathrm{Im}\Sigma(\omega)$ fluctuates. Mahaux and Sartor (1987) have calculated Σ for the center of the ^{208}Pb nucleus; their results have been represented by Brown (1988b) by

$$-\mathrm{Re}\frac{\partial\Sigma}{\partial\omega}=0.32\sin\frac{m\omega}{20\ \mathrm{MeV}}\ . \tag{4.24}$$

The effective nucleon mass m^*/m fluctuates with energy ω by about 30%.

This is compatible with Gogny's result that $m^*/m=0.67$ at the monopole resonance in ^{208}Pb, while it is about 1 for nuclear matter. Recalling that F_0 should be about the same for both cases, and using Eq. (4.14), we conclude that K_0 for nuclear matter should be about $\frac{2}{3}$ of the result of Eq. (4.11) from the Pb monopole, thus

$$K_0=140\pm20\ \mathrm{MeV}\ . \tag{4.25}$$

Brown points out that the central value, 140 MeV, would still be difficult to reconcile with the Landau sum rule, Eq. (4.18), and therefore he favors the lower limit of Eq. (4.25), $K_0=120$ MeV. Pines *et al.* (1988) have carried out a comprehensive calculation using the polarization potential approach. If F_1 is assumed known ($=0$), and F_0 is determined from the sum rule (4.18), the Pines calculation yields $K_0=120$ (see Brown, 1988b), so 120 MeV is a reasonable value to adopt. However, the very careful calculation by Friedman and Pandharipande, who used a very sophisticated interaction between nucleons, gives $K_0=240$ MeV, Eq. (4.4).

D. High-density equation of state[3]

At high densities, the nucleons become to some extent relativistic. Therefore Dirac theory should be used to treat the nuclear matter problem. This is also indicated by experiments on the scattering of nucleons by nuclei in the laboratory. It has been found that especially the polarization and the spin rotation parameter are much better described by a Dirac theory than by Schrödinger wave functions (see Wallace, 1987).

The relativistic interaction has been calculated in a mean-field approximation by Serot and Walecka (1985) and Celenza and Shakin (1986), and this program has been further evaluated by Horowitz and Serot (1987). A detailed Brueckner-Hartree-Fock calculation with relativity has been performed by ter Haar and Malfliet (1986a, 1986b) and by Machleidt, Holinde, and Elster (1987). These authors find results rather similar to those of Horowitz and Serot (1987), i.e., the detailed Brueckner-Hartree-Fock calculation agrees quite well with the mean field. The resulting EOS is quite stiff, even stiffer than that of Friedman and Pandharipande (1981).

One disturbing result is the very small value of the effective mass of the nucleon, m^*/m. Horowitz and Serot found $m^*/m=0.5$, while ter Haar and Malfliet found $m^*/m=0.24$. It is very unlikely that the effective nucleon mass would become this small.

Ainsworth *et al.* (1987) use a simpler and more phenomenological approach. They start from the fact that the standard nonrelativistic Brueckner-Hartree-Fock calculations find the minimum of energy at about $2\rho_{nm}$, twice the observed density of nuclear matter. This has always been a problem with the Brueckner-Hartree-Fock calculations, but Ainsworth *et al.* have made a virtue out of it.

They first note that the energy per nucleon versus density with two-body forces can be well represented by a quadratic expression:

$$E_2=E_{nm}^{(2)}+\frac{K^{(2)}}{18}\left[\frac{\rho-2\rho_{nm}}{2\rho_{nm}}\right]^2\ . \tag{4.26}$$

The density scale here is $2\rho_{nm}$, so they hope to use this simple approximation up to $\rho\approx4\rho_{nm}$.

They then remark that the nonrelativistic two-body force calculation has to be corrected, both for relativity and for three-body forces. Relativity gives a repulsive correction

$$E_{\mathrm{rel}}=B\left[\frac{\rho}{\rho_{nm}}\right]^{8/3}\ . \tag{4.27}$$

Various explicit calculations give

$$1.6<B<3.6\ \mathrm{MeV}\ . \tag{4.28}$$

The correction in Eq. (4.27) is very strongly dependent

[3]A more thorough treatment is given by Brown (1988a).

on density. It therefore shifts the minimum energy to a smaller density. With a reasonable value of B of about 4 MeV, the minimum is shifted to approximately ρ_{nm}.

Three-body forces arise from various sources. They are not strongly dependent on density and therefore do not shift the saturation density appreciably. The simplest type of three-body force, involving the Δ isobar, gives an attractive contribution

$$E_3 \approx -2(\rho/\rho_{nm})^{1/4} \text{ MeV} . \tag{4.29}$$

This contribution is needed to bring about sufficient binding energy at the equilibrium density. A detailed discussion of these three-body and other corrections is given by Jackson, Rho, and Krotschek (1985).

These authors, as well as Ainsworth *et al.*, find that there are very big correction terms from higher-order diagrams. The diagrams involving nucleon loops give a strong repulsive contribution, which could be as large as +100 MeV. On the other hand, diagrams involving meson loops give attraction of about equal magnitude. Jackson *et al.* (1985) calculate the ratio of these two and find that with suitable choice of the scalar-meson mass this ratio can be 1 ± 0.05. In other words, these corrections nearly cancel. Using these three components of the energy, Ainsworth *et al.* (1987) construct an EOS for densities up to $6\rho_{mn}$. This is presented in Fig. 8. They choose $B=4.4$ MeV and the coefficient in Eq. (4.29) to be -3.9 MeV. The basic energy is the two-body interaction E_2. The relativistic correction rises rapidly near ρ_{nm}, but then saturates at about +20 MeV. The three-body forces also saturate, at about -3 MeV. The total energy does not become very large, i.e., the equation of state is rather soft.

To make these complicated corrections manageable,

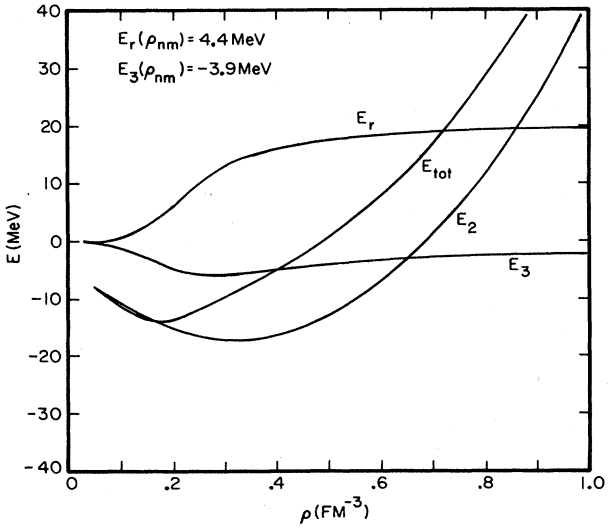

FIG. 8. Various contributions to the energy per nucleon, as functions of density, according to Ainsworth *et al.* (1987). E_2 is the energy due to two-body interactions, E_r the relativistic correction, E_3 the correction due to three-body interactions, and E_{tot} the sum of these.

Brown (1988b) goes back to the constituent quark model. The scalar σ meson that provides the main attraction between nucleons consists of a quark and an antiquark, with little interaction between them. Hence its mass should be close to twice the mass of a constituent quark,

$$m_\sigma^* = 2m_q^* , \tag{4.30}$$

where the star indicates that the masses are to be taken in a medium that contains many nucleons. The nucleon consists of three quarks,

$$m_n^* = 3m_q^* , \tag{4.31}$$

hence

$$m_\sigma^* = (2/3)m_n^* . \tag{4.32}$$

In any theory considered here, the nucleon mass is a decreasing function of the density of matter. The salient point of the Brown theory is that m_σ^* decreases the same way as m_n^*. Decreasing m_σ^* means increasing the range of the attractive force, thus increasing the effective attraction at higher density; this leads to a soft interaction.

The mass of the ρ meson can be expected to scale the same way as m_σ because the ρ meson also consists of a quark and an antiquark. For the ω meson which gives the main repulsion between nucleons, scaling is not so obvious, but it is reasonable to assume it here as well, because QCD has only one scaling parameter, Λ. All interactions then scale as

$$\lambda(\rho) = \frac{m_\sigma^*}{m_\sigma} . \tag{4.33}$$

The distances scale as $1/m_\sigma^*$, and the kinetic energy of the nucleons similarly. It is then easy to see that the entire many-body Hamiltonian H may be written as

$$H(\rho, r) = \lambda(\rho) H_{\text{vac}}(\lambda r) , \tag{4.34}$$

where H_{vac} is the Hamiltonian at zero matter density. The energy can then be calculated taking the vacuum masses for all particles, nucleons as well as mesons, and must then be scaled down by the factor $\lambda(\rho) < 1$.

This makes calculation easy, but it causes serious trouble with saturation: we are back at the simple equation (4.26), which saturates at the wrong density. Worse, Eq. (4.26) will be multiplied by $\lambda(\rho)$, which shifts the energy minimum (slightly) to still higher ρ, so the main problem is to find a new saturation mechanism.

To do this, Brown (1988b) starts from one of the important diagrams producing saturation in the older theory of Ainsworth *et al.* (1987); it is shown in Fig. 9(a). This diagram, which may be considered as a (positive) correction to the mass of the σ meson, is compensated in the new theory by other diagrams that give a net decrease of m_σ^*. However, there is a radiative correction to Fig. 9(a), which is shown in Fig. 9(b), and this is not included in m_σ^*. It has a magnitude and density dependence similar to that of Fig. 9(a). This diagram was invoked earlier by Lee and Margulies (1975) to prevent

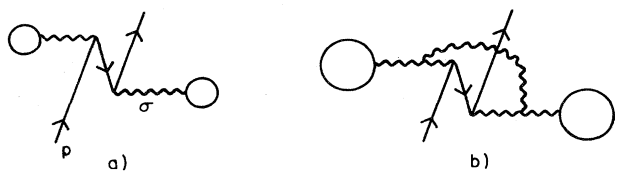

FIG. 9. (a) Interaction making and annihilating a nucleon pair from theory of Ainsworth *et al.* (1987); (b) a radiative correction to (a) by Brown (1988b).

$(m_\sigma^*)^2$ from becoming negative in calculations.

The diagram 9(b) probably will not give enough saturation. It has to be supplemented by higher-order diagrams. These tend to screen out the repulsion at higher density, as is usual for repulsive interactions; the total contribution goes as

$$\Delta U_\sigma \simeq \log\rho \tag{4.35}$$

at high density.

A Dirac-Brueckner-Hartree-Fock calculation has been carried out by Brown *et al.* (1990), using the scalar law (4.34) and adding only the lowest-order saturation term, Fig. 9(b). The energy has its minimum at a Fermi momentum of 1.47 fm^{-1} ($\rho=0.21$ fm^{-3}), somewhat too high, and energy -13 MeV, i.e., not enough binding. The interaction is rather hard, much harder than Sec. IV.C indicates.

Clearly, a calculation with a more complete ΔU_σ will be needed. Some indication of what it should be like is given in the paper by Ainsworth *et al.* (1988). The sum of the loops like Fig. 9(b) levels off at high density, as in Eq. (4.35). For $\rho > 6\rho_0$, the two-body mean field dominates, and this in turn consists mainly of the repulsion due to ω-meson exchange. This would imply a rapid rise of pressure above $\rho=4\rho_0$, which later tails off to $p\sim\rho^2$, i.e., $\gamma=2$. If this picture is confirmed by more detailed calculations, the theory of supernova explosions would involve a rather different regime from that of neutron stars: In the supernova the EOS would be rather soft, since densities up to about $4\rho_0$ are involved; in the neutron star the densities may be $6-7\rho_0$, and the EOS much stiffer.

Brown points out (1988c; see also Ainsworth *et al.*, 1988) that the decrease of m_σ^* with particle density follows from the chiral σ model first introduced by Lee and Wick (1974). The mass m_σ^* should go to zero, or to a small value of the order of the pion mass m_π, when the nucleon-meson gas goes over into a quark-gluon gas, i.e., when chiral symmetry is restored (it is broken in normal nuclear matter). This probably happens at a density of about $10\,\rho_0$. At the same density, according to Eq. (4.32), the nucleon mass should also vanish.

The effective mass m_n^* should be used not only for nucleons but also for antinucleons, i.e., negative-energy nucleons, whenever they appear in a diagram such as Fig. 9. Diagrams containing nucleon lines of negative energy are called "nucleon loop terms."

The density dependence of the effective mass of the nucleon has been obtained by explicit calculations and may be represented by

$$\frac{m_n^*}{m_n}=\frac{1}{1+\beta\rho/\rho_0}\ . \tag{4.36}$$

To find β, we use the determination of Mahaux *et al.* (Johnson, Horen, and Mahaux, 1987) of m_n^*/m_n at the center of the Pb nucleons; this gives

$$\beta=0.18\pm0.004\ . \tag{4.37}$$

E. Heavy-ion collisions[4]

Many experiments have been performed on the collisions of heavy nuclei at high energy, with the hope of obtaining an equation of state at high density. Stock *et al.* (1982) observed collisions of ^{40}Ar with KCl at energies from 0.36 to 1.8 GeV/nucleon at the Bevalac, and used the production of pions as a measure of compression; these experiments were continued by Harris *et al.* (1985). However, Brown and Siemens (1987) showed that pions equilibrate with nucleons down to a density of about $\frac{1}{2}\rho_0$ because of the Δ resonance and are therefore not a good measure of compression.

Renfordt *et al.* (1984) used the deflection angle for intermediate impact parameters to indicate the pressure produced in the collision of ^{40}Ar at 0.772 GeV/nucleon with Pb. This "sideways flow" was analyzed by Molitoris, Hahn, and Stöcker (1985a, Molitoris and Stöcker, 1985) in terms of the Nordheim method of statistical mechanics, commonly called the VUU method (for Vlasov, Uehling, and Uhlenbeck). The result is a very stiff equation of state, shown in Fig. 10, curve VUU. It is much stiffer than the EOS of Friedman and Pandharipande, curve FP, which was discussed in Sec. IV.A.

However, one has to take into account that the interaction depends strongly on the momentum (or energy) of the nucleon, not only on the density. To see this, we remember that in relativistic theory we must distinguish between a scalar and the fourth component of a four-vector. For instance, when we speak of density, we ordinarily mean

$$\rho=\bar\psi\gamma_4\psi\ , \tag{4.38}$$

which is the time component of a four-vector. It must be distinguished from the scalar density

$$\rho_s=\bar\psi\psi\ . \tag{4.39}$$

Similarly, we distinguish between the mean-field scalar potential $\bar U$ and the (fourth component of the) vector po-

[4]For a more detailed treatment, see Brown (1988a).

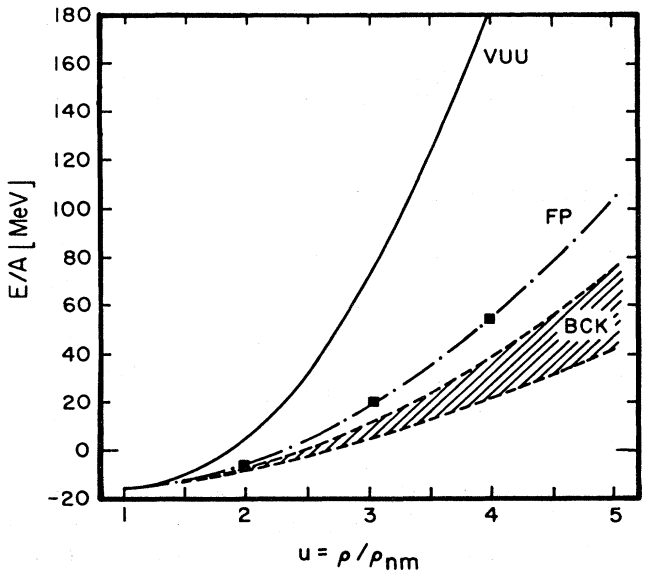

FIG. 10. Interaction energy per nucleon according to various theories. FP=Friedman and Pandharipande, heavy points on this due to Ainsworth *et al.* (1987); VUU due to Molitoris *et al.* (Molitoris, Hahn, and Stöcker, 1985; Molitoris, and Stöcker, 1985); BCK is the range of EOS used by Baron, Cooperstein, and Kahana, 1985a, 1985b.

tential $\bar{V}$. The scalar potential is caused by exchange of σ mesons and is attractive; the vector potential, mainly from exchange of ω mesons, is repulsive.

The mean-field equation involves the operator

$$(E-\bar{V}\rho)\gamma_0-\boldsymbol{\gamma}\cdot\mathbf{p}-m-\bar{U}\rho_s=0\ . \tag{4.40}$$

From this one finds

$$(E-\bar{V}\rho)^2-p^2=(m+\bar{U}\rho_s)^2\ . \tag{4.41}$$

We may define an effective potential energy by writing

$$E=m+p^2/2m+U \tag{4.42}$$

(see Jaminon *et al*, 1985; Serot and Walecka, 1985; Ainsworth *et al.*, 1988; Brown, 1988a). We find

$$U=\bar{V}\rho+\bar{U}\rho_s+\frac{(\bar{U}\rho_s)^2-(\bar{V}\rho)^2}{2m}+\frac{\bar{V}\rho}{m}(E-m)\ . \tag{4.43}$$

The last term in Eq. (4.43) contains the vector interaction V, which is purely repulsive. Therefore, even though $(E-m)/m$ may be rather small, this last term will be quite large, comparable with the sum of the first two terms where attraction and repulsion nearly cancel. Brown (1988a) has shown that the last term joins smoothly to the dependence of the optical potential on energy, which is well known from scattering of low-energy nucleons by nuclei. Gale *et al.* (1987) have used the momentum dependence (4.43) in heavy-ion collisions at 400 MeV/nucleon and have shown that it, together with a soft EOS, can explain the observed sideways flow, and that no stiff EOS is needed. Aichelin *et al.* (1987) have also used momentum dependence but have not reached quite so conclusive results.

A further reason for an apparent repulsion for high relative momentum is the decrease of ρ_s compared with ρ, in the second term of Eq. (4.43); we have

$$\rho_s=\frac{m^*}{E}\rho=\frac{m^*}{[p^2+(m^*)^2]^{1/2}}\rho\ . \tag{4.44}$$

Thus the first two terms in Eq. (4.43), which almost balance at low momentum, give a net repulsion at high momenta.

Finally, it should be remembered that the nucleons are slowed down when two heavy ions collide. This increases the sideway deflection; see Brown, 1988c. In that paper there are also many additional and illuminating arguments about heavy-ion collisions.

Summarizing, there are many effects causing a repulsive force at high energy. The experiments on heavy-ion collisions, therefore, do not give an indication of a strong repulsive force due to compression alone; they are quite compatible with the soft interactions used by Baron, Cooperstein, and Kahan (1985a, 1985b). In the supernova problem the temperatures are relatively low, of the order of 10 MeV, as are the relative momenta of the nucleons, so the "cold" equation of state should be used, with repulsion due only to compression.

F. Thermal effects

Above normal nuclear density, temperature gives only a small correction to the behavior of the nucleons, which form a strongly degenerate gas. Distinguishing between neutrons and protons, $i=1$ and 2, we find that the chemical potentials at $T=0$ are

$$\mu_i(0)=(h^2/2m_i^*)(3\pi^2 n_i)^{2/3}\ , \tag{4.45}$$

where n_i is the number of nucleons of each type per unit volume, usually different for neutrons and protons. The thermal energy of nucleons of type i, per total nucleon, is

$$E_{\mathrm{th},i}=\frac{\pi^2}{4}\frac{n_i}{n}\frac{T^2}{\mu_i(0)}\left[1-\frac{3\pi^2}{20}\frac{T^2}{\mu_i^2}(0)\right]\ , \tag{4.46}$$

with $n=n_1+n_2$ and total energy per nucleon $E=E_1+E_2$. The entropy per nucleon is

$$S=\frac{\pi^2}{2}\frac{T}{n}\sum_i\frac{n_i}{\mu_i(0)}\left[1-\frac{\pi^2}{10}\frac{T^2}{\mu_i^2(0)}\right]\ . \tag{4.47}$$

For lower density, Lattimer has given more general formulae; see Bethe (1988), Sec. 8.

V. THE PROMPT SHOCK

A. Overview

After implosion has compressed the inner core of the star to supernuclear densities, this inner core rebounds

and sends a shock wave out into the star. The hope is that this shock will go through the entire star and expel most of it, thus giving a supernova. The core will of course remain behind and will, in time, become a neutron star; the large negative gravitational energy of that neutron star provides the energy to expel the mantle and envelope against the gravitational attraction of the core, and to give the expelled material considerable kinetic energy. The major part of the released gravitational energy of the neutron star goes into the emission of neutrinos, and most of this emission occurs after the supernova material has been set in outward motion.

Unfortunately, the results of most of the computations do not conform to this appealing scenario. The shock wave always starts, but it rapidly loses energy because it has to dissociate the nuclei into nucleons, at the expense of 9 MeV per nucleon. The shock is therefore apt to stall at some point, typically at a radius of 400 km; it then turns into an accretion shock in which additional infalling matter accretes to the existing core; outward motion has then stopped, and the prompt shock has failed to expel the outer part of the star.

This trouble is aggravated by the emission of neutrinos: Once the shock slows down, there is time for copious neutrino emission, which further saps its energy. Thus a near failure is turned into a complete failure. (If the shock remains strong and fast, neutrino emission gives only a moderate correction to the supernova energy.)

Failure or success of the prompt shock depends primarily on the amount of material the shock has to traverse before it emerges from the Fe core. Thus we need a small Fe core to begin with, and the mass of the inner core which collapses homologously (see Sec. II.C) must be as large as possible. Once the shock is beyond the Fe core, it is likely to succeed (Sec. V.F). If the prompt shock suceeds, it gives, typically, explosion energies of the order of 1 foe$=10^{51}$ ergs ("foe" is derived from 10 to the *f*ifty-*o*ne *e*rgs), the observed energy SN 1987A.

If the shock turns into an accretion shock, this may be revived after about $\frac{1}{2}$ to 1 second by the neutrinos emitted from the hot neutron star. This mechanism, the delayed shock, will be discussed in Sec. VI. It is likely to be the correct explanation for SN 1987A, as well as for heavier stars.

In this section, we discuss the details of the prompt shock. It depends very sensitively on the presupernova evolution. If the mass of the Fe core is more than about 1.2 $M_\odot$, the chance of success of the prompt shock is very slim; at 1.1 $M_\odot$ it is good. The temperature at the beginning of SN collapse is also important. A low temperature of 0.3–0.4 MeV will favor the prompt shock because it will reduce electron capture during collapse and thus is likely to increase the mass of the homologous core. The scattering of neutrinos by electrons acts the opposite way. The use of general relativity rather than Newtonian gravitation is important. Most important is probably the use of a soft equation of state above nuclear density.

Convection apparently does not help the prompt shock; see Sec. V.K. The late-time development of the shock will be discussed in Sec. VI.

B. Formation of the shock

When the center of the star reaches and exceeds nuclear density, the material becomes very hard to compress any further. The pressure builds up, and the inward velocity must ultimately go to zero. A pressure wave will propagate outward. If the infall were to stop suddenly, the velocity would change by

$$\Delta u = -u_{\rm inf} \equiv u \ , \tag{5.1}$$

where $u_{\rm inf}$ is the infall velocity before stopping, and u is defined by Eq. (5.1). According to the usual laws of acoustics, this velocity change is associated with a pressure change,

$$\Delta p = \rho a \Delta u \ , \tag{5.2}$$

where ρ is the local density and a the local sound velocity. This change in pressure will lead to a change in density

$$\frac{\Delta\rho}{\rho} = \frac{u}{a} \ , \tag{5.3}$$

as long as the right-hand side is small compared with 1, which is the condition for the laws of acoustics to hold. The final Δp and $\Delta\rho$, in this case, are the same whether the change in velocity occurs suddenly or gradually.

As we have seen in Fig. 4, the infall velocity u is much smaller than a at small r, so here we get merely a mild pressure wave. This propagates outward, and as it does so, u/a increases. Finally, we get to the sonic point where $u=a$, and the acoustic approximation no longer holds: the mild pressure wave becomes a shock.

The formation of the shock is discussed in much greater detail by Cooperstein and Baron (1990), pp. 252–254. They give a modern version of our Fig. 4 in their Fig. 9.17. Their sonic point occurs at a mass of only 0.53 $M_\odot$ vs about 0.8, and their Mach number reaches about 2. Our Fig. 11 is taken from their paper. It shows how the infall (curves *a* and *b*) stops (curve *c*) by having the inner core come to rest while the outer parts are still falling in rapidly, which is followed by the formation of the shock (curve *d*). The figure is based on calculations by the authors which include general relativity; this enhances the infall velocities.

The shock forms not in the center of the star but at a considerable distance from it, near the surface of the homologous core, and in fact slightly outside it. This is absolutely essential for the further development of the shock, and it is for this reason that the mass of the homologous core is so important.

In a shock, the entropy increases. As long as the shock is weak, the entropy increase is

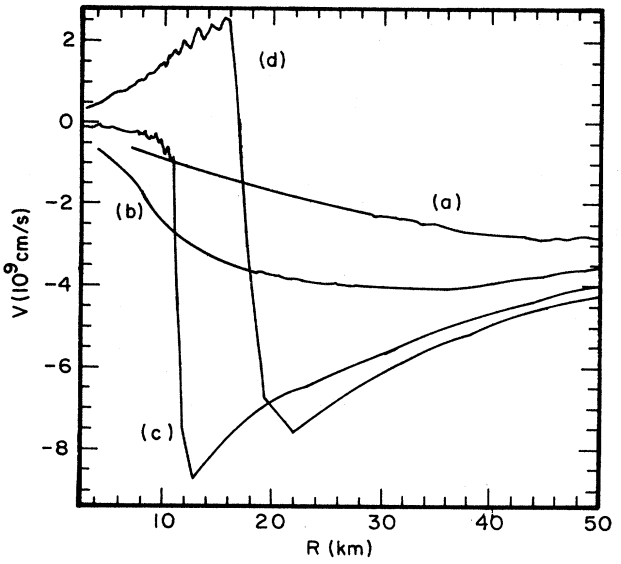

FIG. 11. Start of the shock, according to Cooperstein and Baron (1990). (a) Last time when velocity of infall is roughly proportional to radius; (b) nuclear density has been reached at center; (c) inner 10 km have been brought to rest; (d) shock has started.

$$\Delta S = \frac{\gamma(\gamma+1)}{12}\left[\frac{u}{a}\right]^3 , \tag{5.4}$$

where γ is the adiabatic index, roughly 4/3 where the shock is formed. Once the shock is started, the entropy quickly increases and soon reaches values between 6 and 12. (As will be recalled, we measure the entropy per nucleon in units of Boltzmann's constant.)

In all reasonable equations of state, nuclei dissociate into nucleons at entropy $S\sim 3$, so, behind the shock, the material is mostly nucleons. This dissociation, starting from nuclei near Fe, costs an energy of 8.8 MeV per nucleon, which gradually drains the energy of the shock, as was pointed out in 1981 by Arnett and by Hillebrandt.

C. Neutrinos in the shock

Several phenomena occur in the shock which do not occur in the infall.

We have already mentioned that, behind the shock, nuclei are dissociated into nucleons. Moreover, as the shock proceeds, the density decreases; it is roughly proportional to r^{-3} as in Eq. (2.14). We then have a dilute gas of neutrons and protons, with a compensating number of electrons. Because of the small charge of the proton, there is essentially no Coulomb effect. Because of the low density, nuclear forces are unimportant. Thus we have a very simple equation of state, an almost perfect gas, with the nucleons being nonrelativistic and the electrons relativistic. The difference in chemical potential, neglecting the mass difference between neutron and proton, is

$$\hat{\mu}=\mu_n-\mu_p=T\ln X_n/X_p , \tag{5.5}$$

where X_n is the fraction of neutrons, $X_p=1-X_n$ that of protons. Because of equilibrium,

$$\hat{\mu}=\mu_e . \tag{5.6}$$

Near the center, the temperature is very high, of the order of 10 MeV or more. In these conditions, electron pairs (which are plentiful already at lower temperature) transform rapidly into neutrino pairs,

$$e^+ + e^- \rightarrow \nu+\bar{\nu} . \tag{5.7}$$

The rate of energy transfer from electron to neutrino pairs has been calculated by Beaudet, Petrosian, and Salpeter (1967) and Dicus (1972), supplemented by Soyeur and Brown (1979), with the result

$$\Lambda = 1.06\times 10^{25} T^9 \times(1+0.19n)F(\mu_e/T)\ \text{ergs cm}^{-3}\,\text{s}^{-1} , \tag{5.8}$$

where F is a slowly variable function calculated by Bethe, Applegate, and Brown (1980) from the work of Dicus, as follows:

For $x=$	0	1	2	3
$F(x)=$	0.92	0.89	0.81	0.69,

(5.9)

where $x=\mu_e/T$. In Eq. (5.8), n is the number of types of neutrinos other than ν_e (which has now been determined to be $n=2$).

The most remarkable feature of Eq. (5.8) is the very strong temperature dependence, T^9. Therefore, during the infall, neutrino pair production is negligible, and during the shock phase it is only important in the inner part of the core, typically the inner solar mass or less. Another remarkable point is that Eq. (5.8) is independent of the density of matter, except for the slight dependence through μ_e; the neutrino production is just a certain rate per unit volume. The reason for this is that the density of electron pairs (at high temperature) also depends only on the temperature, not on the material density.

During pair production [Eq. (5.7)] neutrinos of all types, ν_e, ν_μ, and ν_τ, are produced—in each case a given flavor of neutrino together with its antineutrino. This is in contrast to electron capture by protons, free or inside nuclei, in which only electron neutrinos ν_e are produced; in positron capture by neutrons, which also occurs in the shock, only $\bar{\nu}_e$ are emitted. In the pair process (5.7) all types are produced, but ν_μ and ν_τ with less probability because they can only be produced by the neutral weak current, while the ν_e can also be created by the charged current. In Eq. (5.8), the Weinberg angle has been assumed to be

$$\sin^2\theta_W = 0.23 . \tag{5.10}$$

The production of neutrino pairs stops when the neutrino density has become high enough so that the inverse process to Eq. (5.7), $\nu+\bar{\nu}\rightarrow e^+ + e^-$, balances the direct

process. This occurs when the neutrinos have their thermal equilibrium density, which is, for each of the six species ($\nu_e, \bar{\nu}_e$, etc.),

$$W_\nu^o = 0.60 \times 10^{26} T^4 \text{ ergs cm}^{-3} . \tag{5.11}$$

The time for "filling" the $\nu_e, \bar{\nu}_e$ Fermi spheres is thus

$$\tau_{fe} = \frac{2W_\nu^o}{\Lambda_e} = 13 T^{-5} \text{ sec} . \tag{5.12}$$

At the typical temperature $T = 10$ MeV, this is only 0.13 milliseconds, short even on a supernova time scale. For the ν_μ neutrinos,

$$\tau_{f\mu} = 70 T^{-5} \text{ sec} . \tag{5.13}$$

(We use ν_μ for all the species $\nu_\mu, \bar{\nu}_\mu, \nu_\tau, \bar{\nu}_\tau$, since they all behave alike.)

Equation (5.11) assumes $\mu_\nu = 0$, i.e., full thermal equilibrium; in this case, $\mu(\bar{\nu}) = -\mu(\nu)$, and therefore both must be zero. In actual numerical computations by Baron and Cooperstein (1990), the ν_μ (including $\bar{\nu}_\mu, \nu_\tau, \bar{\nu}_\tau$) never reach full thermal equilibrium and can therefore be described by a negative $\mu(\nu)$; their density is less than W_ν^o in Eq. (5.11).

When neutrinos are observed on earth, only $\bar{\nu}_e$ (and ν_e) can be easily detected. The emission of ν_μ and ν_τ is therefore a total loss; see, however, Sec. IX.D.

At high material density, neutrinos continue to be trapped. But as the shock proceeds, the density at its front decreases and finally becomes less than the trapping density. At this point, neutrinos will be released, first those close behind the shock, then those from farther inside as they are able to make their way by diffusion. At this stage, the theory of Cooperstein *et al.* becomes appropriate, which was discussed in Sec. II.G: the neutrinos have a temperature that (at least for $\nu_e, \bar{\nu}_e$) is now close to the matter temperature, and the chemical potential is also in equilibrium,

$$\mu_\nu = \mu_e - \hat{\mu} . \tag{5.14}$$

As the shock proceeds further, neutrino emission occurs far behind the shock. A "neutrino sphere" is formed, from which the neutrinos stream out freely, although they may on the average have one collision outside [see Eqs. (2.36) and (2.40)].

Rather simple results may be derived for the conditions at the neutrino sphere if we assume the total outward flux of neutrinos to be given. A typical number for this is

$$F = 3 \times 10^{52} \text{ ergs/s} \tag{5.15}$$

for each species of neutrino, within a factor of about two. The flux is given by

$$F = \pi c R^2 \times 0.60 \times 10^{26} T^4 = 5.6 \times 10^{48} R_6^2 T^4 , \tag{5.16}$$

so

$$R_6 T^2 \sim 50\text{–}100 . \tag{5.17}$$

The neutrino sphere is defined by

$$\int \alpha \, dr = 2/3 , \tag{5.18}$$

where α is the number of collisions per cm. For ν_e and $\bar{\nu}_e$, the most important collisions are captures by nucleons,

$$\begin{aligned} \nu_e + n &\rightarrow p + e^- , \\ \bar{\nu}_e + p &\rightarrow n + e^+ . \end{aligned} \tag{5.19}$$

Neutrons are more abundant than protons, but for simplicity we shall assume that each is one-half the total number of nucleons. Then

$$\alpha = \tfrac{1}{2} N_A \rho \sigma_c = 3 \times 10^{33} \rho_{10} \times 9 \times 10^{-44} \varepsilon^2 , \tag{5.20}$$

where N_A is Avogadro's number. We shall assume[5]

$$\langle \varepsilon^2 \rangle = 6T^2 . \tag{5.21}$$

Then

$$\int \alpha \, dr = 16 \times 10^{-10} T^2 \int_R^\infty \rho_{10} dr . \tag{5.22}$$

Assuming the density distribution Hr^{-3}, as in Eq. (2.14), we get

$$8 \times 10^{-10} T^2 \rho_{10}(R) R = 2/3 \tag{5.23}$$

$$\rho_{10} R_6 T^2 = 800 . \tag{5.24}$$

Inserting Eq. (5.17), we have

$$\rho_{11}(R) = 0.8\text{–}1.6 . \tag{5.25}$$

Thus the *density* at the neutrino sphere is fairly well determined.

If we assume the density distribution (2.14), the constant H is about 10^{31} when the neutrino sphere is first formed, and goes down to about 10^{30} in half a second. Accordingly,

$$R \sim 50 \text{ km early} \quad \sim 20 \text{ km late} . \tag{5.26}$$

The flux tends to decrease, so in Eq.(5.17) $R_6 T^2 \sim 100$ is apt to be correct early, 50 late, and T is likely to be fairly

[5]Because we are interested in the number of neutrinos *emitted,* we think it is reasonable to average the mean free path $\lambda \sim \varepsilon^{-2}$ over the neutrino distribution. Neglecting the difference between Fermi and Boltzmann statistics, and remembering that we are interested in the neutrino energy rather than their number, we have

$$\langle \varepsilon^{-2} \rangle = \int \varepsilon \, d\varepsilon \, e^{-\varepsilon/T} \Big/ \int \varepsilon^3 d\varepsilon \, e^{-\varepsilon/T} = 1/(6T^2) .$$

constant at

$$T \simeq 5 \text{ MeV} . \tag{5.27}$$

We shall see in Sec. IX that this is in good agreement with observations.

If, instead of capture by nucleons, we assume scattering of the neutrinos, we should remember that there are no heavy nuclei outside the neutrino sphere, so scattering is done only by nucleons, and the scattering mean free path is

$$\lambda_s = \frac{10^8}{\rho_{12}\varepsilon^2} . \tag{5.28}$$

Going through an argument similar to that leading to Eq. (5.25), we find that the required $\rho(R)$ is about four times larger than Eq. (5.25),

$$\rho_{11}^s(R) \simeq 5 \pm 2 . \tag{5.29}$$

This is reasonable because here we are dealing with the neutral weak current, while in Eqs. (5.20)–(5.25) the charged weak current was involved.

The result of Eq. (5.29) is appropriate for μ and τ neutrinos and their antineutrons. Computer results indicate that the total outward flux for each of these types is similar to that of ν_e and $\bar{\nu}_e$, so that RT^2 is about the same (except at very early times when the flux of ν_μ is less). Hence the μ-type neutrinos emerge at a higher density and smaller R than the e-type. Their temperature is also apt to be higher, since RT^2 is about the same, by our assumption. These points have been emphasized by Burrows.

Electron neutrinos, ν_e and $\bar{\nu}_e$, are subject to both capture and scattering. On the other hand, their capture is somewhat reduced by blocking, since some electron states are already occupied. We therefore consider Eq. (5.25) a good approximation.

According to Eq. (5.20), higher-energy neutrinos have a larger capture coefficient α than lower-energy. Therefore the neutrino sphere is actually not the same for all energies, as we assumed in Eq. (5.25), but is at a larger radius for higher-energy neutrinos, and at a correspondingly lower temperature, a somewhat paradoxical result. Accordingly, the neutrino spectrum should fall off more steeply at high energy than a Maxwellian. There are indications of this in Wilson's and Bruenn's computer outputs. The observations on SN 1987A (see Sec. VIII) involved too few neutrinos to show this effect; a supernova in our own galaxy would be necessary.

Cooperstein and Baron (1990) discuss the effects of including all, or only some, types of neutrinos in numerical calculations. Including only ν_e gives a stronger shock than including all types. The ν_μ simply take energy away from the shock at an early stage. The electron antineutrino $\bar{\nu}_e$ permits the two processes (5.19) to occur alternately, resulting in an urca mechanism which continually saps the energy.

Capture of electrons by protons has an absorption coefficient similar to Eq. (5.20), except that (1) it should be divided by 2, because of statistical weights, (2) it should be multiplied by $2Y_p$ where Y_p is the fraction of protons in the medium behind the shock, and (3) ε should be the energy of the electrons to be captured, usually of the order of the chemical potential μ_e. Then the rate of capture is

$$\alpha_e c = 8\rho_{10} Y_p \varepsilon_e^2 \text{ sec}^{-1} . \tag{5.30}$$

The time available in the shock wave is usually a few milliseconds. Thus there is little capture at density 10^{10} and less, but substantial capture at $\rho = 10^{11}$. Accordingly, Y_e close behind the shock is likely to remain nearly the same as in the undisturbed material outside the shock, usually nearly 0.5, but farther behind the shock, where the density gets to 10^{11} or more, the electrons (and protons) may be greatly depleted. If the shock is slowed down, e.g., to a velocity of 10^9 or less, due to having lost energy to dissociation, electron capture will be severe.

D. Shock equations

At the shock front, there is a discontinuity described by the Hugoniot equations. Because the material outside the shock is in motion (inwards), these equations are slightly different from those usually quoted. We denote quantities outside the shock by the subscript 1, those behind (inside the shock) by subscript 2. The shock velocity (relative to the center of the star) is U, material velocities are u_1, and u_2, and $\varepsilon_1, \varepsilon_2$ are the internal energies. Then the Hugoniot equations are

$$\rho_1(U-u_1) = \rho_2(U-u_2) , \tag{5.31}$$

$$(U-u_1)^2 = \frac{\rho_2}{\rho_2-\rho_1}\frac{p_2-p_1}{\rho_1} , \tag{5.32}$$

$$(u_2-u_1)^2 = (p_2-p_1)\left[\frac{1}{\rho_1}-\frac{1}{\rho_2}\right] , \tag{5.33}$$

$$\varepsilon_2-\varepsilon_1 = \tfrac{1}{2}(p_2+p_1)\left[\frac{1}{\rho_1}-\frac{1}{\rho_2}\right] . \tag{5.34}$$

If the shock is strong, $p_2 \gg p_1$, as is the case in the supernova out to quite large radii ($R > 1000$ km), Eqs. (5.34) and (5.33) give

$$2(\varepsilon_2-\varepsilon_1) = (u_2-u_1)^2 . \tag{5.35}$$

If we set $\varepsilon_1 = 0$ and assume that behind the shock the material is a perfect gas, i.e.,

$$\varepsilon_2 = \beta p_2/\rho_2 , \tag{5.36}$$

the density ratio is

$$\frac{\rho_2}{\rho_1} = 2\beta+1 . \tag{5.37}$$

Equation (5.35) holds for any equation of state and is often useful for estimating the material velocity u_2 behind the shock.

Our ε is just the *internal* energy. It is often useful to consider the energy including the gravitational potential,

$$e_{\rm pm}=\varepsilon-GM_r/r\ , \tag{5.38}$$

where $e_{\rm pm}$ means "energy per unit mass" and M_r is the included mass. If $e_{\rm pm}>0$, and if there are no further pressure gradients acting on it, the mass element can escape from the gravitation of the star. In judging the success of the shock, it is useful to consider $e_{\rm pm}$. If all the material behind the shock has negative $e_{\rm pm}$, the shock has failed.

The material velocity u_2 applies only directly behind the shock. Further behind, the material usually slows down, both because of gravitational attraction and because the pressure is likely to be lower than at the shock itself. Therefore the kinetic energy, $\frac{1}{2}u^2$, generally is much lower than the internal ε. In many computations, the material settles down to very low velocity. In particular, the inner core (homologous core) quickly loses its "bounce," as was shown by Brown, Bethe, and Baym (1982).

In computer calculations, the shock is usually treated by the artificial viscosity method due to Richtmyer (see Richtmyer and Morton, 1957). A large viscous pressure is introduced proportional to the square of the velocity gradient $\partial u/\partial r$. This quickly dissipates the shock discontinuity into heat, usually in about three or four of the zones into which the material is divided in computer calculations. Since conservation laws hold, the Hugoniot equations (5.31)–(5.35) continue to be true to some distance from the shock. But it is difficult to determine the exact conditions at the shock itself because the shock is smeared out.

E. Computations

Quantitative results on the prompt shock can only be obtained from extensive computations. Dozens of computations have been carried out. The grand master of these computations is James Wilson of Livermore, who includes elaborate calculations of neutrino diffusion by considering some 16 energy groups of neutrinos, each comprising an interval of $\sqrt{2}$ in energy; see Bowers and Wilson, 1982b, Wilson, 1985 (later papers by Wilson deal mainly with the delayed shock; see Sec. VI). Other important computations were performed by Arnett (1983), Bruenn (1989), Hillebrandt (1982a, 1982b, 1984), and the Stony Brook group, Cooperstein, Bethe, and Brown (1984) and Baron and Cooperstein (1989, 1990). In nearly all these computations the shock got stuck and turned into an accretion shock between 100 and 200 km radius, corresponding to an included mass M_r between 1 and 1.2 $M_\odot$. On this basis it was concluded that the prompt shock will fail if the mass of the Fe core resulting from presupernova evolution is greater than about 1.25 $M_\odot$.

Success was obtained by Baron, Cooperstein, and Kahana (1985a, 1985b) when they assumed a softer nuclear equation of state above nuclear density and at the same time used general relativity. As we have discussed in Sec. IV.C, such a softer equation of state appears now quite likely. The Fe cores they used had masses of 1.2–1.25 $M_\odot$. Many further calculations have been carried out by Baron and Cooperstein (unpublished); in some of them the shock succeeded, in others it stalled at a fairly large radius like 500 km.

In these calculations Baron and Cooperstein did not include neutrino-electron scattering, which we discussed in Sec. II.F and which considerably decreases the mass of the homologous core, hence increasing the amount of Fe that must be dissociated. Bruenn (1989a, 1989b), who has studied neutrino-electron scattering in detail, has done an approximate calculation of its effect on the shock and found that the mass of the Fe core has to be reduced to about 1.1 $M_\odot$ before the prompt shock will succeed.

Baron and Cooperstein, in their latest calculation (1990), have also included neutrino-electron scattering, as well as the formation of μ-neutrino pairs, and find that the shock suffers greatly from both these effects. They have considered stars with a Chandrasekhar mass before collapse of 1.1 $M_\odot$, and with varying structures of Y_e and entropy. In their nine models, they obtained widely varying results: In some cases, the shock got stuck at a radius of about 300 km, including (surprisingly) a case with an iron-core mass of less than 1.0 $M_\odot$; the reason is not known. Three of the models led to success, in that the shock was still propagating at an enclosed mass of 1.2 $M_\odot$ and a radius of $\gtrsim 2000$ km. They are all characterized by very low precollapse entropy at the center, 0.5. The "best" of these, in which a soft equation of state was used above nuclear density, gives an energy release of 1.5 foe, in accord with the observation of SN 1987A (see Sec. VII).

Baron and Cooperstein, in this and earlier papers, emphasize the importance of the value of the nuclear symmetry energy $W_{\rm sym}$, for which they take 31.5 MeV, on the basis of the observed atomic weights in the region $A=50-80$. This value is in agreement with the value 250 MeV ($=8W_{\rm sym}$) in Eq. (3.1a). Higher $W_{\rm sym}$ suppresses electron capture, which is favorable for the shock but cannot be justified empirically.

For the electron capture during infall, Baron and Cooperstein considered only capture by free protons. This is greatly suppressed by the low temperature, which is the result of the low initial entropy. The capture by heavy nuclei has yet to be considered, and this will reduce the strength of the prompt shock, probably greatly. On the other hand, Baron and Cooperstein made conservative assumptions in some other respects.

F. Success or failure

As we mentioned earlier, the shock loses energy constantly by the dissociation of heavy nuclei (mainly Fe) into nucleons. This costs about 8.8 MeV per nucleon, equivalent to 1.7 foe (1 foe $=10^{51}$ ergs) for each one-tenth of a solar mass traversed. In addition, some energy is

TABLE VI. Mass of Fe core (units of $M_\odot$).

M(star)/$M_\odot$	12	15	18	25
Weaver and Woosley, 1978		1.6		
Weaver and Woosley, 1985	1.31	1.35		2.0
Nomoto, 1986	1.18	1.25		1.65
Woosley and Weaver, 1988			1.33	

lost by emission of neutrinos. The total energy initially in the shock is of the order of 10 foe, perhaps somewhat more in general relativity. It is, therefore, critically important how much matter the shock has to traverse before it comes to the surface of the iron core. This mass is:

$$M_{\rm sh} = \text{Mass of Fe core minus mass at which the shock starts .} \quad (5.39)$$

The latter quantity is about 0.7 $M_\odot$ in general relativity, but without considering neutrino-electron collisions; these may bring the mass down to 0.6 $M_\odot$.

Our estimate of the mass of the Fe core, calculated from the presupernova evolution of the star, has undergone many changes in the last 12 years, as shown in Table VI. It has generally decreased: In 1978 the core of a 15-$M_\odot$ star was calculated to be 1.6 $M_\odot$. In 1986 it had gone down to 1.25. As discussed in the previous paragraph, this change is favorable to the success of the prompt shock.

The change has come about by a combination of four causes:

(1) The nuclear reactions going from ^{16}O to Fe have been more carefully considered. In particular, the role of nuclei like Si^{29} and Si^{30}, i.e., nuclei that are not just multiples of the α particle, has been studied: they capture α particles more easily, and they are also more likely to undergo β decay and electron capture. In these latter processes, neutrinos are emitted, which decreases the entropy of the material.

(2) The Coulomb interaction between nuclei and electrons has been taken into account. This effect was first emphasized by Nomoto and is the reason why Nomoto's 1986 figures are lower than those of Woosley and Weaver (1986). The Woosley and Weaver 1988 figure includes this effect.

(3) Different assumptions have been made about certain convective processes in the star. (For instance, we have learned that certain types of convection must be suppressed in order that the progenitor of SN 1987A evolve back to the blue, after its red giant stage; see Sec. VII.D).

(4) The cross section for the reaction

$$^{12}\mathrm{C}+{}^{4}\mathrm{He}={}^{16}\mathrm{O}+\gamma \quad (5.40)$$

appears to be lower, according to recent experiments, than was assumed in 1978.

From our previous discussion and from Sec. V.H, it is clear that an Fe core of mass 1.6 or larger is hopeless for the prompt shock. It may explode by the delayed shock, see Sec. VI. So, according to the 1978 presupernova calculations, the prompt shock would be impossible. On the other hand, SN 1987A did explode; its mass is believed to have been 18 ± 2 $M_\odot$ (see Sec. VII).

The reported presupernova Fe core mass for an 18-$M_\odot$ star is 1.33 $M_\odot$, and for a 15-$M_\odot$ star 1.25 $M_\odot$. These are still too high for the most recent implosion-explosion calculation by Baron and Cooperstein (1990), reported in Sec. V.E, which require about 1.1 $M_\odot$.

Baron and Cooperstein point out that it is really not the Fe core mass that is significant, but rather the Chandrasekhar mass. They have shown a considerable dependence on the detailed distribution of Y_e and S versus enclosed mass in the presupernova star. In particular, they find for a given Chandrasekhar mass, of 1.1 $M_\odot$, a model with an especially low Fe core mass of 1.0 $M_\odot$ that will not explode by prompt shock; I believe that this paradoxical result is a freak, due to other assumptions.

G. General relativity

Most of the early computations (until 1984) were done with Newtonian gravitation. Apart from simplicity, this had the advantage that quantities like $e_{\rm pm}$, Eq. (5.38), could be defined, that there was a simple virial theorem (see Sec. V.I), and that generally the computer results could be understood in a qualitative manner.

Some of the early computations did use general relativity and found in some cases that the prompt shock was strengthened compared with Newtonian gravitation, while in other cases it was weakened.

This result was understood by Baron, Cooperstein, and Kahana (1985a), and the following discussion is quoted from their paper. "We find . . . that [in some respects] general relativistic corrections are harmful to the shock. This stems from two sources: (i) There is an increase in the energy expended for shock propagation, since the shock now moves against the stronger gravity of general relativity; (ii) more importantly, the critical adiabatic index for stability ($\Gamma_{\rm crit}$) is raised above its Newtonian value of $\frac{4}{3}$. Yahil (1985) has shown that the size of the homologous core, and hence the point where the shock forms are [sic] very sensitive to the difference, $\Gamma-\Gamma_{\rm crit}$. This is borne out in our calculations. In our Newtonian calculations the shock forms at a mass point of approximately 0.8 $M_\odot$ while in the general relativistic calculations this is moved in to about 0.7 $M_\odot$. (We define the point where the shock forms as the point where the entropy first reaches 2.7, the 50% nuclear-dissociation point.) Formation at a smaller mass point requires the shock to expend more energy before it reaches the edge of the iron core. [These two effects dominate if the EOS (equation of state) above nuclear density is stiff, e.g., if the compression modulus at nuclear density is $K_0=220$ MeV.]

"There is a threshold point, however, when the EOS is soft enough that the increased binding energy of the final

hydrostatic core (essentially the shock energy *modulo* neutrino losses) overcomes the above impediments to the success of the shock. Since gravity is stronger in the general relativistic formulation, a higher central density will be reached. When the EOS becomes soft enough the extra energy gained from 'digging deeper' into the gravitational well overcomes the other energy costs to the shock due to general relativity. Another effect of general relativity is that the central regions collapse faster than under Newtonian gravity. Thus, when the shock reaches the outer parts of the core, they have not collapsed as far and therefore are at lower density and have a smaller infall velocity; the outward shock propagation is eased."

We shall see in Sec. V.H that general relativity makes the prompt shock succeed in some cases where it fails for Newtonian gravitation. Aside from this most important effect of general relativity there are others. For instance, a neutrino emitted at radius r and emerging without collision will at infinity have a reduced energy, by a factor

$$\phi=(1-R_S/r)^{1/2}\ , \tag{5.41}$$

where R_S is the Schwarzschild radius

$$R_S=\frac{2GM}{c^2}\ . \tag{5.42}$$

This factor must be taken into account when neutrinos from the supernova are observed on earth. It also enters when neutrino absorption at some intermediate radius, like 100–200 km, revives a shock (see Sec. VI).

H. Results for soft equation of state

Baron, Cooperstein, and Kahana (1985a, 1985b) have carried out many computations using general relativity and a soft equation of state. They parametrize the EOS in the form

$$P_{\rm cold}=\frac{K_0\rho_0}{9\gamma}(u^\gamma-1)\ , \tag{5.43}$$

$$u=\rho/\rho_0\ . \tag{5.44}$$

They also assume that ρ_0 and K_0 depend on the proton fraction Y_p, which they assume to be 0.33. Table VII gives some of their results.

The first column of the table gives the mass of the star, in units of the solar mass. K_0 and γ are the assumed parameters in Eqs. (5.43) and (5.44). The next column states whether or not general relativity was used. The following gives the maximum compression attained. E is the total energy of explosion, and E_ν the energy of the emitted neutrinos, both in foes.

Without general relativity, no explosion is obtained (the 0.1 foe in the second line is not sufficient to expel the mantle and envelope of the star, which are bound with a gravitational energy of several tenths of a foe). With general relativity, both models for mass 12 explode. As might be expected, the softer EOS, $\gamma=2$, gives a larger explosion energy, 3 foe.

TABLE VII. Results of Baron, Cooperstein, and Kahana (1985a, 1985b) for soft equation of state.

$M/M_\odot$	K_0	γ	GR	$\rho_{\max}/\rho_0$	E	E_ν
12	220	2	No	1.7		2.6
12	140	2	No	2.3	0.1	3.2
12	140	2	Yes	12	3.2	2.2
12	140	3	Yes	3.1	0.8	3.3
15	140	3	Yes	3.1		2.5
15	140	2.5	Yes	4.1	1.7	3.4
15	120	3	Yes	3.3		3.0
15	90	3	Yes	4.0	0.8	3.2

For a star of mass 15, it is not enough to use general relativity; the EOS must also be quite soft. With $K_0=140$, a likely value, it must be assumed that $\gamma=2.5$, not 3; this is also quite likely (see Sec. IV.D). If $\gamma=3$ is assumed, K_0 must be as low as 90 MeV, which is rather unlikely. For $M=18\ M_\odot$ presumably an even softer EOS is needed; $K_0=140$ and $\gamma=2$ is not an unlikely combination from the considerations of Sec. IV.

Successful shocks generally involve large compressions at the center of the star. In one case in Table VII, the compression is as high as 12, but, according to Cooperstein (private communication), this is due to an extreme assumption about the symmetry energy; the correct value should be about 6 to 7. In most cases, the compression is by a factor of about four.

The energy lost in neutrinos is near 3 foe in all cases and does not seem to be closely correlated with the explosion energy E.

I. Net ram

Behind the shock wave, nuclear material quickly settles down to hydrostatic equilibrium (Brown, Bethe, and Baym, 1982). In such equilibrium, a gas sphere of $\gamma=4/3$ can have any radius whatever; if the radius is smaller, the gravitational potential is bigger, but this is compensated by higher pressure. We shall here estimate the energy of the star by a method introduced by Cooperstein, Bethe, and Brown (1984).

The material of a supernova that is at a density below nuclear gets its pressure mostly from relativistic electrons that have $\gamma_e=4/3$, but there are some deviations due to the nuclei, as described in Sec. III. The energy of this region of the star may be written

$$E_e=V_e+3W_e+\Delta_e\ , \tag{5.45}$$

where

$$V=-G\int\frac{M(r)}{r}dM\ , \tag{5.46}$$

$$W=\int(p/\rho)dM\ , \tag{5.47}$$

$$\Delta_e=\int_{R_i}^{R_o}(\varepsilon-3p/\rho)dM\ . \tag{5.48}$$

Here $M(r)$ is the mass included in the sphere r, the sub-

script e refers to the region in which electron pressure dominates, and R_i, R_o are the inner and outer radius of that region. Further, ε is the internal energy per unit mass. If the gas had exactly $\gamma=4/3$, then we would have $\varepsilon=3p/\rho$, Eq. (5.48) would be zero. This is the motivation for writing the energy in the form of Eq. (5.45). In reality, Δ_e is not zero, but small compared with V_e and W_e. The integrals V_e, W_e extend from R_i to R_o.

The inner core of the star is at or above nuclear density. We assume (arbitrarily) that it has a constant adiabatic index γ_N, i.e.,

$$p\sim\rho^{\gamma_n} \tag{5.49}$$

where p is the total pressure, due to electrons plus nucleons, and $\gamma_N>4/3$ (Cooperstein *et al.*, 1984, assumed that $\gamma_N=3$). The outer radius of this core is at R_i, and we may choose R_i such that there is no nuclear contribution to pressure at that point; then

$$\varepsilon_i=3p_i/\rho_i \ . \tag{5.50}$$

Then at higher density, the energy per unit mass is

$$\varepsilon(\rho)=\varepsilon_i+\int_{\rho_i}^{\rho}p\,d\rho/\rho^2 \ , \tag{5.51}$$

remembering that the material is on an adiabat. Using Eq. (5.49),

$$\varepsilon(p)=\frac{p/\rho}{\gamma_N-1}+\left[3-\frac{1}{\gamma_N-1}\right]\frac{p_i}{\rho_i} \ . \tag{5.52}$$

Then the total energy of the inner core, called the "dense pack" by Cooperstein *et al.* (1984), is

$$E_N=V_N+\int_0^{R_i}\varepsilon\,dM=V_N+\frac{W_N}{\gamma_N-1}+\left[3-\frac{1}{\gamma_N-1}\right]\frac{p_i}{\rho_i}M_N \ , \tag{5.53}$$

where M_N is the mass of the dense pack, while V_N and W_N are as defined in Eqs. (5.46) and (5.47) with the integrals extended over the dense pack. The total energy of the star up to radius R_o is then E_N+E_e.

We now derive the virial theorem. Because the entire material out to R_o is supposed to be at rest,

$$\frac{dp}{dr}=-\rho G\frac{M(r)}{r^2} \ . \tag{5.54}$$

We multiply both sides by r and integrate over the volume

$$4\pi\int r^3dr\,dp/dr=-G\int\frac{M(r)}{r}dM(r) \ . \tag{5.55}$$

The right-hand side is just V of Eq. (5.46). The left-hand side can be integrated by parts,

$$\text{LHS}=4\pi pR^3|-3\int(p/\rho)dM \ . \tag{5.56}$$

The integral is just W as defined in Eq. (5.43). Therefore

$$V_N+3W_N=4\pi p_iR_i^3 \tag{5.57a}$$

$$V_e+3W_e=4\pi p_0R_o^3-4\pi p_iR_i^3 \ . \tag{5.57b}$$

The total energy inside R_o is now

$$E_o=E_N+E_e=V_N+\frac{1}{\gamma_N-1}W_N+\left[3-\frac{1}{\gamma_N-1}\right]\frac{p_i}{\rho_i}M_N+4\pi p_oR_o^3-4\pi p_iR_i^3+\Delta_e \tag{5.58}$$

$$=\left[V_N+3\frac{p_i}{\rho_i}M_N-4\pi p_iR_i^3\right]\left[1-\frac{1}{3(\gamma_N-1)}\right]+4\pi pR_o^3+\Delta_e \ . \tag{5.59}$$

In going from Eq. (5.58) to Eq. (5.59), we have eliminated W_N by using Eq. (5.57a). Cooperstein *et al.* (1984) then imply, without proof, that the bracket in Eq. (5.59) is

$$[\ ]=\frac{\gamma_N-1}{\gamma_N}V_N \ , \tag{5.60}$$

so that

$$\text{NR}\equiv4\pi p_oR_o^3-E_o=-V_N\frac{3\gamma_N-4}{3\gamma_N}-\Delta_e \ . \tag{5.61}$$

Cooperstein *et al.* (1984) call this the net ram pressure. V_N is approximately equal to the gravitational self-energy of a uniformly dense sphere of mass M_N,

$$-V_N=\frac{3}{5}\frac{GM_N^2}{R_i} \ . \tag{5.62}$$

They show that this is accurate to 1%.

The importance of Eq. (5.61) is that the first term on its right-hand side is independent of R_o, and the second term is much smaller, so the net ram does not depend strongly on the outer radius R_o. In practice, one may take the left-hand side of Eq. (5.61) from a computer calculation at *some* radius, and then extrapolate to larger radii by adding the change of Δ_e. The first term on the right-hand side of Eq. (5.61) is about +10 foe.

Comparing the net ram (NR) at two values of the included mass, we have [cf. Eq. (5.48).]

$$(\text{NR})_2-(\text{NR})_1=\int_{M_1}^{M_2}N(m)dM \ , \tag{5.63}$$

where

$$N(m)=3p/\rho-\varepsilon \ . \tag{5.64}$$

One advantage of the net ram is that gravitation has been eliminated; it largely compensates the electron pressure.

This pressure, which dominates at subnuclear densities, gives zero contribution to Eq. (5.64), so we are concerned only with the nuclear contribution, which we denote by subscript n. At subnuclear density, this contribution is usually negative. This is due to the dissociation of nuclei with increasing temperature. As nuclei dissociate into nucleons, the internal energy ε_n becomes large, while p_n/ρ remains moderate. Complete dissociation into nucleons occurs at about $T=1.4$ MeV, and $p_n/\rho \sim T$ after complete dissociation. On the other hand,

$$\varepsilon_n = D + \tfrac{3}{2}T \tag{5.65}$$

where the dissociation energy (per nucleon) is

$$D = 8.8 \text{ MeV} , \tag{5.66}$$

hence

$$3p_n/\rho - \varepsilon_n = \tfrac{3}{2}T - D . \tag{5.67}$$

This is negative for $T < 6$ MeV.

For low temperature, $0.5 < T < 1.4$ MeV, dissociation only goes to α particles. Disregarding the fact that neutrons may also be formed, we have then

$$D = 1.7 \text{ MeV} , \tag{5.65a}$$

$$\varepsilon_n = D + \tfrac{3}{8}T , \tag{5.68}$$

$$p_n/\rho = \tfrac{1}{4}T , \tag{5.68a}$$

$$3p_n/\rho - \varepsilon_n = \tfrac{3}{8}T - D . \tag{5.69}$$

This is still negative, but smaller in magnitude than Eq. (5.67). Thus the net ram decreases more slowly once the temperature behind the shock falls below 1.4 MeV. Below about 0.5 MeV, there is no dissociation, and Eq. (5.64) becomes positive again. However, because of the shock condition (5.33), the shock then moves very slowly.

It is sometimes useful to write

$$p/\rho = (\Gamma - 1)\varepsilon , \tag{5.70}$$

where Γ is one of the many definitions of the adiabatic index; then

$$(\mathrm{NR})_2 - (\mathrm{NR})_1 = \int_{M_1}^{M_2} (3\Gamma - 4) dM . \tag{5.71}$$

In the dense pack, $\Gamma = \gamma = 3$, the right-hand side is positive, so the dense pack gives a positive contribution to the net ram. Using Eq. (5.62), this is of the order of 10 foe.

To use the net ram, one goes back to the definition (5.61),

$$\mathrm{NR} = 4\pi p R^3 - E . \tag{5.61a}$$

The energy inside a given mass point M is nearly always negative: It is slightly negative before collapse because of the gravitational potential, and neutrino energy is lost continually. Thus $4\pi p R^3 < \mathrm{NR}$, and NR would give an upper limit of the shock pressure.

Cooperstein, Bethe, and Brown (1984) considered two computer calculations with artificial initial conditions, with initial Fe core masses of 1.25 and 1.35 $M_\odot$. The first gave a successful prompt shock, the second was unsuccessful. For either case, the net ram at the surface of the homologous core, R_o, is 4 foe. The integral of Eq. (5.63) from there to the shock, when the latter is at $R = 500$ km, is -1.5 foe. The energy $E_2 - E_1$ is also about -1.5 foe, due to neutrino emission. Therefore, near the shock,

$$4\pi p R^3 \sim 4 - 1.5 - 1.5 \sim 1 \text{ foe} . \tag{5.72}$$

Computer calculation gave 0.4 foe; the agreement is not bad, considering the large individual terms involved in Eq. (5.61).

In either case, pR^3 is small. But, as Cooperstein *et al.* (1984) showed, it is large enough to propel the shock outward at $v = 10^9$ cm/s. This is due to the very low density of infalling material (Sec. VI.F).

J. Convection theory

If the shock begins to weaken, the entropy behind the shock decreases. Since the entropy of a given mass element is nearly constant with time, the entropy decreases with increasing M_r. This is shown in Cooperstein, Bethe, and Brown, 1984, Fig. 2, as well as in our Fig. 13. Such a situation generally leads to convection.

In this section, we develop the general theory of convection. While in stellar evolution a very small negative gradient of entropy, dS/dr, is sufficient to drive convection, in a supernova the gradient has to be substantial in order to cause appreciable convection in the short times involved, milliseconds or at most seconds. Our aim is to obtain a relation between energy transport and entropy gradient. In the next section, we shall apply the theory of *two* specific computations of prompt shocks.

In laboratory experiments, in the Earth's atmosphere, and in the Sun's envelope, convection cells are formed that have dimensions small compared to the total dimension of the system. We shall assume the same here. We shall assume the height of a convection cell to be equal to a pressure scale height,

$$L = -dr/d\ln p , \tag{5.73}$$

and the width of the same order. Usually, in supernova conditions,

$$p \sim r^{-4} , \tag{5.73a}$$

and so

$$L \sim r/4 . \tag{5.74}$$

This means that there are about 200 cells on the surface of a sphere. (The Sun's surface has many more.) Considering such cells makes it possible to do most of the calculation analytically, rather than requiring a three-dimensional computer calculation, which would be difficult and probably not reliable.

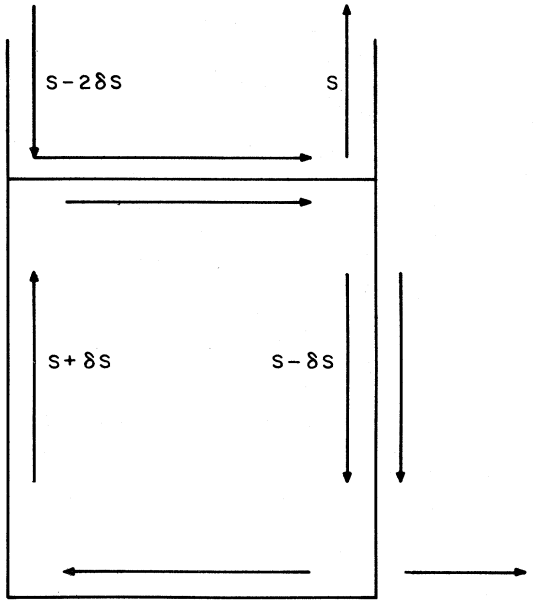

FIG. 12. Streaming in a convection cell.

It is reasonable to assume that, even in the presence of convection, the surfaces of constant pressure are still spheres, i.e., the pressure is a function of r only. In a cell, we assume there is an up stream on one side, having a higher entropy than the down stream on the other side (see Fig. 12). The mass transport of the two streams must of course be equal, but there is a net energy transport up. In the neighboring cell, the stream "on the other side of the wall" is parallel to that in our cell (see Fig. 12), which makes the circulation of the neighboring cell opposite to that in our cell. We adopt a mixing-length idea, i.e., at the top of a cell, the streams get mixed, so that the up stream in the next higher cell starts with the *average* entropy in our cell. For the moment, we assume that only entropy changes with r; near the end of this section we shall consider the case in which the electron fraction Y_e also changes.

Our assumptions and results are essentially the same as those of Böhm-Vitense (1958). However, our mathematics is simpler, because we use the entropy as an independent variable, rather than the temperature. Thus, for instance, the density is taken to be

$$\rho=\rho(p,S,Y_e) \tag{5.75}$$

and the temperature likewise.

Our cell has a certain average entropy S. The up stream has entropy $S+\delta S$, the down stream $S-\delta S$. To derive the conditions in the two streams, we start from quantities per *gram* of material, denoted by subscripts 1. The second law of thermodynamics is

$$dE_1+p\,dV_1=T\,dS_1\ . \tag{5.76}$$

Since we have postulated that the pressure is the same in up and down streams, it is convenient to introduce the enthalpy

$$H_1=E_1+pV_1\ , \tag{5.77}$$

so that

$$dH_1=T\,dS_1-V_1dp\ , \tag{5.78}$$

and the last term is zero. For a change of temperature,

$$dH_1=C_p dT \tag{5.79}$$

with C_p the specific heat at constant pressure, and

$$dE_1=C_v dT\ . \tag{5.79a}$$

The difference in energy content between the up stream and the average is δH_1, where

$$\delta H_1=TN_A k_B\delta S\ . \tag{5.80}$$

Here N_A = Avogadro's number, and

$$N_A k_B T=0.96\times10^{18}T_{\rm MeV}\ . \tag{5.81}$$

The buoyancy of the up-stream material, relative to the average material in the cell, of density ρ_0, is

$$\ddot{R}_b=\left[\frac{1}{\rho_0}-\frac{1}{\rho}\right]\frac{\partial p}{\partial r}=-\delta V_1\frac{\partial p}{\partial r} \tag{5.82}$$

(note $\rho_0V_1=1$). This acceleration acts over one mixing length, which we take to be equal to a pressure scale length L [Eq. (5.75)]. For the average upstream material, we assume that the acceleration has acted only over half a scale height. Then the velocity acquired by the upward stream is given by

$$\tfrac{1}{2}v_c^2=\tfrac{1}{2}\ddot{R}_b L \tag{5.82a}$$

$$v_c^2=\delta V_1 p \tag{5.83}$$

(c for convection). From Eqs. (5.76) and (5.78),

$$p\delta V_1=T\delta S_1-\delta E_1=(C_p-C_v)\delta T$$
$$=\frac{C_p-C_v}{C_p}\delta H_1\ . \tag{5.84}$$

This equation holds for an arbitrary EOS.

The energy flow through any spherical surface, carried by the up stream, is

$$J'=\tfrac{1}{2}\rho 4\pi r^2\delta H_1 v_c\ . \tag{5.85}$$

Here $\frac{1}{2}\rho$ appears because half the material flows up, the other half down. The down stream carries a negative energy, $-\delta H_1$, downward, so it contributes the same net upward energy current. The total upward convection current is therefore

$$J=4\pi\rho r^2\delta H_1 v_c=4\pi\rho r^2\left[\frac{C_p-C_v}{C_p}\right]^{1/2}(\delta H_1)^{3/2}\ . \tag{5.86}$$

For a monatomic, nonrelativistic, perfect gas (e.g., nucleons),

$$\frac{C_p-C_v}{C_p}=\frac{2}{5}\ ; \tag{5.87}$$

for a relativistic perfect gas, e.g., electrons or radiation,

$$\frac{C_p - C_v}{C_p} = \frac{1}{4} . \tag{5.87a}$$

If the convective zone is less than one pressure scale height, Eq. (5.82) should not be used, but the actual height h of the convective zone should be inserted in Eq. (5.82a) instead of L. The δS, in this case, is simply given by

$$2\delta S = \Delta S , \tag{5.88}$$

where ΔS is the difference in entropy between the top and bottom of the convective zone.

If the height of the convective zone is more than one pressure scale height, we use the mixing-length idea described above, namely, that after rising by a pressure scale height, the entropy of the up stream becomes equal to the average entropy in the cell below. Thus the *average* entropy of the material changes in one mixing length by

$$L\frac{dS}{dr} = -\delta S . \tag{5.88a}$$

Inserting L from Eq. (5.73), we find

$$\delta S = p\frac{dS}{dp} . \tag{5.89}$$

When we insert this into Eq. (5.86), the energy current becomes

$$L = 4\pi w r^2 \left[\frac{C_p - C_v}{C_p} H_1 \right]^{1/2} \left[\frac{d \ln S}{d \ln p} \right]^{3/2} \tag{5.90}$$

where

$$w = \rho H_1 \tag{5.90a}$$

is the enthalpy per unit volume.

In an actual computation, S is given at one time as a function of p. This gives $\delta S(p)$, hence δH_1 from Eq. (5.80) and the energy current J from Eq. (5.90). This in turn will give the entropy distribution at the next instant, $t + dt$.

In equilibrium, the energy current $J(r)$ will become independent of r over most of the convective zone. In such dynamic equilibrium, therefore,

$$A(\delta H_1)^{3/2} = \text{const} = \text{indep. of } r \tag{5.91}$$

with

$$A = 4\pi\rho r^2 . \tag{5.92}$$

In computer calculations, A is usually nearly independent of r; then

$$\delta H_1 / 0.96 \times 10^{18} \equiv B = T_{\text{MeV}} \delta S = \text{const} , \tag{5.93}$$

a very convenient result. Using Eq. (5.90), we find that the difference between the entropy inside, S_3, and that at the shock, S_2, is

$$S_3 - S_2 = \int \delta S \frac{dp}{p} = B \int_{p_2}^{p_3} \frac{dp}{pT} . \tag{5.94}$$

The integral can be calculated from the computer output; so can $S_3 - S_2$, and so δH_1 can be calculated. This then gives the energy current J from Eq. (5.86).

The energy current, together with the hydrodynamics, gives the change of S_2 with time so that $S_3 - S_2$ at the next time step can be obtained.

So far we have assumed that density and temperature depend only on entropy (and pressure). In reality, they depend also on Y_e, the number of electrons per nucleon (in the following, just denoted by Y).

The general condition for convection to occur in this case is the Ledoux criterion,

$$\frac{dS}{dr} + \frac{(\partial\rho/\partial Y)_{S,p}}{(\partial\rho/\partial S)_{Y,p}} \frac{dY}{dr} < 0 . \tag{5.95}$$

The total derivatives in Eq. (5.95) are taken for the actual distribution in our star. The partial derivatives refer to the equation of state (5.75).

Generally,

$$(\partial\rho/\partial S)_{p,Y} < 0 \tag{5.96}$$

$$(\partial\rho/\partial Y)_{p,S} < 0 . \tag{5.97}$$

To see Eq. (5.97), recall that, at constant density and temperature, the pressure increases with increasing Y_e. Hence, to get back to the original pressure, the density must decrease. Using Eqs. (5.96) and (5.97), we find that Eq. (5.95) becomes

$$\frac{dS}{dr} + a\frac{dY}{dr} < 0 , \tag{5.98}$$

where a is a *positive* coefficient. Thus a negative slope of S, and a negative slope of Y_e, favor convection. Usually, the slope of S is more important.

We have evaluated a for our equation of state at $S = 9$, $Y_e = 0.19$, $\rho = 5 \times 10^9$, which are typical values for a shock at $r = 200$ km, and find

$$a \sim 7 . \tag{5.99}$$

Assuming that a stays nearly constant with r, the Ledoux condition becomes

$$\frac{dS'}{dr} \equiv \frac{d}{dr}(S + aY_e) < 0 . \tag{5.100}$$

In our theory, then, S must be replaced by S'.

K. Effect of convection on the shock

The effect of convection is best studied by means of the net ram concept, which we have described in Sec. V.I. We have argued that a large net ram will increase the strength of the shock. Bethe, Brown, and Cooperstein (1987) showed that, in general, convection will *decrease* the net ram.

They consider a typical example, Fig. 13, taken from Baron *et al.* 1985a, 1985b. The entropy has a maximum of 9.4 at point B ($M = 1.06$) and falls to 7.7 at $M = 1.19$ (point A). If convection were complete, the material at A, which has a density $\log\rho = 9.6$, would have its entropy

raised from 7.7 to 9.4, and the material at B, $\log\rho=10.2$, would undergo the opposite change of S. This would cause changes in the *differential* net ram,

$$N(m)=3p/\rho-\varepsilon\ , \tag{5.64}$$

as follows:

At A, $\log\rho=9.6$, $S=9.36$, $N=-5.78$
$S=7.69$, $N=-4.70$
Change of $N(m)$
due to convection: $\Delta N=-1.08$ MeV

At B, $\log\rho=10.2$, $S=7.69$, $N=-5.03$
$S=9.36$, $N=-5.23$
Change: $\Delta N=+0.20$ MeV.

The same amount of material is involved at A and B, so the integrated net ram changes by -0.88 MeV (times the amount of material convected). Thus convection will decrease the total net ram and weaken the shock.

Of course, in reality convection will not simply exchange the entropies at points A and B, but will bring both entropies to some intermediate level: this will have a smaller effect on net ram than that indicated above, but the sign will remain the same. Moreover, the convection is rather slow, so it will not equalize the entropies at A and B but leave the slope negative; this will further diminish the effect, but we shall still have a decrease in the net ram.

The result is rather paradoxical. It is strange that increasing entropy will decrease the differential net ram. We have therefore investigated the behavior of $N(m)$ at several different densities, of which we reproduce four examples in Table VIII. For $\log\rho=9$, the net ram *decreases* monotonically with increasing S; for $\log\rho=10$, it reaches a minimum at $S=9$; for $\log\rho=11$, the minimum is shifted to $S=8$, and the N then increases strongly for larger S. For $\log\rho=12$, the increase is monotonic, and N becomes positive for $S\gtrsim 7.3$.

This behavior can be correlated to the fraction of α particles in the medium, given in part B of Table VIII. Taking, for example, $\log\rho=11$, increasing S from 6 to 8, serves primarily to dissociate α particles into nucleons, and the temperature increases only modestly. This means that p/ρ increases only slightly, while the internal energy ε increases strongly because of the dissociation; hence the decrease of the net ram as defined in Eq. (5.64). Further increase of S from 8 to 10 no longer needs to dissociate α particles, so that all the energy can go into raising the temperature and hence the pressure.

It appears from Table VIII that the "critical" fraction of α particles is $\sim 10\%$: for $X_\alpha > 10\%$, most of the energy causes dissociation into α particles: for $X_\alpha < 10\%$, it goes into raising the temperature and pressure of the nucleon gas. Thus, for $\log\rho=12$, where X_α is only 13% at $S=6$, the net ram starts increasing already at that point.

Referring again to Fig. 13, in the region from A to C ($M=1.17$–$1.30\ M_\odot$), the electron fraction increases rapidly with M. By use of Eq. (5.98), it can be shown that this region is stable against convection by the Ledoux criterion. Thus convection can occur only between the entropy maximum (which lies slightly outside the neutrino sphere) and the region of rapidly increasing Y_e (which is well inside the shock).

TABLE VIII. Net ram vs S for $Y_e=0.30$.

	S				
$\log\rho$	6	7	8	9	10
	(A) Net ram in MeV per nucleon				
9	−3.57	−4.07	−4.44	−4.99	−5.58
10	−3.99	−4.56	−5.18	−5.70	−5.38
11	−4.12	−4.66	−4.94	−3.79	−2.17
12	−2.79	−0.87	+2.82	+6.22	+3.87
	(B) Percentage of material in α particles, X_α				
9	40	59	45	39	27
10	53	39	24	8	3
11	40	23	6	1	0.01
12	13	0.8	0.03	0	0

Bethe and Brown (1989, unpublished) have investigated two shocks computed by Baron and Cooperstein (1988). One of these was successful: it went through the entire Fe core. Bethe and Brown found that, in this star, convection was confined to the region between $M=1.12$ and $1.20\ M_\odot$, and the loss in net ram was less than 0.02 foe, essentially negligible.

The other computation, by Baron and Cooperstein, yielded a shock that almost succeeded; it got stuck at about 400 km. This shock has a substantial convective region and is appreciably hurt by convection. The convected material moves with a velocity of 5–8×10^8 cm/s; the convective energy transport decreases from 6×10^{52} ergs/s at 6 milliseconds after collapse, to 0.6×10^{52} at 21 ms; it is 10–20% of the work which the shock does on the infalling material.

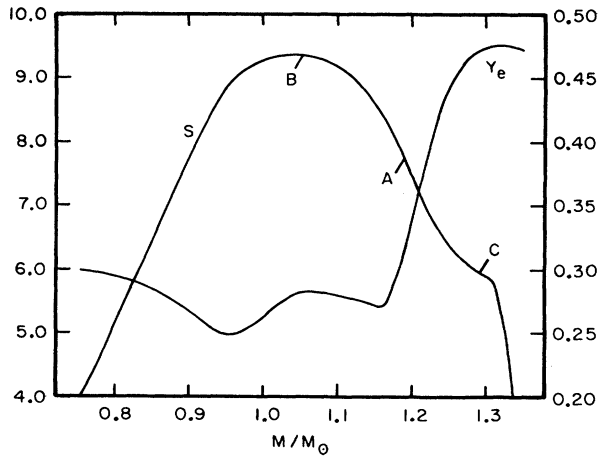

FIG. 13. Entropy S and electron fraction Y_e in a supernova computation used by Cooperstein, Bethe, and Brown (1984). Left scale gives S, right scale Y_e. See text for points A,B,C.

At the early times relevant for the prompt shock, i.e., up to about 0.05 sec, there is no convection inside the neutrino sphere. The increase of entropy from the unshocked core to the ν sphere, from about 2 to 8 units, is far more important than the decrease of Y_e, from about 0.35 to 0.25; thus the Ledoux criterion for convection [Eqs. (5.95) and (5.98)] is not fulfilled. At late times, like 1 sec, which are important for the delayed shock (Sec. VI), convection inside the neutrino sphere is possible.

L. Stars of masses 8–11 $M_\odot$

Stars in this mass range do not have an Fe core, but their core consists of O+Ne+Mg. It might be expected that the energy liberated when these nuclei go to nuclear statistical equilibrium could help a supernova explosion.

With this in mind, Hillebrandt, Nomoto, and Wolff (1984) calculated the collapse and explosion of a star of 9 $M_\odot$ and found a sizable explosion, about 2 foe. Before collapse, the core of their star had a mass of about 1.2 $M_\odot$, and outside of the core the density dropped sharply. The core contracts slowly. When the center reaches sufficient temperature, the nuclei begin to react. This reaction heats the material, and the nuclear burning spreads outward as a deflagration wave. Since the material gets heated, it expands, so that the deflagration wave involves a discontinuous decrease in density. The infall velocity also decreases, by as much as 30% in the calculation of Hillebrandt *et al.* They state that the ram pressure ρv^2 of the infalling material decreases by a factor of 4–10 in the deflagration wave. This greatly facilitates propagation of the prompt shock, which starts, as usual, when the central density exceeds nuclear density. At this time, they find an entropy of 1.0 at the center of the star. Their shock starts at 0.63 $M_\odot$. Its velocity is high, about 5×10^9 cm/s, and it accelerates further after it overtakes the deflagration wave. The entropy in the shock is typically about 11 and increases to 15 after entering the very dilute region outside the core. In this manner, Hillebrandt *et al.* find the very substantial energy of 2 foe in the supernova.

Unfortunately, repetitions of this calculation by Burrows and Lattimer (1985), by Baron, Cooperstein, and Kahana (1987), and especially by Mayle and Wilson (1988) gave quite different results. Baron *et al.* start from Nomoto's (1984) calculation of the evolution of a star of 9 $M_\odot$. Like Hillebrandt, Nomoto, and Wolfe, they find a deflagration wave, but the decrease of velocity at its front is only 5% instead of the 30% found by Hillebrandt *et al.* Their smaller result agrees with an analytical calculation. They also find a much smaller density reduction. Instead, they find a very large increase of entropy in the burned material, to 1.3–2.0, while Hillebrandt *et al.* found only about 1.0 at bounce. The increase of entropy is due to the energy release when the core burns to nuclear statistical equilibrium; there is no time for this energy to be emitted in the form of neutrinos. The high resulting temperature leads to a high abundance of protons, and thereby to copious capture of electrons. The lepton number per nucleon at bounce is only $Y_L=0.36$, in contrast to $Y_L=0.40$ for the successful calculation of a 12-$M_\odot$ star by Baron, Cooperstein, and Kahana, reported in our Table VII; in neither calculation were neutrino-electron collisions (Sec. II.F) taken into account. The shock accordingly forms at a very small mass, $M_r=0.46$ or 0.50 $M_\odot$ (Hillebrandt *et al.* had 0.63 $M_\odot$), and has to traverse a very large mass which it must dissociate into nucleons. It gets stuck at 150 km—it is a failure. Mayle and Wilson (1988) fully confirm the result of Baron *et al.* (1987).

The conclusion is that release of thermonuclear energy before complete collapse is harmful because it increases entropy and electron capture. On the other hand, such release in the outgoing shock wave when it traverses the Si and O layer is probably helpful.

A star of mass 9 $M_\odot$ probably explodes by the delayed mechanism discussed in Sec. VI. For stars of mass 12–20 $M_\odot$, it is also likely that the delayed mechanism is responsible (see Sec. VI.I). And stars heavier than 20 $M_\odot$ surely explode by the delayed mechanism, or not at all.

VI. THE DELAYED SHOCK

A. The proto-neutron star

The unshocked core of the star does not have a large net energy. The very large gravitational energy (several times 10^{53} ergs) has been converted largely into chemical potential of electrons and neutrinos. The core has to get rid of this potential energy, chiefly by emitting neutrinos, before it can become (the inner part of) a neutron star: it has to be deleptonized.

The chemical potentials are large. Typically, the density at the center is

$$\rho_c\sim6\times10^{14}\ \mathrm{g/cm^3}\ , \tag{6.1}$$

and the neutrino fraction is

$$Y_\nu\sim0.08\ . \tag{6.2}$$

Then the chemical potential is

$$\mu_\nu=111(2\rho_{13}Y_\nu)^{1/3}\ \mathrm{MeV}=235\ \mathrm{MeV}\ . \tag{6.3}$$

The electron chemical potential is even larger,

$$\mu_e=\mu_\nu+\hat{\mu}\ , \tag{6.4}$$

where $\hat{\mu}=\mu_n-\mu_p$ is typically 50–100 MeV, At $r>0$, μ_ν decreases, mainly because ρ decreases. The temperature, at early times, is of the order of 10 MeV, much smaller than μ_ν.

The neutrinos will diffuse out of the core, due to the gradient of the density n. The theory of this diffusion has

been given by Burrows *et al.* (1981). The outward flux is

$$F_n = -\frac{\lambda c}{3}\frac{\partial n}{\partial r} . \tag{6.5}$$

The mean free path is

$$\lambda(\varepsilon) = \lambda_1(\varepsilon_1/\varepsilon)^2 , \tag{6.6}$$

where λ_1 is the mean free path for some neutrino energy ε_1. Since the neutrinos are highly degenerate, $\mu \gg T$, only the neutrinos near the Fermi energy μ will diffuse, so we may put $\varepsilon = \mu_\nu$ in Eq. (6.6). The density n is proportional to μ_ν^3; thus Eq. (6.5) becomes

$$F_n = -\lambda_1 c\frac{n_1}{\varepsilon_1}\frac{\partial \mu_\nu}{\partial r} , \tag{6.7}$$

where n_1 is the neutrino density corresponding to $\mu = \varepsilon_1$. The mean free path is of the order of 10 cm, extremely small compared to the radius of the core of about 10 km, so that the diffusion approximation in Eq. (6.5) is excellent.

The density changes with time according to

$$\frac{\partial n}{\partial t} = -\nabla\cdot\mathbf{F} . \tag{6.8}$$

However, as the neutrino density decreases, the chemical equilibrium between neutrinos and electrons is disturbed, and electrons will convert into neutrinos until the equilibrium (6.4) is restored. Hence Eq. (6.8) describes the change of the total *lepton* density,

$$\frac{dn_L}{dt} = -\nabla\cdot\mathbf{F} , \tag{6.9}$$

while F denotes the neutrino current, these being the only particles that can diffuse. Likewise, in Eq. (6.5) n is the neutrino density, not the total lepton density.

The flux brings to a given mass element neutrinos of higher μ than it takes out. The internal energy of the mass element changes by

$$\frac{\partial w}{\partial t} = -\mathbf{F}\cdot\nabla\mu , \tag{6.10}$$

assuming the mass element does not change its specific volume (see Burrows *et al.*, 1981, for details). Inserting Eq. (6.7), we find

$$\frac{\partial w}{\partial t} = \lambda_1 c\frac{n_1}{\varepsilon_1}\left[\frac{\partial \mu}{\partial r}\right]^2 , \tag{6.11}$$

so the mass element heats up. As Burrows *et al.* (1981) point out, this is analogous to Joule heat in ordinary electric conduction.

The major problem is the determination of the mean free path λ. This is discussed in Sec. IX.A, and in more detail in Burrows *et al.*, 1981.

Having obtained λ as a function of ρ and μ, Burrows *et al.* calculated the time required to reduce Y_L in the core to half its value; they find that this is about a second and that the temperature in the outer core is raised from 10 to about 18 MeV. A later calculation, by Burrows and Lattimer (1987), and more careful determination of λ, shows heating up to $T \sim 40$ MeV; this result agrees well with computations by Wilson (1985). (Wilson's calculation was already carried out in 1982, but publication was delayed.) Burrows and Lattimer (1987) find that it takes about five seconds for the Y_L in the core to be reduced to one-half.

B. Neutrino sphere, μ and τ neutrinos

The diffusion of neutrinos in the mantle, i.e., the region outside the unshocked core, has been treated by Cooperstein, van den Horn, and Baron (1986). They assume that the neutrinos, at any mass point, have a temperature T_ν and chemical potential μ_ν which differ from T_e and μ_e of the electrons. They derive the flux of neutrino number and energy in terms of the gradients of T_ν and μ_ν and appropriate Fermi integrals. This description remains valid out to the neutrino sphere.

The neutrino sphere R_ν, in analogy to the photosphere for ordinary stars, is defined by the condition that its optical depth should be 2/3 [cf. Eqs. (2.36) and (2.40)],

$$\int_{R_\nu}^{\infty} dr/\lambda(\rho,\varepsilon) = 2/3 . \tag{6.12}$$

Following Eddington, we take the right-hand side to be 2/3 rather than 1 because the neutrinos are generally emitted at some angle with the radius. In general, R_ν will depend on the neutrino energy: since (roughly)

$$1/\lambda \simeq \rho\varepsilon^2 . \tag{6.13}$$

higher-energy neutrinos will have their neutrino sphere at lower ρ, i.e., larger R_ν. If the neutrinos are represented by a thermal distribution, a suitable average must be taken. A simple case will be treated in Sec. VI.H.

From the neutrino sphere, the neutrinos move in straight lines; at large r, they move in the radial direction. Some are absorbed on the way out. The total emission of $\nu_e + \bar{\nu}_e$ is

$$L = 1.20\times 10^{26}\pi R^2 c T^4 \text{ ergs/sec} , \tag{6.14}$$

where c is the velocity of light, R is the radius of the neutrino sphere, and T its temperature in MeV. Actually, the emission is determined by the rate at which neutrinos are delivered to the neutrino sphere by diffusion, and Eq. (6.14) then gives the relation between radius and temperature of that sphere in terms of the (known) L. Most of the time, T is about 4–5 MeV (see Sec. VI.H).

The emitted neutrinos are far more numerous than the neutrinos that come from the core by deleptonization. The latter have an energy μ, as discussed in Sec. VI.A, and the average of μ over the core is about 150 MeV. The average energy of neutrinos in a Fermi distribution of temperature T is about $3T$, hence about 15 MeV. Thus about ten neutrinos are emitted from the neutrino sphere for every one from the core. The total energy of these ten is equal to the energy of the core neutrino. One

of the ten must be a ν_e to carry away the lepton number. If we assume that the rest of the energy is equally distributed over the six species ν_e, $\bar{\nu}_e$, ν_μ, $\bar{\nu}_\mu$, ν_τ and $\bar{\nu}_\tau$, then there will be 1.5 neutrinos of each species. In particular, the energy flux in ν_e will be a fraction of the total flux in $\nu_e+\bar{\nu}_e$, like this:

$$\frac{L(\nu_e)}{L(\nu_e)+L(\bar{\nu}_e)}=\frac{1.5+1}{3+1}=\frac{5}{8}\ . \tag{6.15}$$

This being $>\frac{1}{2}$ means that there is a chemical potential μ_ν for the electron neutrinos. As discussed in Sec. III.A, the energy emitted in ν_e and $\bar{\nu}_e$ is, respectively, proportional to the Fermi integrals

$$F(\eta_\nu) \text{ and } F(-\eta_\nu)$$
$$\eta_\nu=\mu_\nu/T_\nu\ . \tag{6.16}$$

With the ratio given by Eq. (6.15),

$$\eta_\nu=0.29\ . \tag{6.17}$$

This result depends somewhat on T_ν and on the average μ_ν in the core. There is a small correction to Eq. (6.14), an increase by a factor of about $1+\eta_\nu^2$. The μ and τ neutrinos have $\mu=0$, of course.

The μ and τ neutrinos are produced by the plasma process

$$e^+ + e^- \rightarrow \nu_i + \bar{\nu}_i\ , \tag{6.18}$$

where $i=\mu$ or τ. This process has been calculated by Beaudet, Petrosian, and Salpeter (1967), by Dicus (1972), and by Soyeur and Brown (1979). Of course, pairs of electron neutrinos are also produced, but this is unimportant in comparison to the single production by $p+e^-\rightarrow n+\nu_e$ and the like. Bethe, Applegate, and Brown (1980) showed that the quantum states of ν_μ are filled at the rate

$$\kappa'=0.016T^5\ \text{sec}^{-1}\ , \tag{6.19}$$

where T is the electron temperature in MeV. Relevant times are from 0.01 to 1 sec; therefore the ν_μ will be essentially in equilibrium with electrons for $T>6$ MeV (or even less for 1 sec). This means that they will be in equilibrium essentially up to their neutrino sphere, which is at somewhat higher temperature than that of the ν_e, because the ν_μ have a longer mean free path. The ν_μ species are not directly observable because

$$\nu_\mu + n \rightarrow \mu^- + p \tag{6.20}$$

would require an energy greater than the rest mass of the μ meson, about 100 MeV.

We have emphasized here neutrino emission after the shock reaches the neutrino sphere, which happens a few milliseconds after bounce. For phenomena at earlier times, see Bethe *et al.* (1980).

C. The Wilson mechanism

James R. Wilson (1985) found that the neutrinos from the core can be absorbed by material at $r=100$–200 km and can heat this material sufficiently to revive the shock, which will then expel the material from the star. If the prompt shock (Sec. V) fails, I believe that this is the likely mechanism for the supernova explosion. It is interesting that Colgate and White had already found (1966) that neutrino heating at 100–200 km was the only mechanism that produced an explosion, while the prompt shock did not.

The cross section for the absorption of an electron neutrino by a neutron (or an antineutrino by a proton) is

$$\sigma=9\times10^{-44}\varepsilon^2\ \text{cm}^2\ , \tag{6.21}$$

where ε is the neutrino energy in MeV. If L' is the luminosity in neutrinos (or antineutrinos) in ergs/sec, the energy gain of a free nucleon at distance R_m is

$$\left[\frac{dE}{dt}\right]_{\text{abs}}=\frac{L'\sigma}{4\pi R_m^2}=\frac{L'\times9\times10^{-44}\varepsilon^2}{4\pi\times1.6\times10^{-6}\times10^{14}R_{m7}^2}$$
$$=0.45\times10^{-52}\frac{L'\varepsilon^2}{R_{m7}^2} \tag{6.22}$$

(1 MeV $=1.6\times10^{-6}$ ergs). The average gain per nucleon is then

$$\left[\frac{dE}{dt}\right]_{\text{abs}}=0.22\frac{L_{52}\varepsilon^2}{R_{m7}^2}X_N\ \text{MeV/sec}\ , \tag{6.23}$$

where L_{52} is the total luminosity in ν_e and $\bar{\nu}_e$ in units of 10^{52} ergs/sec, and X_N is the fraction of nucleons that are free.

Bound nucleons, in He^4 or O^{16}, contribute little. If they were to absorb a neutrino, the nucleon would have to be promoted to the next shell in the nucleus, i.e., we would have a forbidden transition whose probability is reduced at least by the factor $(kR)^2$ where $k=1/\lambda$ is the wave number of the neutrino and R is the radius of the nucleus. For a 20-MeV neutrino (which is typical), $\lambda=10$ fermi, while R for the He and O nucleus is 2 and 3 fm, respectively. Therefore absorption by nucleons in He (O) is down by a least a factor 25 (10) compared with free nucleons, actually more because the factor is less than $(kR)^2$.

The material located at $r=100$–300 km after collapse is mostly O^{16} before the shock reaches it. Thus it must be dissociated by the shock in order to effectively absorb neutrinos. Dissociation into α particles is not enough—there must be at least some nucleons. The energy required to dissociate O^{16} into α's is 0.9 MeV per nucleon. To get 10% of the α's dissociated into nucleons takes an additional 0.7 MeV. The temperature required to dissociate α particles is about 1.4 MeV, and we need a thermal energy per nucleon of about this amount. The total energy required is then

$$3\ \text{MeV per nucleon}\sim3\times10^{18}\ \text{ergs/g}\ . \tag{6.24}$$

The shock, by the time the Wilson mechanism operates, is an accretion shock. We may assume that the gravitational energy of the infalling material is converted into internal energy when the material is stopped and accreted. Thus we need to have

$$\frac{GM}{r} > 3\times 10^{18} \text{ ergs/g} . \tag{6.25}$$

The mass is typically 1.5 $M_\odot$, so $GM = 2\times 10^{26}$ cgs units; thus

$$r < 7\times 10^7 \text{ cm} = 700 \text{ km} . \tag{6.26}$$

For total dissociation into nucleons, $r < 200$ km. if the material is only partially dissociated by the shock, the absorption of neutrinos will in time complete the dissociation.

In Wilson's computations, typically

$$L_{52}=5, \quad \langle \varepsilon^2 \rangle = 100 , \qquad r_7 = 1.5, \quad X_N = 1 , \tag{6.27}$$

so that Eq. (6.23) gives

$$\frac{dE}{dt} = 50 \text{ MeV/sec} . \tag{6.28}$$

The heating is thus quite rapid; in 1/4 second the material acquires an energy larger than $GM/r = 13$ MeV (for $r = 150$ km), and can therefore be expelled from the star.

Equation (6.23) is not complete: the material absorbing the neutrinos will also emit neutrinos spontaneously. The emission is (per free nucleon)

$$\left[\frac{dE}{dt}\right]_{\text{em}} = -\sigma(T_m) a c T_m^4 , \tag{6.29}$$

where T_m is the temperature of the material and $\sigma(T_m)$ is the corresponding neutrino absorption cross section, assuming a Fermi distribution of temperature T_m; aT^4 is the energy density of neutrinos. Writing in Eq. (6.22)

$$L' = \pi R_\nu^2 a c T_\nu^4 , \tag{6.30}$$

i.e., assuming that the neutrinos from the core are a Fermi distribution of the temperature T_ν of the neutrino sphere, we find the sum of absorption and emission

$$\frac{dE}{dt} = ac\left[T_\nu^4 \sigma(T_\nu)(R_\nu/2R_m)^2 - T_m^4 \sigma(T_m)\right] . \tag{6.31}$$

Since

$$\frac{\sigma(T_m)}{\sigma(T_\nu)} = \left[\frac{T_m}{T_\nu}\right]^2 , \tag{6.32}$$

the total energy change may be written

$$\frac{dE}{dt} = \left[\frac{dE}{dt}\right]_{\text{abs}} \left[1 - \left[\frac{2R_m}{R_\nu}\right]^2 \left[\frac{T_m}{T_\nu}\right]^6\right] . \tag{6.33}$$

Equation (6.33) assumes that the neutrinos from the neutrino sphere actually have a thermal (Fermi) distribution in energy.

Some corrections are discussed in Bethe and Wilson (1985). Equation (6.22), and hence (6.33), is only valid if $R_m \gg R_\nu$, so that the outgoing neutrinos go in the radial direction; at smaller R_m, the absorbed energy is greater than that shown in Eq. (6.22). It is interesting that Eqs. (6.22) and (6.33) are independent of the material density.

Colgate and White (1966) were the first to suggest that neutrinos from the core would heat the imploding matter and cause the explosion. However, the neutrino physics, equation of state of dense matter, and the diffusion processes were not treated with sufficient accuracy to reliably model the process.

D. Results on Wilson mechanism

Wilson (1985) has carried out many computations based on the mechanism described in Sec. VI.C. The result of one of these is shown in Fig. 14, which shows the trajectories of various mass points as a function of time. The inner dashed curve shows the location of the neutrino sphere; it moves from about 60 km shortly after collapse time ($t=0$) to about 22 km at $t=0.65$. The outer dashed curve is the shock, starting at about 100 km and generally moving out. Up to a certain mass M_1, the material collapses at $t=0$ and then continues to move further in. Beyond M_1, the material is hit by the shock, which stops the rapid infall, but (in this computation) the mass points still fall in slowly; once they have fallen below about 150 km, the infall accelerates and stops only at the neutrino sphere. (In other computations the prompt shock is more successful, i.e., the mass element moves outward after the shock hits it, but may ultimately again fall inward.) However, the mass point $M_r = 1.665$ $M_\odot$ is different; it moves decisively outward after it crosses the shock, at about $r = 170$ km, and then continues to move out. The same happens to larger M_r; the

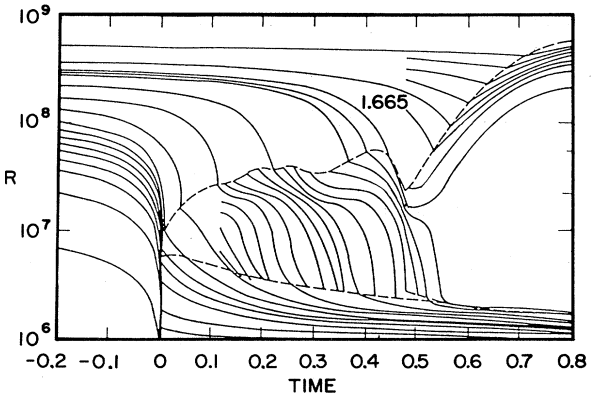

FIG. 14. Trajectories of various mass points, in an early calculation of J. R. Wilson (1985). Time after bounce is in seconds. Mass 1.665 $M_\odot$ is the first mass point which is propelled outward by the second shock, which is due to neutrino heating. The empty region on the right is the "bubble," filled by electromagnetic radiation. The upper dashed curve is the shock, the lower one the neutrino sphere.

shock has been revived by neutrino heating. This happens at $t \sim 0.5$ seconds. Below the trajectory $M = 1.665$, there is a large empty space, i.e., a large region of very low density, which will be discussed in Sec. VI.E.

The shock also moves in an interesting way: At $t = 0.42$ s, it is at 600 km, but it then recedes to about 230 km before it finally turns outward decisively. (Of course, the shock always moves outward relative to the material.) The recession of the shock is important because it brings the shocked material to smaller r, where it can be more effectively heated by the neutrinos.

In many computations by Bowers and Wilson (1982a, 1982b), Wilson (1985), and Wilson and Mayle (1989), the revived shock was successful. In some others, especially for stars of large mass (like 50 $M_\odot$), the shock went out, but then receded once more, to give neutrino heating a second chance; in some cases, recession and renewed bounce occurred several times.

Generally, these computations give a rather low energy, 0.3–0.4 foe, while the observed energy in Supernova 1987A (see Sec. VII) is at least 1.0 foe. Two additional mechanisms apparently cure this trouble; see Secs. VI.H and VI.I.

The Wilson-Mayle calculations already include a contribution from nucleosynthesis. To be observable in the supernova, this explosive nucleosynthesis must take place outside the bubble. Before the supernova implosion the material just outside the bubble was mostly ^{16}O and ^{20}Ne. Nucleosynthesis then begins with the process

$$^{16}\mathrm{O} \rightarrow \text{nuclear statistical equilibrium (NSE)} .$$

This releases about 0.5 MeV energy per nucleon or 0.1 foe per 0.1 $M_\odot$. We know from observation of 1987A that 0.07 $M_\odot$ of ^{56}Ni was formed as part of this process. Assuming the total NSE produced to be 0.2 $M_\odot$ we get an energy of 0.2 foe, a sizable fraction of the Wilson-Mayle result.

Obtaining the observed amount of ^{56}Ni, 0.07 $M_\odot$ is an important test of the theory. Wilson and Mayle (1989) find 0.065 $M_\odot$.

E. Thinning of the infalling material

Before the supernova collapse, the density distribution is typically of the form

$$\rho_0(r) = 10^{31} C r^{-3} , \tag{6.34}$$

where C is a coefficient between 1 and 10, r is in cm, and ρ in g/cm^3. The mass in an interval dr is then

$$4\pi\rho r^2 dr = 1.26 \times 10^{32} C\, dr/r , \tag{6.35}$$

i.e., of the order of $10^{32}\, dr/r$ grams. In the collapse, the material falls in with a velocity

$$u = \alpha (2GM/r)^{1/2} , \tag{6.36}$$

where the coefficient α is usually between 1/2 and 1, tending toward 1 at late times. The time required to fall from an initial position r_0 to r is

$$t(r_0, r) = (2GM)^{-1/2} \alpha^{-1} \int_r^{r_0} \frac{dr'}{\sqrt{1/r' - 1/r_0}} \tag{6.37}$$

$$= (2GM)^{-1/2} \alpha^{-1} (\tfrac{1}{2}\pi r_0^{3/2} - \tfrac{2}{3} r^{3/2}) , \tag{6.38}$$

where the latter expression holds only for $r \ll r_0$. At relevant times, of the order of one second, $(2GM)^{1/2} \sim 2 \times 10^{13}$, and the point of origin of the material is $r_0 \sim 10^8$. For given t, r_0 depends only very slightly on r.

As a consequence, the density of the material becomes very low. We have

$$\rho(r) r^2 dr = \rho_0(r_0) r_0^2 dr_0 . \tag{6.39}$$

Inserting Eq. (6.38), we get

$$\rho(r) = \rho_0(r_0) \frac{4}{3\pi} \left[\frac{r_0}{r} \right]^{3/2} . \tag{6.40}$$

Using Eq. (6.34), and expressing r_0 in terms of t by using just the first term in Eq. (6.38), we find

$$\rho(r) = \frac{2}{3} \frac{10^{31} C}{\alpha (2GM)^{1/2}} t^{-1} r^{-3/2} . \tag{6.41}$$

Setting $(2GM)^{1/2} = 2 \times 10^{13}$,

$$\rho = \frac{10^7 C}{\alpha t\, r_7^{3/2}} . \tag{6.42}$$

Thus, at given r, the density decreases as t^{-1}, and for $t \sim 1$, $r_7 \sim 1$ the density is of the order of 10^7, extremely small compared to the density in the core, which is several times 10^{14}, and also compared to the initial density at the same r, Eq. (6.34), which is of the order of 10^{10}. This argument was given by Cooperstein *et al.* (1984).

This explains the region of very low density, that Wilson found in his computations at r around 10^7 (see Fig. 14). In Sec. VI.F we shall see that this low-density region is filled by radiation, and in Sec. VI.G that the low density has great influence on the absorption of neutrinos and the revival of the shock.

F. The radiation bubble

Because the density is low, the energy supplied by neutrinos, Eq. (6.28), soon raises the temperature enough so that most of the energy resides in radiation rather than in matter. By "radiation" we mean the sum of electromagnetic radiation and electron-positron pairs. Assuming $T > m_e c^2 \sim 0.5$ MeV we find the radiation energy density

$$w_r = a_r T^4 = 3.75 \times 10^{26} T^4 \text{ ergs/cm}^3 , \tag{6.43}$$

where T is in MeV, while the energy density in nucleons is

$$w_m = 1.5 \times 0.96 \times 10^{18} T\rho \text{ ergs/cm}^3 . \tag{6.44}$$

Hence the ratio

$$w_r/w_m = 2.6\times 10^8 T^3/\rho \ . \tag{6.45}$$

The entropy in radiation per nucleon is (see Bethe and Wilson, 1985)

$$S_r = 2w_r/w_m \ . \tag{6.46}$$

Since ρ is quite small [se Eq. (6.42)], S_r can reach very high values, several hundred. By contrast, the entropy in the material is always of the order of 10 or less. Both entropy and energy reside mostly in the radiation.

We thus have a bubble that is almost free of matter, but has high pressure due to radiation. This radiation bubble is a natural way for the star to separate into a core, which will ultimately become a neutron star, and an envelope, which will be expelled. The envelope is supported and propelled by the radiation; see, however, Sec. VI.J. The core mass is all the material that has been accreted by about 1 second, i.e., by the time the radiation pressure has become sufficient to support the envelope.

The pressure is essentially all in radiation,

$$P = w_r/3 \ . \tag{6.47}$$

The equation of motion of the matter is

$$\ddot{R} = -\frac{GM_r}{R^2} - \frac{1}{\rho}\frac{\partial P}{\partial R} \ . \tag{6.48}$$

The first term alone is of the order of 10^{11} cm s^{-2}; since the relevant times are of the order of tenths of a second, this term would give enormous velocities. Therefore, inside the radiation bubble, there should be near compensation of the two terms; in other words, we have hydrostatic equilibrium. The radiation, which gives the main contribution to the pressure, is tied to the matter, because opacity for radiation is extremely great. The entropy S_r for a given mass element can only change when additional neutrino energy is absorbed. If S_r is large, this can only happen by neutrino-electron scattering, (see Sec. VI.H) or neutrino pair annihilation (Sec. VI.I). If S_r is known, P is a known function of ρ, and the hydrostatic equation, $\ddot{R}=0$, can be solved for $\rho(R)$. This is simplified by the fact that, in the bubble, M_r is essentially constant. Assuming $M_r = 1.65\ M_\odot$ according to Wilson's results, we have

$$GM_r = 2.2\times 10^{26} \ . \tag{6.49}$$

G. The cliff

Since the density of the matter in the radiation bubble is low [Eq. (6.42)], the core decouples from the surrounding material. The boundary condition at the surface of the core is, to a good approximation,

$$P(R_c) = 0 \ . \tag{6.50}$$

The mass of the core is just the mass that has accumulated by accretion up to the time when the radiation bubble is established. The temperature distribution is determined by neutrino diffusion and decreases very slowly with time. Thus the calculation of the density distribution is essentially a hydrostatic problem. We have, similar to Eq. (6.48),

$$\frac{1}{\rho}\frac{\partial P}{\partial R} = -\frac{GM_r}{R^2} \ . \tag{6.51}$$

Near the surface of the core, the right-hand side is essentially constant. In the Wilson computation underlying Fig. 14, at a time $t=0.8$ s after bounce,

$$\begin{aligned} &M_r = 1.66\ M_\odot \ , \\ &R = 19.6 \text{ km} \ , \\ &GM_r/R^2 = 5.6\times 10^{13} \text{ cm s}^{-2} \ . \end{aligned} \tag{6.52}$$

From the same computation, again near the core surface,

$$P \sim \rho^\gamma \quad \text{with } \gamma = 1.188 \tag{6.53}$$

$$\begin{aligned} \frac{d(P/\rho)}{dR} &= \frac{\gamma-1}{\gamma}\frac{dP}{\rho dR} \\ &= \frac{0.188}{1.188}\times 5.6\times 10^{13} \\ &= 0.89\times 10^{13} \ . \end{aligned} \tag{6.54}$$

This agrees well with Wilson's computed distribution of P/ρ. Using again Wilson's computer output, one can obtain

$$P/\rho = 0.89\times 10^{18}(25.4-R) \ , \tag{6.55}$$

where R is in km. Using γ from Eq. (6.53) and Wilson's output, we find

$$\rho = A\,(25.4-R)^{5.3}, \quad A = 1.28\times 10^{17} \ . \tag{6.56}$$

Of course, Eq. (6.56) is only valid as long as it gives a result greater than the density in the radiation bubble Eq. (6.42). The temperature is related to the density by

$$T \sim \rho^{\gamma'}, \quad \gamma' = 0.123 \ , \tag{6.57}$$

again using Wilson's output.

If the density is plotted against R, it looks like a cliff at a surface of the core, [cf. Eq. (6.56) and Fig. 15]. This means that essentially all neutrinos originate from the same sphere, about $R=20$ km. The cliff feature greatly simplifies the discussion of the core surface. Of course, the cliff comes about only when the material outside the core gets very thin, according to Secs. VI.E and VI.F.

At a later time, 3.6 s after bounce, and in a more recent calculation, Wilson and Mayle (1989) find the temperature in the cliff nearly constant. Then in the region where the material pressure dominates over radiation pressure, i.e., $S_r < 2$, the density distribution is given by a barometric formula,

$$\rho = A\exp(-r/H) \ , \tag{6.58}$$

where A is a constant and the scale height is

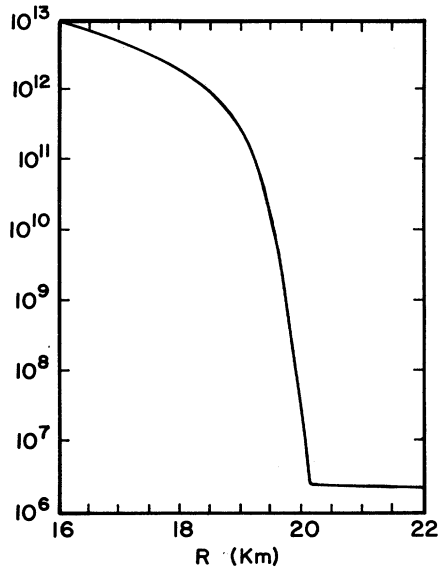

FIG. 15. Density, in g cm^{-3} vs position R, at late stage of computation. The density falls off precipitously, as in a cliff.

$$H=\frac{0.96\times10^{18}T(1+Y_e)r^2}{GM} . \tag{6.59}$$

With the figures from Wilson and Mayle, $T=3.35$, $Y_e=0.23$, $r=12.2$ km,

$$H=0.27 \text{ km} . \tag{6.60}$$

Thus the scale height is a small fraction of the radius—there is a cliff.

H. Neutrino-electron scattering

The radiation bubble separates the outgoing material (ejecta) from the core, which ultimately becomes a neutron star. The core continues to emit neutrinos for many seconds but the ejecta are too far away to effectively absorb them. But in the bubble itself there are negative and positive electrons, and these also can absorb neutrino energy, by elastic scattering. This has been emphasized by Wilson and Mayle (1989).

The transfer of energy from neutrinos to electrons takes place by elastic scattering. This does involve substantial energy transfer because the electron mass is small compared with the average neutrino energy (in elastic collisions of neutrinos with nucleons, very little energy is transferred because the nucleon is heavy).

The scattering of neutrinos has been calculated by Tubbs and Schramm (1975). If electron and neutrino energy are $\gg m_e$, and if the electrons and positrons are in a Fermi distribution with $\mu_e=0$, the absorption coefficient for electron neutrinos (or antineutrinos) by electrons and positrons is

$$\alpha=2.68\times10^{-2}\varepsilon_\nu T^4 \text{ km}^{-1} . \tag{6.61}$$

In the collision, the neutrino transfers approximately half its energy to the electron-positron gas. In the Wilson-Mayle computation, at $t=3.6$ sec,

$$\int T^4 dr=404 \tag{6.62}$$

(r in km). The average neutrino energy is

$$\varepsilon_\nu=4T_\nu=17 \text{ MeV} , \tag{6.63}$$

so the fraction of neutrino energy transferred to the electrons is

$$f_e=0.9\times10^{-3} . \tag{6.64a}$$

The μ-type neutrinos have a cross section smaller by a factor 4.7, but an average energy larger by a factor 1.6, so the fraction of *their* energy transferred to the electron gas is

$$f_\mu=0.3\times10^{-3} . \tag{6.64b}$$

Assuming, then, a total energy of 10^{53} in $\nu_e+\bar{\nu}_e$, and equal amounts in $\nu_\mu+\bar{\nu}_\mu$, and in $\nu_\tau+\bar{\nu}_\tau$, we find that this mechanism contributes to the shock an energy

$$E_\nu=0.15 \text{ foe} . \tag{6.65}$$

This is quite appreciable because the Wilson mechanism described in Secs. VI.C and VI.D yields only about 0.3 foe.

I. Neutrino pair annihilation

In 1989, Wilson and Mayle (1989) used a new mechanism, which apparently greatly enhances the delayed shock. It is the annihilation of neutrino pairs,

$$\nu_i+\bar{\nu}_i\rightarrow e^++e^- . \tag{6.66}$$

Its cross section is proportional to the square of the relative kinetic energy of the two colliding neutrinos, which is given by

$$\varepsilon^2=2\varepsilon_1\varepsilon_2(1-\cos\theta) , \tag{6.67}$$

where ε_1, ε_2 are the energies of the two neutrinos in the rest system of the star, and θ is the angle between their directions of motion. Therefore these collisions are highly effective only if the neutrinos collide more or less head-on. As Wilson and Mayle emphasize, this becomes possible when the cliff forms (Sec. VI.E).

It is a good approximation, then, to assume that the neutrinos originate from a definite neutrino sphere of radius R^*. The main condition for this is that $R^*\gg\lambda$ where λ is the neutrino mean free path at R^*; this is well satisfied when the cliff exists. Goodman, Dar, and Nussinov (1987), who first pointed out the importance of reaction (6.66) found that the rate of energy transfer to electron pairs at distance R from the center is

$$\dot{q}(R)=KF(\nu)F(\bar{\nu})(\varepsilon_\nu+\varepsilon_{\bar{\nu}})(1-x)^4(5+4x+x^2) , \tag{6.68}$$

where

$$x=[1-(R^*)^2/R^2]^{1/2} . \tag{6.69}$$

In Eq. (6.68), K is a constant, $F(\nu)$ and $F(\bar{\nu})$ are the energy fluxes of neutrinos and antineutrinos, and ε_ν and $\varepsilon_{\bar{\nu}}$ their average energies. $F(\nu)$ is essentially independent of R.

The averages of ε_ν, $\varepsilon_{\bar{\nu}}$ are proportional to the neutrino temperature. Therefore μ neutrinos are more effective for this process than e neutrinos. In the Wilson and Mayle calculation, the average neutrino energies are

$$\begin{aligned}\langle\varepsilon(\nu_e)\rangle&=10\text{ MeV},\\ \langle\varepsilon(\bar{\nu}_e)\rangle&=15\text{ MeV},\\ \langle\varepsilon(\nu_{\mu,\tau})\rangle&=24\text{ MeV}.\end{aligned} \tag{6.70}$$

(These were derived by me from the flux and the R_ν for the two types of neutrinos.) Wilson and Mayle point out that the *radii* of the two neutrino spheres should not be too different, because otherwise the energy gain from ν_μ annihilation by Eq. (6.66) will be lost immediately by emission of ν_e.

The total energy transfer from neutrinos to electrons may then be written as

$$\dot{Q}=b(t)L_\nu^2 , \tag{6.71}$$

where b is a function of neutrino temperature, or average energy, which is slowly decreasing with time. The neutrino luminosity L_ν is also slowly variable, so we may write

$$\dot{Q}=a(t)L_\nu , \tag{6.72}$$

which is the expression Wilson and Mayle use. This means that the total energy transfer to electron pairs is essentially proportional to the total energy emitted in neutrinos

$$Q=\langle a(t)\rangle E_\nu , \tag{6.73}$$

and E_ν, in turn, is essentially the gravitational energy released in the collapse—or better, the part released after the cliff forms, i.e., after about two seconds. This is about 10^{53} ergs. Wilson and Mayle find

$$\langle a(t)\rangle\sim 0.01 , \tag{6.74}$$

yielding an energy transfer of about 1 foe, the correct order of magnitude to agree with the observed energy release in SN 1987A (see Sec. VII.H).

In calculating this process, care must be taken that the electrons to which the energy is transferred not get so hot that they in turn reradiate the energy in the form of neutrinos. This effect has been taken into account by Wilson and Mayle in calculating Eq. (6.74).

The great advantage of neutrino pair annihilation over other mechanisms is that it persists as long as there is a neutrino energy flux out of the proto–neutron star [Eqs. (6.71) and (6.72)]. Thus the bubble continues to receive new energy all the time, and continues to exert pressure on the ejecta and thus to drive the shock, in spite of the fact that the bubble energy gets distributed over an ever-increasing volume. Colgate has emphasized (1971, 1989) that this is essential because otherwise some of the ejecta would continue to rain back on the proto–neutron star.

The electrons, + and −, produced in the process (6.66), have initially the same average energy as the neutrinos, i.e., of the order of 20 MeV. They quickly settle down, by emission of radiation and production of further electron pairs, to a thermal distribution of a temperature appropriate to their energy per unit volume. Because $\dot{q}$ decreases rapidly with R, so does the electron temperature. The inner, hot electron-photon gas exerts pressure on the gas further out, leading towards more uniform pressure. However, at 3.6 sec in the calculation of Wilson and Mayle, the pressure is still far from uniform.

Wilson and Mayle calculate that, after inclusion of the neutrino pair annihilation (6.66), the final energy of the supernova is about 1.5 foe. This is just about the energy observed in SN 1987A (see Sec. VII.G). It is therefore likely that the delayed shock, including the effects discussed in Secs. VI.C, VI.H, and VI.I, is the correct mechanism of supernova explosion.

J. Convection

The bubble is paradoxical in an important respect: density increases outward near its outer surface. Thus dilute material in the bubble has to support and push denser material in the ejecta. This clearly causes Rayleigh-Taylor instability. "Mixing," however, does not make sense because the material in the bubble and in the ejecta is of the same kind, nuclei and radiation.

The answer is convection: the entropy has an enormous negative gradient, being as large as 1000 or more in some region of the bubble and only about 10 at the shock. Hence the Schwarzschild condition for convection,

$$dS/dr<0 , \tag{6.75}$$

is amply fulfilled, and the Ledoux correction, $a(dY/dr)$ in Eq. (5.98), is negligible. Hence convection will occur.

Convection is very fast, and it will make the entropy more uniform. The theory of Sec. V.J may be used, in particular, Eq. (5.90), which relates dS/dp to the total energy current J. We assume that the pressure gradient exactly balances the gravitation [see Eq. (6.48)]. Radiation will still dominate; thus ρ can be written as

$$\rho=\frac{p^{3/4}}{KS} , \tag{6.76}$$

with

$$K=0.75\times 10^{11} .$$

We then have two equations connecting p and S with r. They can be integrated from the outside in; we choose to start at 4000 km, assumed to be the location of the shock. For the energy current, we assume

$$J=0.25 \text{ foe/sec} . \tag{6.77}$$

The results are as follows:

(1) The pressure rises only slowly, going from $r=4000$ to 1000 km; at smaller r, it rises very fast to compensate for gravitation. Because of the slow rise over the major part of the volume, it is a good approximation to assume that the pressure behind the shock is the same as if the net energy (internal minus gravitational) E were uniformly distributed over the volume. This gives a shock pressure

$$P_s=\frac{E}{4\pi R_s^3} . \tag{6.78}$$

This assumption has, in fact, been made in most calculations of nucleosynthesis (see Sec. VI.L).

(2) The entropy rises only moderately as we proceed inward. It is about 40 at $r=16$ km; it would be somewhat higher if we had assumed a higher energy flux than (6.77). This $S=40$ is much lower than the entropies, 100 to over 1000, obtained by Wilson and Mayle without convection. Lower entropy means lower matter temperature T_m. In Eq. (6.33) we have shown that the energy loss by reemission of neutrinos is proportional to T_m^6; therefore convection should reduce that energy loss. Wilson and Mayle point out (private communication) that, without convection, the neutrino flux is not quite sufficient to drive the revived shock. It may be hoped that the convection discussed here will make it sufficient.

(3) I have been able to show that convection will remedy this situation. The absorption of neutrino energy, as in the Wilson-Mayle theory, takes place mainly at r between 100 and 200 km. But the convection brings this energy to the shock front, whether that is at $R=300$ or $R=4000$ km, and thereby continually supports the shock. The shock will succeed in ejecting the material outside the bubble. About 1% of the energy of the ν_e and $\bar{\nu}_e$ is absorbed and given to the shock. Since $\nu_e+\bar{\nu}_e$ get about one-third of the energy released by gravitational collapse, and since that energy is about 3×10^{53} ergs, the mechanism gives a supernova energy of about 1 foe, in agreement with the observations discussed in Sec. VII.

K. Separation of ejecta from neutron star

The bubble that is formed in the delayed-shock mechanism appears to provide a natural way to separate the ejecta from the rest of the star. The material outside the bubble would be ejected, that inside would fall back on the core and become part of the neutron star. The bubble itself contains very little material, typically less than $0.01\ M_\odot$.

This simple picture is invalidated by convection. However, we may consider the net energy per unit mass,

$$e_{\rm pm}=3\frac{p}{\rho}-\frac{GM}{r} . \tag{6.79}$$

In the solution with convection discussed in Eqs. (6.76) and (6.77), this quantity remains positive down to $r=16$ km. We may surmise that separation occurs where $e_{\rm pm}=0$, i.e., very close to the surface of the proto-neutron star.

At what mass, then, does the separation occur? The computations of Wilson and his group show the bubble at an included mass of 1.6–1.67 $M_\odot$. How does this number come about?

The bubble forms about $\frac{1}{2}$ second after the center reaches nuclear density. Collapse has been going on for about $\frac{1}{2}$ sec before that time. Let us take a total elapsed time of 1 second since the gravitational collapse started. Inserting this into Eq. (6.38), we can calculate the radius r_o from which the material started that reaches the bubble location at $t=1$; we find

$$r_o=4.5\times10^8\alpha^{2/3} \text{ cm} . \tag{6.80}$$

Setting arbitrarily $\alpha=1$, Woosley's (1988) presupernova calculation yields, for the mass included in a sphere of radius $r_o=4.5\times10^8$,

$$M_r=1.63\ M_\odot . \tag{6.81}$$

This is just the mass found in Wilson's various calculations.

The choice of $\alpha=1$ may be approximately justified by the low density, which means that pressure gradients are likely to be small compared with gravitation. The choice of $t=1$ second is a very rough approximation, but at least the order of magnitude of the separation mass comes out correctly, especially since in Woosley's calculation the included mass is not very sensitive to r_o; approximately,

$$M_r\sim r_o^{0.10}\sim(\alpha t)^{0.07} . \tag{6.82}$$

The mass (6.81) agrees remarkably well with results previously derived from a totally different model. In these calculations, it was assumed that in the whole region behind the shock (and outside the neutron star), radiation pressure dominates over material pressure and is essentially uniform. This assumption was first made by Weaver (1980), and was used especially by Thielemann *et al.* (1990); it was justified in the convection calculation in Sec. VI.J and leads to an energy density

$$w=\frac{E}{(4\pi/3)R^3} , \tag{6.83}$$

where R is the shock radius. The energy is mainly in radiation and electron pairs. Thielemann *et al.* note that ^{56}Ni was observed in the ejecta from 1987A. To form ^{56}Ni from ^{28}Si by successive addition of α particles, the temperature must be above $T=350$ keV$=4\times10^9$ K. When the material subsequently cooled adiabatically, the ^{56}Ni will persist because it is the most strongly bound nucleus that is just a multiple of α particles. We therefore postulate that the energy density [Eq. (6.83)] be equivalent to $T=350$ keV; assuming (as above) that the energy is mostly in radiation and electron pairs, $T=350$ keV corresponds to

$$w = 3.5 \times 10^{24} \text{ ergs/cm}^3 . \quad (6.84)$$

Using Eq. (6.83), we find that the shock radius corresponding to this temperature is

$$R = (4100 \text{ km}) E_{51}^{1/3} , \quad (6.85)$$

where E_{51} is the total energy in foe. Taking $E_{51} = 1.5$, we get

$$R = 4\,700 \text{ km} . \quad (6.86)$$

Rather accidentally, this agrees with Eq. (6.80), the result derived from the Wilson model.

The calculated mass at the separation point, 1.63 ± 0.03 $M_\odot$, will be the baryonic mass of the neutron star. Once that star loses its heat, it contracts under gravitation, and its gravitational mass is between 1.4 and 1.5 $M_\odot$, just like the best-measured neutron stars. Since neutron stars are generally believed to be the remnants of supernova II events, it is tempting to assume that this mass is determined by the separation mass of the supernova. This will depend only slightly on the mass of the progenitor, which might vary from about 10 to about 30 $M_\odot$.

The mass of 1.6 $M_\odot$ is in good agreement with the total release of gravitational energy, as measured by neutrino emission (see Sec. IX).

The mass of 1.6 $M_\odot$ of the proto–neutron star is much larger than the homologous core of about 0.7 $M_\odot$ at which the shock first forms (Sec. V.B). The difference of 0.9 $M_\odot$ is picked up by the shock, but then falls back onto the core. The details of this process have been computed for the delayed shock. It is noteworthy that most of this accretion happens *before* the shock is revived by neutrino absorption; only about 0.05 $M_\odot$ accreted afterwards.

The separation mass is also larger than the mass of the Fe core, which is about 1.3 $M_\odot$, as we have discussed in Sec. V.F. In fact, according to Woosley's presupernova calculations, it is in the region in which ^{16}O and ^{20}Ne are the dominant nuclides. The transformation of these nuclides into ^{28}Si and ^{32}S is, of course, very rapid at $T = 350$ keV, and from there we proceed to ^{56}Ni. Starting from ^{16}O and ^{20}Ne has the advantage of providing additional energy to the shock, as compared with starting from ^{28}Si.

L. Nucleosynthesis

Nucleosynthesis in the supernova has often been calculated, making the assumption of uniform radiation pressure [see Eq. (6.83)]. Good agreement with observed distribution of nuclides has been achieved (Woosley, Pinto, and Weaver 1989; Thielemann *et al.*, 1990).

In their calculation, Wilson and Mayle (1989) find that 0.065 $M_\odot$ of ^{56}Ni are produced, in good agreement with the 0.075 $M_\odot$ observed in SN 1987A (see Sec. VII). Other nuclides have been calculated in Thielemann *et al.* (1990); they can of course not be measured as accurately as ^{56}Ni.

VII. SUPERNOVA 1987A

A. General

On 24 February 1987, Ian Shelton, a graduate student of astronomy at the University of Toronto, who was making observations at the 10-inch telescope at Las Campanas Observatory in Chile, noticed a spot on his photograph of the Large Magellanic Cloud (LMC) that had not been there the previous night. He first thought this was some dirt on the plate, but he then stepped outside and clearly saw a new star in the LMC (Shelton *et al.*, 1987). O. Duhalde, at the same location, also made this visual observation; both observations were on Feb. 24.23 Universal Time. They had discovered the first supernova since 1604 that was visible with the naked eye.

Slightly later, on Feb 24.37, Albert Jones, an amateur astronomer in New Zealand, saw 1987A in his routine monitoring of the LMC. On the previous night, at 23.39 he had not seen it; this puts its brightness at that time at magnitude 7.5 or higher, an important datum in the analysis, (see Sec. VII.C). On the other hand, R. M. McNaught had exposed a plate at date 23.443 (McNaught, 1987) and found the supernova at magnitude 6.5, at least one magnitude unit brighter and only about one hour later than Jones. This shows that SN 1987A brightened extremely rapidly, indicating that it started from a compact star.

The progenitor was Sanduleak $-69\,202$. Its location coincided with SN 1987A, and after the supernova had become transparent in the ultraviolet, it was found that Sk $-69\,202$ had disappeared. Our supernova thus was the first for which the progenitor is known except for "the very strange case of SN 1961V" as stated by Arnett, Bahcall, *et al.*, 1989. The progenitor was a B3I blue supergiant, of luminosity 4×10^{38} ergs/s (range $3-6 \times 10^{38}$). From this, one can deduce the mass of its He core to be 6 ± 1 $M_\odot$, corresponding to a main-sequence mass of

$$M = 16-22 \ M_\odot . \quad (7.1)$$

Its radius was $(3 \pm 1) \times 10^{12}$ cm, while a red supergiant would have a radius about 10 times larger.

These facts, as well as the observations and conclusions on SN 1987A, are very well summarized in the review article by Arnett, Bahcall *et al.* (1989), on which this and the next section are largely based.

A very important number is the distance of the LMC from the Earth. The accepted number is (Andreani *et al.*, 1987)

$$\begin{aligned} D &= 50 \pm 5 \text{ kiloparsecs} \\ &= (160 \pm 16) \times 10^3 \text{ light years} \\ &= (1.5 \pm 0.15) \times 10^{23} \text{ cm} . \end{aligned} \quad (7.2)$$

The events we are observing took place about 160 000 years ago, but it is customary and sensible to speak of the time they were observed on Earth. The distance must be

used to deduce absolute luminosities from observed brightness.

B. Neutrinos

SN 1987A also was the first supernova from which neutrinos were observed, in fact the first extraterrestrial source other than the sun. This was extremely important because the neutrino signal indicates the time when the explosion actually happened: the neutrinos get out of the supernova essentially without resistance, while electromagnetic radiation is closely tied to the material and can get out only when the shock reaches the surface of the star.

Neutrinos were observed by two laboratories, Kamiokande II in Japan (K II; see Hirata *et al.*, 1987, 1988), and IMB near Fairport, Ohio (see Bionta *et al.*, 1987; Bratton *et al.*, 1988). Both detectors consisted of very large tanks of highly purified water, deep underground to minimize cosmic-ray muons. Both were set up originally to detect the spontaneous decay of protons expected in some unified theories; no decay has been found so far. Both laboratories were equipped with automatic recording devices which also registered the time of events, so that, after the optical discovery of SN 1987A, the scientists could go back over the records and discover the neutrino signal from the SN.

The water detector responds primarily to electron antineutrinos,

$$H+\bar{\nu}_e \rightarrow n+\varepsilon^+$$

(n=neutron). The positron emits Cherenkov radiation, which is detected by thousands of photomultiplier tubes (PMT) ranged around the water container. These give the spatial distribution of the Cherenkov radiation, and thus the direction of the positron. The number of PMT responding is a measure of the energy of the positron, which is essentially that of the antineutrino. The K II detected is under 2700 m of water equivalent, which eliminates cosmic-ray mu mesons very effectively; they use special 20-inch PMT which permit them to detect $\bar{\nu}_e$ down to a threshold of about 8 MeV. The IMB detector is under only 1570 m water equivalent and has a larger cosmic-ray background; therefore it is not worthwhile to use very big PMT. They use 8-inch tubes and have a detection threshold of about 20 MeV. IMB has a bigger water tank, with a fiducial volume of about 5000 tons, while the fiducial volume of K II is 2140 tons.

Both laboratories are in the northern hemisphere, while SN 1987A is in the southern, but neutrinos, of course, penetrate through the Earth with ease. K II observed 12 neutrinos, IMB (because of its higher energy threshold) only 8. The time at IMB was accurately recorded as 7:35:41.37 UT for the first count and then continuing for about 6 seconds. At K II, the seconds were not accurately recorded (by their own statement); they give the time as 7:35:35, but there is little doubt that the first counts at the two laboratories were simultaneous within fractions of a second; the K II signal lasted for about 12 seconds.

Both laboratories made a monumental effort. The K II term included 15 Japanese and 8 Americans, the IMB had 37 members, including one Englishman and one Pole. Both published one preliminary report in April 1987, and one final in 1988. It is indeed fortunate that these two laboratories were operating at the time of the supernova explosion.

Two other laboratories also reported neutrino signals, Baksan in the Caucasus, and Mont Blanc. Compared with K II and IMB, both of them had rather modest amounts of material, in these cases liquid scintillator, namely 200 and 90 tons, respectively. Therefore only about one count could be expected from either one. Baksan reported five counts, but the first came 25 seconds after IMB, when the neutrino emission was expected to be essentially over; there was a big cosmic-ray background. It is unlikely that their counts are significant for SN 1987A.

Mont Blanc, which also reported five counts, has been very controversial (see, for example, de Rujula, 1987). I believe, as do also Arnett *et al.* (1988) and most other authors, that the Mont Blanc signal was unrelated to SN 1987A. Some of the reasons are (1) the signal occurred three hours before IMB. No signal at that time was found in the records of either IMB or K II. The K II detector, having about 20 times the volume of Mont Blanc and a similar energy threshold, should have found about 100 counts. (2) With the small mass of the Mont Blanc detector, five counts would have indicated a gravitational energy release of at least 10 times that which can be expected from the collapse of a star of about 20 $M_\odot$, or indeed of any star because much heavier stars would collapse into black holes and only emit a small fraction of their gravitational energy in the form of neutrinos. (3) A neutrino pulse at the Monte Blanc time would not fit to the observed light curve [see, for example, Woosley, 1988, Fig. 8(b)], while the K II–IMB time fits well, (see Fig. 16 below). Further arguments are given in Arnett *et al.*, 1989.

The neutrino observations from K II and IMB are extremely important for several reasons:

(1) The signal gives an exact time for the start of the explosion to which the light curve can be normalized.

(2) The number of the observed neutrinos (20), together with the calculable efficiency of the neutrino detectors, permits a calculation of the energy released in the gravitational collapse. This has been carried out by several authors, e.g., by Burrows (1987) and by Cooperstein (1988). The latter finds

$$E_g=(2.5\pm1)\times10^{53}\ \text{ergs}\ . \tag{7.3}$$

Spergel *et al.* (1987), having analyzed the temperature as well (see below), give

$$E_g=(3.7\pm2.1)\times10^{53}\ \text{ergs}\ , \tag{7.4}$$

assuming that there is equal energy emitted in each of the

six neutrino species $\nu_e, \bar{\nu}_e, \nu_\mu$, etc. From this, using the analysis of Cooperstein, one may deduce the baryon mass of the neutron star,

$$M = 1.6 \pm 0.4\ M_\odot\ . \tag{7.5}$$

This is compatible with the mass 1.6 $M_\odot$ derived in Sec. VI.J, but does not tie it down.

(3) The energy distribution of the neutrinos gives a measure of the temperature of the neutrino sphere. This again has been evaluated by many authors. The most careful evaluation is that of Spergel *et al.* (1987), who consider the K II and IMB observations together. They find best agreement if they assume an exponential decay of T^4 with a time constant $\tau = 4.5 \pm 2$ s and an initial temperature of

$$T = 4.2^{+1.2}_{-0.8}\ \text{MeV}\ . \tag{7.6}$$

A simpler analysis, assuming constant temperature, was made by Bahcall *et al.* (1987) and yielded

$$T = 4.1\ \text{MeV}\ . \tag{7.6a}$$

(4) The time distribution of the neutrinos is in reasonable agreement with theoretical predictions (see Sec. IX.A). On the face of it, there was a puzzle in the K II observations: there were 9 events in 2 seconds, followed by a gap of 7 seconds, followed by 3 more events. Some authors have speculated that this gap might indicate two separate pulses of high neutrino temperature. But in fact the gap seems to be a statistical accident: (a) Two of the IMB events fall right in the middle of the gap, between 5 and 6 seconds; (b) Similar gaps appear with appreciable frequency in Monte Carlo simulations of sparse events (Bahcall *et al.*, 1988).

Some conclusions from the neutrino observations have been drawn on the properties of neutrinos as such, for instance,

(1) Neutrinos survive a flight through space for 160 000 years. This excludes decay of the neutrino as an explanation of the deficit in detectable neutrinos from the sun. If the neutrino has a mass m_ν, its lifetime in its rest system is bounded by

$$t_0 > 5 \times 10^5\ \text{s}\ m_\nu \tag{7.7}$$

where m_ν is the mass in eV.

(2) An upper limit can be placed on the mass of the electron neutrino. Assuming a distance of 50 kiloparsec, the extra time Δt that a finite-mass neutrino requires to reach the earth, compared with a zero-mass particle, is

$$\Delta t = 2.6\ \text{s} \left[\frac{10\ \text{MeV}}{E_i} \right]^2 \left[\frac{m_\nu}{10\ \text{eV}} \right]^2 . \tag{7.8}$$

Many authors have exploited the time distribution of neutrino arrivals to find limits on m_ν. Some authors disregarded that the emission of neutrinos by the supernova was distributed in time. Arnett and Rosner (1987) and Bahcall and Glashow (1987) derived an upper limit of 11 eV for m_ν, assuming that the observed 2-s half-width of the neutrino pulse was not narrowed in transit by more than a factor of two. The most thorough statistical treatment was given by Spergel and Bahcall (1988), yielding

$$m_\nu < 16\ \text{eV}\ . \tag{7.9}$$

The same result was obtained independently by Burrows (1988). Laboratory measurements have given a similar limit.

(3) A limit can be placed on the magnetic moment of the neutrino, μ_ν. Lattimer and Cooperstein (1988) have shown that this moment cannot be greater than 10^{-12} Bohr magnetons, μ_B, provided the right-handed neutrino ν_R has a mass less than 10 MeV. If this condition is fulfilled, a normal, left-handed neutrino, ν_L, will turn into ν_R upon scattering by an electron at the rate

$$\alpha = (10^{12} \mu_\nu / \mu_B)^2 Y_e B_f \rho / \rho_0\ \text{sec}^{-1}\ , \tag{7.10}$$

where B_f is a blocking factor due to electron degeneracy, ρ is the density at which the scattering takes place, and ρ_0 is normal nuclear density. The scattering is supposed to flip the neutrino spin, making a ν_L into a ν_R. The latter has no interaction with ordinary matter, cannot be detected by present experiments, and will escape quickly from the supernova. Lattimer and Cooperstein show that appreciable spin flip of this kind would contradict the experimental observations and conclude that

$$\mu_\nu < 10^{-12} \mu_B\ . \tag{7.11}$$

C. Optical observations

After its discovery, SN 1987A was observed systematically every night by observatories in the southern hemisphere. Prominent among them were the Cerro Tololo Inter-American Observatory (CTIO; Blanco *et al.*, 1987), and the South African Astronomical Observatory (Menzies *et al.*, 1987; Catchpole *et al.*, 1988). This was a monumental effort: in the first paper 12 authors were involved, in the second 16, and in the third 20.

As a result, we have light curves from both observatories over a very long period, and they agree well with each other (see Fig. 16). Looking at the bolometric intensity, it starts from a very high maximum before the observations began, drops to a minimum at about 7 days with a magnitude $M_{\text{bol}} \sim 4$, then rises slowly to a maximum of magnitude about 2.4 at 85 days, drops fairly quickly to $M = 3.4$ at 125 days, and drops slowly from then on, following an exponential decay with a half-life of about 77 days. The *visual* magnitude follows a similar curve after 7 days, but at early times it has a sharp rise followed by a plateau at magnitude about 4.5 (see Fig. 18 below). These observations will be analyzed in Sec. VII.E.

From the spectral indices, like Blue minus Visual (B−V), and Visual minus Infrared (V−I), the effective

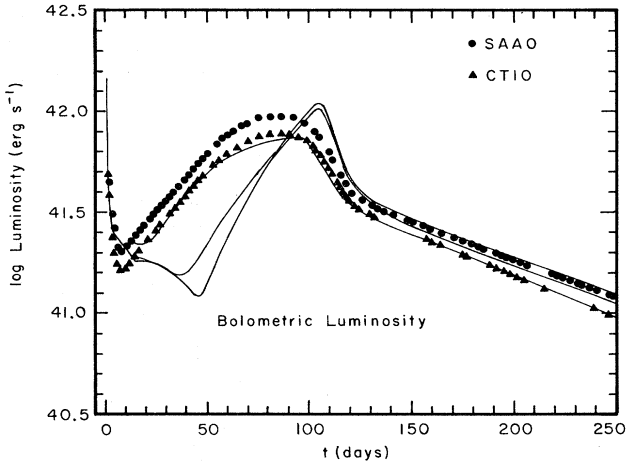

FIG. 16. Bolometric luminosity of Supernova 1987A, as observed by the Cerro Tololo Inter-American Observatory (CTIO) and the South African Astronomical Observatory. The three theoretical curves are from Woosley, Pinto, and Weaver (1989); the one that fits CTIO includes mixing, the other two do not.

tempera ure can be deduced (Catchpole *et al.*, 1988; Hamuy *et al.*, 1987). It starts out very high ($>15\,000$ K), since the material emerges from the star very hot and well ionized, hence opaque. It then drops rapidly and, after about 20 days, settles down at 5500 K. This is, at the prevailing density, the temperature at which atomic hydrogen gets ionized. The interpretation is that inside the photosphere, hydrogen is ionized and hence opaque to visible (and infrared) radiation whereas outside hydrogen is neutral and transparent. As times goes on, the material cools, and more hydrogen recombines; a recombination front travels inwards through the hydrogen envelope (Hamuy *et al.*, 1988; Woosley, 1988). The photosphere indicates the present position of that front. Its position in space can be calculated from the instantaneous, measured intensity of radiation and the radiation per unit area aT^4 ($T=5500$ K). Physically, the motion of the recombination front is determined by the rate at which radiation (aT^4) can dispose of the energy residing behind the photosphere (see Sec. VII.H).

Spectra were observed from early on, showing prominent hydrogen lines, making this a Type II supernova The width of the Hα line is very large to begin with, indicating (from the Doppler effect) a velocity near 20 000 km/s. It becomes narrower with time, indicating at 40 days a velocity of 7000 km/s. The velocities indicated by Hβ and Hγ are slightly smaller. These strong hydrogen lines indicate the velocity far out in the exploding supernova because only a small amount of H is needed to give optical depth one. The lines are therefore not significant for information on the photosphere.

The velocity of the material at the photosphere is probably best indicated by two Fe II lines, of wavelengths 5018 and 5169 Å, yielding $v=8000$ km/s early and 2100 km/s after about 40 days. This latter number may be considered the velocity of the slowest hydrogen, at the bottom of the H envelope. The Brackett γ line, transition from $n=4$ to $n=7$ in H, shows the same velocity as Fe II, up to about 100 days (Phillips, 1988, Elias *et al.*, 1988): For this transition between high levels of H, the intensity is much lower than for Hα, so that the absorption line presumably refers to the photosphere. After 100 days, the velocity indicated by Brackett γ remains at 2100 km/s, indicating that this is indeed the bottom of the H envelope, while the Fe II velocity declines again, which indicates that the photosphere now recedes into the He mantle.

Later spectroscopic data show the appearance of a host of nuclei formed by nucleosynthesis in the explosion. This is discussed, for example, by Woosley *et al.*, 1989.

D. Why was progenitor blue?

The progenitor of SN 1987A was a blue supergiant, Sanduleak $-69\,202$. This was a great surprise because it had generally been believed that stars at the end of their life, before they become supernovae, are *red* supergiants. In fact, in early discussions, astronomers looked on plates exposed before the explosion, for red stars close to the location of 1987A (e.g., Blanco *et al.*, 1987). Woosley, Pinto, and Ensman (1988) showed theoretically, from the observed light curve, that the progenitor had to have properties very close to those of Sanduleak $-69\,202$. Then, when the supernova had become transparent in the ultraviolet it was observed that Sk $-69\,202$ had indeed disappeared, settling the question (Gilmozzi *et al.*, 1987; Sonneborn, Altner, and Kirshner, 1987; Walborn *et al.*, 1987).

The question was then hotly discussed how a blue supergiant could become a supernova. For a while, some theorists (Arnett, 1987; Truran and Weiss, 1987; Hillebrandt *et al.*, 1988) proposed that Sk $-69\,202$ had been blue all its life. But this has become unlikely because of the observation of low-velocity (15–20 km/s) nitrogen-rich gas (Casatella *et al.*, 1987; Kirshner *et al.*, 1987), presumably a circumstellar shell. This indicates that Sk had some mass loss, and mass loss is much more likely for an extended, red supergiant. The observed shell then represents material from deep inside the star which had undergone the CNO cycle and was dragged up by convection; the CNO cycle converts most of the C and much of the O into N, hence the observed large ratio of N/C in the circumstellar gas. Another argument for a red phase of Sk is the large number of red supergiants found in the Magellanic Cloud near SN 1987A. (There are also many blue supergiants.)

The most thorough study of the "blue problem" has been made by Woosley, Pinto, and Weaver (1989). They computed the evolution of stars between 15 and 25 $M_\odot$, varying many parameters. The fundamental reason for some stars to end their life in the blue is the existence of two solutions for the stellar envelope for a given mass of

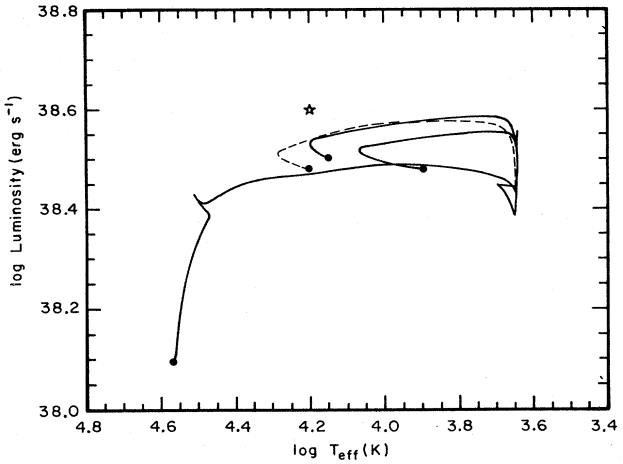

FIG. 17. Theoretical evolution of the progenitor of SN 1987A, from the blue ($\log T_{\rm eff}=4.6$) to red ($\log T_{\rm eff}=3.6$) to blue. From Woosley *et al.* (1989).

the He core, one solution having an extended, convective envelope (red), the other a compact, radiative one (blue). This was pointed out by Barkat and Wheeler (1988) and by Woosley, Pinto, and Ensman (1988).

Figure 17 shows the evolution of three stars of 18 $M_\odot$ according to Woosley *et al.* (1989); their caption reads "Hertzsprung-Russell diagram for three 18-$M_\odot$ stars evolved through hydrogen, helium, and carbon burning with a small semiconvective diffusion coefficient (10^{-4} that of radiation) and two different mass loss rates. The left-most of the two solid lines corresponds to a star having a mass loss rate three times that of de Jager (1985) and a final stellar mass of 16.2 $M_\odot$ (model 18A; hydrogen envelope equals 11.5 $M_\odot$). The right-most solid line is a model that used three times the de Jager rate on the main sequence (as before), but six times the de Jager prescription when the star was a red supergiant. This star ended up with a mass of 14.7 $M_\odot$ (model 18B; hydrogen envelope 9.2 $M_\odot$). This latter star died in a state of thermal disequilibrium while making a transition back to the red during carbon burning. 18 $M_\odot$ stars that have lost this much mass or more cannot have been SN 1987A. The dashed line is a variation of model 18A that was artificially made to mix up more helium into the envelope."

All three stars start their lives in the blue on the main sequence. Most of their He-burning phase is spent in the red, but then they return to the blue during C burning. The model 18A stars end their life in the blue, as desired, while 18B is on the way back to the red.

Woosley *et al.* conclude that several features have to come together to make a star blue before explosion:

(1) The abundance of elements heavier than He (metallicity) must be low. Specifically, they choose this to 0.5% by weight, one quarter of that in the sun. This reduces both the opacity and the rate of the CNO cycle, specifically the reaction $^{14}{\rm N}(p,\gamma)^{15}{\rm O}$, which determines the rate of the cycle. They show that both these reductions are necessary to make the star return to the blue.

(2) The star must have a mass between about 10 and 20 $M_\odot$ (perhaps 25 $M_\odot$), no matter what the metallicity. Heavier and lighter stars, for different reasons, will stay red.

(3) The mass loss during the red supergiant stage must be moderate. This is illustrated in Fig. 17, where model 18B is on the way back to the red before exploding. This model had twice the mass loss of 18A, and Woosley *et al.* conclude that the mass loss should not be more than 3 $M_\odot$. (On the other hand, the existence of the circumstellar shell makes a mass loss >1 $M_\odot$ likely.) If we accept the main-sequence mass of 18 $M_\odot$ and the corresponding He core mass of 6 $M_\odot$, the mass of the hydrogen envelope should be between 9 and perhaps 11 $M_\odot$, in agreement with the result of many model calculations (Sec. VII.E), which favor an envelope of about 10 $M_\odot$.

(4) "Semiconvection" should be small. This is a phenomenon that occurs when convection is allowed by the Schwarzschild criterion, $dS/dr>0$ (S=specific entropy), but is forbidden according to the Ledoux criterion (see Sec. V.J), which takes the gradient of chemical composition into account. Astrophysicists engaged in calculating stellar evolution believe that in these circumstances a slow diffusion takes place, with a diffusion coefficient a fraction α of that for radiation. Conventionally, α has been assumed to be 0.1, but this value will make the star remain in the red. Values of $\alpha=10^{-3}$ or less are needed to make the star end up in the blue. Woosley *et al.* warn that this may not indicate that α is always this small; it may depend on special circumstances.

They conclude that supernovae like SN 1987A may be uncommon events.

E. Theoretical model of Woosley

Very thorough theoretical studies of 1987A have been made by Woosley's and Nomoto's groups. Woosley's results are summarized in his paper (1988). He starts from a presupernova model that gives the initial distribution of density. The mass of the He core is known to be 6 $M_\odot$ (see Sec. VII.D), and the total main-sequence mass is then 18 $M_\odot$. However, it was not known *a priori* how much of the H envelope had been lost during the red supergiant stage. That *some* had been lost was shown by the discovery of the circumstellar shell, which was highly enriched in N (see Sec. VII.D). Some authors suggested that the remaining hydrogen envelope might be as thin as 1 $M_\odot$; therefore Woosley investigated envelope masses of 1, 3, 5, 10, and 14 $M_\odot$. By his analysis, he shows that 10 $M_\odot$ is the most likely mass of the envelope. A similar conclusion has been reached by Nomoto and his collaborators (see Sec. VII.F).

Woosley then makes a schematic study of the explosion, in which he assumes that a piston expels the material with a certain kinetic energy E, starting from the sur-

face of the iron core at $M=1.33$. He chooses two values of the explosion energy, 0.65 foe (called L, low energy) and 1.4 foe (called H, high energy). H generally fits the observed light curve better, but the final decision is due to the observed *velocity* of the material, which indicates the kinetic energy per unit mass (Arnett, 1988; Nomoto, and Shigeyama 1988). As will be discussed in Sec. VII.H, once an envelope mass of $M_\odot$ is chosen, the observed velocities lead essentially uniquely to the high explosion energy of about 1.4 foe.

Woosley then follows the shock wave to the time when it reaches the outer surface of the star. Then, and only then, can the light break out of the star, because the electromagnetic radiation is firmly tied to the matter. This breakout occurs 1.7 hours after the initial collapse if we take the preferred model 10 H (i.e., mass 10 $M_\odot$ of the H envelope, and high energy release). Other theoretical models gives similar results. This shows clearly that the neutrino pulse at Kamiokande and IMB, not that at Mont Blanc, signals the initial collapse of the star (see Sec. VII.B). This is even more closely shown by the time at which McNaught observed the first light from the supernova, and by the fact that Jones did not observe light [see Sec. VII.A and Woosley, 1988, Fig. 8(a) and (b)].

At breakout, the radius of the star is 3×10^{12} cm; at McNaught's time it is $2-3\times10^{13}$. Woosley deduces from this that 10^{23} g of material traveled at a speed of 40 000 km/s. The temperature of the surface at breakout is about 4×10^5 K. After half a day, it has decreased to 2×10^4 K. The total energy emitted in the first day, in hard ultraviolet, was about 10^{47} ergs. The total energy of radiation during the whole time of observation was of order 10^{49} ergs (see below). The temperature of the radiating surface was observed from day 2 on; it decreased to 5500 K after 20 days (Sec. VII.C).

Figure 18 shows the predicted visual magnitude of 1987A for the first two days, according to Woosley (1988), compared with observations. The agreement is excellent for the first point (McNaught's observation) and fair for the observations after 1.3 days. But at intermediate times, 0.3 to 1.3 days, the observed luminosity falls short of that calculated by Woosley by about a factor of two (see Fig. 18) This discrepancy has been explained by Pizzochero (1990): it is due to Woosley's assumption that the radiation is blackbody. In reality, this is not the case because the radiating gas is very dilute, and therefore there is no local thermal equilibrium (LTE). Radiation from the hotter interior is merely scattered (not absorbed) by the electrons in cooler layers; it keeps the color temperature from the hot layer and is hence rich in ultraviolet and relatively poor in the visible, relative to blackbody. The Woosley calculation of the total radiation must be somewhat corrected downward because the scattering dilutes the flux, but the main change is that the visible radiation is a smaller fraction of the total. Pizzochero has estimated the expected visible radiation for the time 0.5 d, considering the scattering by free electrons from H and He and the opacity arising mainly from the

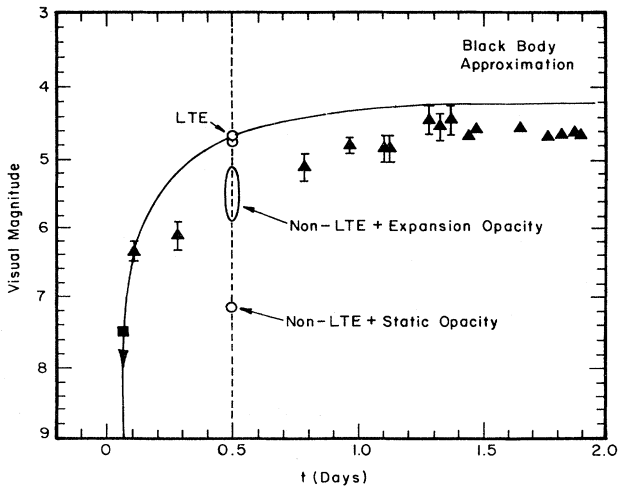

FIG. 18. Early visible light, as observed by CTIO and South Africa. The theoretical curve is from Woosley (1988), assuming the mass of the hydrogen envelope to be 10 $M_\odot$ and the explosion energy 1.4 foe. The theoretical curve must be corrected for deviations from local thermal equilibrium (LTE); see text. These deviations, as calculated by Pizzochero (1990), are given at $t=0.5$ days.

spectral lines of heavier elements. The latter is greatly increased by the Doppler effect due to the high velocity of the material, which varies with altitude and hence effectively broadens the lines. This opacity is difficult to calculate, which accounts for the large uncertainty of Pizzochero's result, marked "non-LTE, expansion opacity" in Fig. 18, but it is clear that his theory brings the visual luminosity down into the range of the observations. Also given in Fig. 18 is the theoretical luminosity assuming only the Doppler effect due to temperature, the "static opacity."

At breakout again, the specific internal energy of the matter (calculated from the model) is nearly constant throughout the star; it is about 10^{16} ergs/g. (Only at the very outside is it larger, because that material, being very dilute, was traversed by the shock much faster than the bulk of the star.) After breakout each material element travels at nearly constant speed because the gravitational energy, GM/r for $M\sim20\ M_\odot$ and $r>10^{13}$ cm, is very small ($<2\%$) compared to the kinetic energy, $\frac{1}{2}v^2$ for the observed velocity at the photosphere, $v>2\times10^8$ cm/s (see also Sec. VII.H). Hence r for a given mass element is proportional to t, and the density to t^{-3}. The internal energy is mainly in the form of radiation, so that the adiabatic index $\gamma=4/3$; therefore the temperature will go down as t^{-1}. Thus most of the initial internal energy is used up in pdV work. The total internal energy in an H envelope of 10 $M_\odot$ is initially 2×10^{50} ergs (note: much less than the kinetic energy of 10^{51} ergs), but only about 0.7×10^{48} of this appears as radiation.

The radiation cannot come out all at once but is limited by the blackbody emission from the photosphere, aT_e^4. The radius of the photosphere increases steadily, and this

increase is more important than the decrease in temperature, except for the first few days, so the bolometric luminosity increases with time, from a minimum of $\log L=41.2$ at 7 days to a maximum of $\log L=41.9$ at about 90 days. The observed luminosity and temperature can be used to derive the radius of the photosphere versus time; the photosphere moves outward relative to the center of the star while it moves inward as a recombination wave (Sec. VII.C) relative to the material. The difference is the velocity of the material at the photosphere, which is measured by the Doppler effect of the Fe II lines (Sec. VII.C).

If the internal energy of the matter (deposited by the shock) were the only source of energy, the radiation would stop abruptly after the recombination wave had gone through the H envelope. Woosley (1988) has shown this in a model calculation, his Fig. 15(a). But there is another source of energy, the radioactive decay of ^{56}Co. The supernova shock produces ^{56}Ni by explosive nucleosynthesis. The half-life of ^{56}Ni is too short, six days, to be directly seen in the supernova, but that of the daughter nucleus, ^{56}Co, is 77 days. The luminosity of SN 1987A, after 120 days, falls off with exactly that half-life, showing that ^{56}Co radioactivity is the source of energy at these late times. The decay of ^{56}Co to iron gives an energy of 6.4×10^{16} ergs/g; therefore from the observed luminosity Woosley deduced that the amount of ^{56}Ni formed was 0.075 $M_\odot$. This is a very important result, which should be reproduced by any correct theory of the explosion.

Counting also the energy release by ^{56}Ni, of 3.0×10^{16} ergs/g, one finds that the total energy supplied by the radioactivity is 1.3×10^{49} ergs. Some of the radioactive energy, but not very much, is again lost by adiabatic expansion of the material to which it is supplied, but the integrated luminosity in the radioactive phase is about 6×10^{48} ergs, roughly eight times that from the shocked material (see above).

Since there are two sources of energy, the shocked material and the radioactivity, we might expect some discontinuity in the luminosity in the transition from one to the other. None is observed. The observed luminosity is a completely smooth function of time. Woosley argues that this indicates that the radioactive energy arrives at the photosphere before the latter has gone through all the hydrogen. If the mass of the hydrogen envelope is small, 1 or 3 $M_\odot$, this happens very quickly, then the luminosity reaches a maximum much too early (see Fig. 19). The luminosity then drops abruptly until the radioactive energy reaches the photosphere. Maximum L is reached after 28, 36, 53, 90 days if the mass of the H envelope is 1, 3, 5, 10 $M_\odot$ and the high explosion energy (1.4 foe) is assumed. The latter is reasonable for 10 $M_\odot$ but not for the lower masses; the best known quantity is the ratio of energy to mass (see Sec. VII.H). If we accordingly choose the low energy, 0.65 foe, for the case of 5 $M_\odot$, the maximum is shifted to 73 days. Thus either 5 or 10 $M_\odot$, with appropriate explosion energy, is acceptable from this point of view, but Woosley shows that 1 or 3 $M_\odot$ are hopeless.

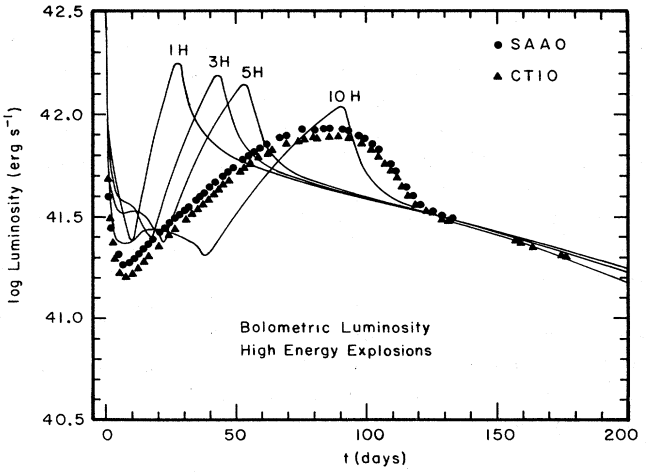

FIG. 19. Models of light curve for high explosion energy (1.4 foe) and for several assumed masses of the hydrogen envelope, from 1 to 10 solar masses. From Woosley (1988). No mixing was assumed.

A different method of determining the envelope mass was used by Saio *et al.* (1988b). They use the observed N/C and N/O ratios in the shell of expelled material (see Sec. VII.C) to put limits on its mass and hence on that of the envelope. They find $7\ M_\odot < M_{\rm env} < 11\ M_\odot$. From an analysis of the structure of the progenitor itself, Barkat and Wheeler (1988) find $M_{\rm env} > 7\ M_\odot$ if the He abundance in the envelope is $Y=0.4$, a value consistent with that of Saio *et al.* (1988b).

Even with the best mass, between 7 and 11 $M_\odot$, and the correct ratio of explosion energy to mass, the theoretical light curve is still not satisfactory: it has too sharp a maximum. In particular, it falls off too sharply after the maximum. Woosley's remedy is to assume mixing of elements in the various regions of the star. One part is mixing of some He into the inner part of the envelope. This, he points out, is likely to happen near the end of the main-sequence stage of the star. The second type of mixing concerns the distribution of ^{56}Ni in the star; originally, this isotope is formed at the inner edge of the ejecta, but the γ-ray observations (Sec. VII.I) show that some of it must be widely distributed through the mantle and also through some of the envelope. This makes the radioactive energy appear near the photosphere.

Pinto and Woosley (1988a) derived a distribution of ^{56}Ni from the early appearance of x rays and γ rays (Fig. 1 of Pinto and Woosley, 1988a). This was then used to calculate the light curve, Fig. 16.

It is seen that the theoretical curve in Fig. 16 matches closely the observed light curve. Undoubtedly, the details of the mixing are not uniquely determined by the light curve, but the fact of mixing is unquestionable. So is the approximate value of the envelope mass.

We have discussed earlier the fact that the luminosity

after 120 days behaves exactly as the energy released by the radioactivity of Co. However, at the maximum, about 90 days, the luminosity is about twice that given by the instantaneous radioactive energy. The energy deposited by the original shock, as we discussed earlier, is used up by about 40 days. The luminosity at the maximum should therefore be interpreted as due to radioactive energy released earlier than day 90, energy which was stored in the material and gradually made its way to the photosphere.

After about 500 days, the visual light from SN 1987A fell below the level expected from decay of ^{56}Co, but when infrared emission (out to 20 microns) is included, the theoretical curve is still followed very well (S. E. Woosley, private communication).

F. Theoretical model of Nomoto

Nomoto and his group emphasize the mixing of heavy materials, including the radioactive ^{56}Co, through large parts of the star. No longer is the star a well ordered onion, with the heavy elements C, O, Si, and ^{56}Co at the center, He next to these in the mantle, and an envelope of H. Instead, the heavy elements penetrated far out into the envelope, all in qualitative agreement with Woosley.

The evidence comes chiefly from the γ- and x-ray observations (see Sec. VII.I). These radiations became observable much earlier than expected, indicating that the ^{56}Co was closer to the surface of the star. Kumagai *et al.* (1989) exploit the observations in great detail. They find that the radioactive ^{56}Co extends out to $M_r = 9.5\ M_\odot$, as do C, N, O, Si, and S. Helium dominates out to 5 $M_\odot$ from the surface and is still 45% of the material at 1 $M_\odot$ below the surface of the star. Their distribution of ^{56}Co is in reasonable agreement with Pinto and Woosley (1988a).

The physical mechanism for this extensive mixing is Rayleigh-Taylor instability at the surface between the original He and H (see Sec. VII.J).

The conclusions of Nomoto's group are summarized by Shigeyama and Nomoto (1990). Apart from somewhat increased mixing, their conclusions are generally similar to those of Woosley *et al.* They also favor a mass of the envelope of about 10 $M_\odot$ (they quote the mass of the ejecta as 14.6 $M_\odot$; the ejecta include about 4.5 $M_\odot$ which were originally He and heavier elements). Nomoto noticed already in 1987 that the light curve determines the *ratio* of supernova energy to ejecta mass, not the absolute energy; their result for the absolute energy is

$$E = 1.0 \pm 0.4 \text{ foe} . \tag{7.12}$$

Using the distribution of materials derived by Kumagai *et al.* (1989), Shigeyama and Nomoto can reproduce the early light curve (Fig. 18; this figure is actually taken from Woosley) and the late light curve (Fig. 20) very well, including especially the broad peak from 50 to 100 days. In Fig. 20 they include, for comparison, the light curve that would be predicted if all the ^{56}Ni

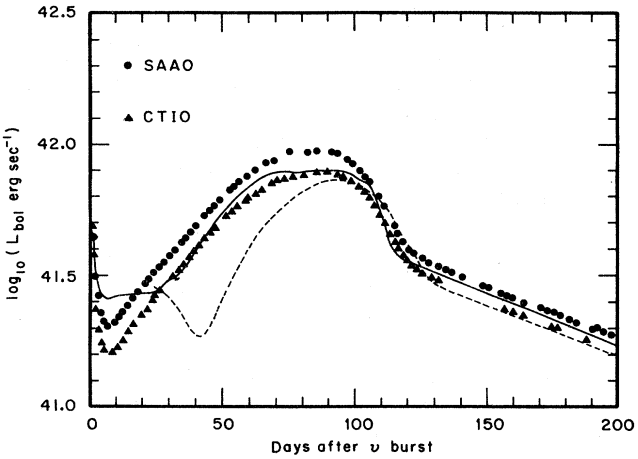

FIG. 20. Measured bolometric light curves compared with theory of Shigeyama and Nomoto (1990). Solid curve assumes full mixing, dashed curve assumes no mixing, with ^{56}Ni confined in innermost layer.

remained near the inner edge of the ejecta where it is produced (dashed curve). It is very convincing that mixing does occur.

Further evidence for mixing comes from the observation that the spectrum appears different from day 25 on. Shigeyama and Nomoto suggest (in agreement with other authors) that this indicates the arrival of radioactive material near the photosphere. They point out that this indicates *early* mixing, before the ejecta actually emerge.

Shigeyama and Nomoto have found an explicit formula for the inward velocity of the recombination front relative to the material; it is of order 1000 Km/s. Using this, they find that the front arrives at the bulk of ^{56}Co at about $t = 37$ days (but it meets some low density of ^{56}Co already at day 25, in accord with the discussion in the last paragraph). Using this relative motion of the recombination front, together with their calculated velocity of the matter, they find that the front is nearly stationary at $r = 8 \times 10^{14}$ cm (relative to the center of the star) from $t = 60$ to 100 days, i.e., during the broad maximum of light. They point out that this plateaulike maximum comes about because both the effective temperature and the radius of the photosphere stay constant.

The picture of very extensive mixing at an early stage explains in a natural way the absence of any break in the light curve at the time when the energy source changes from stored shock energy to radioactive energy.

G. Calculations of Arnett

Arnett and his group have made two important contributions to the theory of supernovae of Type II, viz., (a) semianalytic treatment of the light curve and (b) a detailed computation of the mixing.

The analytic treatment starts from a previous theory (Arnett, 1982) of the light curve of supernovae of Type I which derive their luminosity chiefly from radioactivity.

He shows that their light curve is determined by one parameter,

$$y=\tau_m/2\tau_{\rm rad}\ , \tag{7.13}$$

where $\tau_{\rm rad}$ is the lifetime of the radioactive nucleus (^{56}Ni in SN I, ^{56}Co in SN II) and τ_m is the geometric mean of the radiation diffusion time

$$\tau_0=\frac{9}{4\pi^3}\frac{\kappa M}{cR_o} \tag{7.14}$$

and the hydrodynamic time of the homologous expansion of the ejecta,

$$\tau_h=R_o/v_{\rm sc}\ . \tag{7.15}$$

He notes that τ_m is independent of the radius R_o of the supernova. Knowing $v_{\rm sc}$ from observation one can thus deduce the product of the mass and the mean opacity κ.

In SN 1987A, the light curve depends also on the distribution of radioactivity in the star, i.e., on the fraction b of the star radius occupied by ^{56}Co and its distribution within this radius. Arnett and Fu (1989) find that $b=0.4$ gives good agreement with the observed light curve; this value is in good accord with the distributions derived by Woosley (Sec. VII.E) and Nomoto (Sec. VII.F). Arnett and Fu show that their analytic light curve agrees with observation as well as the model calculations (Secs. VII.E and VII.F).

In this statement, they must exclude the first 20 days, when the luminosity is provided by energy stored in the material due to the shock. Arnett and Fu discuss the luminosity provided by radioactivity.

For any values of the parameters, the light curve has a broad maximum. The time of this maximum depends on the initial radius of the supernova. For a large radius, the maximum occurs late and is correspondingly low. It also depends on the temperature of H recombination. For the observed $T=5500°$, the maximum occurs at the right time (about 90 days); for $T=11\,000°$, it would occur too early, while it would come too late if there were no recombination. The ejected mass influences the light curve after the maximum. For 15 $M_\odot$ the light decreases with just the exponential given by the radioactive decay of ^{56}Co; if the mass were only 7.5 $M_\odot$, the light would decrease faster, because the γ rays could easily escape from the star instead of depositing their energy inside it.

The extent of mixing of Co influences mostly the γ detection. The most important parameter is b, the radius out to which the Co is spread: $b=0.1$ and 0.2 give far too few γ rays and too late; $b=0.4$ is more acceptable, but better agreement is achieved if in addition 1% of the Co extends as far as $b=0.9$. This parameter has little influence on the light curve.

Arnett and Fu finally calculate the late light curve in the presence of a neutron star pulsar. They can exclude a pulsar luminosity of 5×10^{39} ergs/s by using the observed curve up to 340 days, and predict the behavior up to 1500 d for pulsars of 2 and 1×10^{39}.

In the *mixing* calculation, Arnett, Fryxell, and Müller (1989) and Fryxell *et al.* (1990) start from a presupernova distribution of a 15-$M_\odot$ star by Arnett (1987). They evolve this for 300 seconds using a one-dimensional Eulerian code and find regions of Rayleigh-Taylor instability just inside the interface between heavier elements (C,O, etc.) and He, and again inside the He-H interface. They then impose a fluctuation of the density contours of 10 (or 1) percent and follow the further motion in two dimensions, using cylindrical coordinates. The computations are carried out with a very sophisticated method, which achieves high resolution. Artificial viscosity is not required to stabilize shocks. They were able to use as many as 500×500 spatial zones and obtained very impressive density contours after three hours for an explosion energy of 1 foe, and after two hours for 2 foe. Long fingers of high density project into the less dense material. Similarly, much mixing of C and O into the outer He layers was found, as well as He into the H envelope and vice versa.

H. Energy

Many authors have derived the energy of SN 1987A from the light curve using models, e.g., Arnett, 1988; Shigeyama, Nomoto, and Hashimoto, 1988; Woosley, 1988; Shigeyama and Nomoto, 1990). We have discussed Woosley's calculations in Sec. VII.E, those of Nomoto *et al.* in Sec. VII.F, and those of Arnett in Sec. VII.G; they show that an energy of at least 1 foe is most likely.

Nomoto has emphasized repeatedly that the optical data determine primarily the *ratio* of the energy to the mass of the hydrogen envelope. That mass has been determined by studies of the progenitor star and of the circumstellar shell (see Sec. VII.C) by Saio *et al.* (1988a, 1988b) and by Barkat and Wheeler (1988); the result is

$$M_{\rm env}=7 \text{ to } 11\ M_\odot\ . \tag{7.16}$$

Woosley's model calculations (Sec. VII.E) and his study of the "blue problem" (Sec. VII.D; Woosley *et al.*, 1989) also favor a mass in this range.

Bethe and Pizzochero (1990) have found a method for deriving the specific energy (i.e., energy per unit mass) from the observations essentially without a model. The most important ingredient is the material velocity at the photosphere. As we discussed in Sec. VIII.C, this is well indicated by the Doppler effect of the Fe II lines: the velocity decreases from about 12 Mm/s at three days after the explosion (1 Mm = 1000 km = 10^8 cm) to 6 Mm/s at 10 days to 2 Mm/s after about 40 days.

The kinetic energy is by far the largest component of the energy; with $v=2\times10^8$ cm/s the specific energy is

$$\varepsilon_{\rm kin}>2\times10^{16}\ \text{ergs/g}\ . \tag{7.17}$$

The radius of the photosphere, estimated from the velocity, is at least 10^{14} cm, so the specific energy of gravitation is

$$GM/r < 2\times 10^{13} \text{ ergs/g} . \quad (7.18)$$

The internal energy is measured by the total light emitted in the time when the internal energy is the energy source; this total light is obtained by integrating the luminosity over time and is

$$E_{\text{light}} = 7\times 10^{47} \text{ ergs} . \quad (7.19)$$

Assuming the mass of the envelope to be 9 $M_\odot$ this corresponds to

$$\varepsilon_{\text{int}} = 4\times 10^{13} \text{ ergs/g} . \quad (7.20)$$

Of course, the internal energy was originally much higher, but adiabatic expansion has diminished it and converted it into kinetic energy.

In order to calculate the total kinetic energy, we need to average $\frac{1}{2}v^2$ over the envelope. In order to do this, we need the position in mass of the photosphere as a function of time. At the photosphere, the internal energy of the matter is released to the outside as radiation.

The kinetic energy of the hydrogen envelope of SN 1987A is given by

$$K_{\text{env}} = \tfrac{1}{2}\int_0^{M_{\text{env}}} v^2(t)\,dM(t) = \tfrac{1}{2}\int_0^{t_H} v^2(t)\frac{dM(t)}{dt}\,dt , \quad (7.21)$$

where M_{env} is the mass of the envelope, $dM(t)/dt$ is the mass swept up per unit time by the photosphere at time t, and t_H is the time it takes the photosphere to cross the whole envelope and reach the outer edge of the helium core. Observations do not make it possible to determine t_H precisely; however, an analysis of when the velocity from the infrared hydrogen lines reaches its lower limit shows that 25 d $< t_H <$ 40 d (see Woosley, 1988), and the Fe II lines further show that quite likely $t_H \sim 35$ d. Bethe and Pizzochero assume that the He mantle is clearly separated from the H envelope; according to Sec. VII.F, this may not be the case.

In order to follow the position in mass of the photosphere of SN 1987A as a function of time, they use the observed luminosities $L(t)$; they write

$$\frac{dM(t)}{dt} = \frac{L(t)}{(dE/dM)} , \quad (7.22)$$

where dE/dM is the specific internal energy (energy per unit mass) of the matter behind the photosphere. This consists of two terms, the radiation and the recombination energy density,

$$\frac{dE}{dM} = \varepsilon_{\text{rad}} + \varepsilon_{\text{rec}} . \quad (7.23)$$

Here ε_{rec} is essentially 13.6 eV per hydrogen atom, with a correction for the fact that some of the material in the envelope is He; a He fraction $Y=0.3$ was assumed in the calculations.

The radiation energy ε_{rad} is what is left over from the energy originally deposited by the shock. Bethe and Pizzochero argue that the specific energy deposited originally is the same everywhere in the stellar envelope. For the temperatures and densities prevailing, this energy is mostly in the form of radiation and hence has $\gamma = 4/3$. As the envelope expands adiabatically, the temperature decreases as $\rho^{1/3}$. The energy per unit mass, being in radiation, behaves as $T^4/\rho \sim \rho^{1/3}$. Because the gravitational energy is small compared with the kinetic, each material element moves at constant speed, so that its r is proportional to t, hence $\rho \sim t^{-3}$. Hence the specific energy

$$\varepsilon_{\text{rad}} \sim C/t \quad (7.24)$$

where C is a constant independent of both the mass coordinate M and t. The constant C is then determined from the integrated luminosity, Eq. (7.19), and the envelope mass.

On this basis, Bethe and Pizzochero determine the average specific energy. They show that this is nearly independent of the assumed envelope mass and also of the time t_H at which the photosphere has crossed the envelope and reached the helium core. They assume alternatively $t_H = 31$ or 39 days. They also make a (small) correction for the kinetic energy of the helium core, and they show that the result depends very little on arbitrary assumptions made. Their result for the average specific energy is

$$E/M = 0.15 \text{ foe}/M_\odot . \quad (7.25)$$

Taking the average of the estimated masses, 9 $M_\odot$, we get an energy

$$E = 1.4\pm 0.4 \text{ foe} , \quad (7.26)$$

just the "high" value assumed by Woosley.

The result of 1.4 foe does not agree well with that of Shigeyama and Nomoto [Eq. (7.12)], although the given error limits overlap. The difference is due to the fact that Bethe and Pizzochero assume that the recombination front has gone through the entire hydrogen envelope, with a mass of 9 ± 2 $M_\odot$. Shigeyama and Nomoto, on the other hand, assume thorough mixing and find that at $t = 35$ d the recombination front has gone through only about 6.5 $M_\odot$. With this assumption, the analysis of Bethe and Pizzochero gives an energy of

$$E = 0.9 \text{ foe} , \quad (7.26a)$$

in good agreement with Eq. (7.12). I am inclined, however, to believe the result (7.26).

I. Gamma rays and x rays

It was shown in Sec. VII.E that the largest part of the luminosity of SN 1987A was due to γ rays from ^{56}Co. Therefore direct observation of these γ rays was eagerly awaited and was indeed accomplished less than a year after the explosion. A detailed discussion is given by Arnett *et al.* (1989).

Both the prominent γ lines from ^{56}Co were indeed observed, at 847 and 1238 keV. At their maximum, their intensities were about

$$1\times10^{-3} \text{ photons/cm}^2\text{ sec for 847}$$
$$2\times10^{-3} \text{ photons/cm}^2\text{ sec for 1238 .} \quad (7.27)$$

The maximum comes about because the total energy in γ rays decreases with time, but their chance of getting out of the star increases. The maximum was observed at about 350 days after the explosion, much earlier than it could have occurred if the Ni and Co had stayed where they were formed, near the inner edge of the ejecta. Thus the γ rays are very strong evidence for mixing.

The most satisfactory observations were made on balloon flights, mostly from Alice Springs, Australia, by the University of Florida together with the Goddard Space Flight Center, and independently by the Jet Propulsion Laboratory in California. The observations of the two groups agree well with each other. The Solar Maximum Mission satellite was handicapped by the fact that it could not point directly at the supernova; there were results from several other balloon flights, none in conflict with Eq. (7.27).

X rays were observed already six months after the supernova exploded, by the Japanese satellite Ginga (Dotani *et la.*, 1987: Tanaka, 1988) and the Soviet satellite Mir (Sunyaev *et al.*, 1987a, 1987b). They got spectra from 2 to 400 keV, as functions of time. Most of the x rays are presumably due to cobalt γ rays, degraded in the SN material by repeated Compton scatterings. The theory of this process has been calculated by several groups, including Pinto and Woosley (1988a, 1988b), and especially Kumagai *et al.* (1989). There is good agreement between theory and observation (apart from the lowest x-ray energies, below 16 keV), provided substantial mixing is assumed, as in the case of γ rays, above. The early appearance of the x rays in itself indicates mixing.

Pinto and Woosley (1988b), stimulated by the early observation of x rays, calculated the expected intensities of both γ-ray lines, assuming different envelope masses, energies, and mixing. Since we now know (Sec. VII.E) that the envelope mass was about 10 $M_\odot$, only the results for this mass are still relevant (see Fig. 21). Assuming no mixing, the γ-ray lines would have been unobservable, "coming on" only after 350 days and reaching a maximum of about 1/10 of the observed values [Eq. (7.27)]. But when they assumed mixing well into the H envelope, out to a velocity of 3000 km/s, they predicted an intensity curve that was subsequently well verified.

A similar analysis was made by Kumagai *et al.* (1989) in order to deduce the distributions of various elements in the exploding supernova. Like Pinto and Woosley, they found that the radioactive ^{56}Co was distributed out to a velocity of at least 3000 km/s. They found that the bulk of ^{56}Co extended to within 6 $M_\odot$ of the surface of the star and perhaps 1% of it within 1 $M_\odot$. From the slow decay of the x-ray signal from Ginga, they deduce

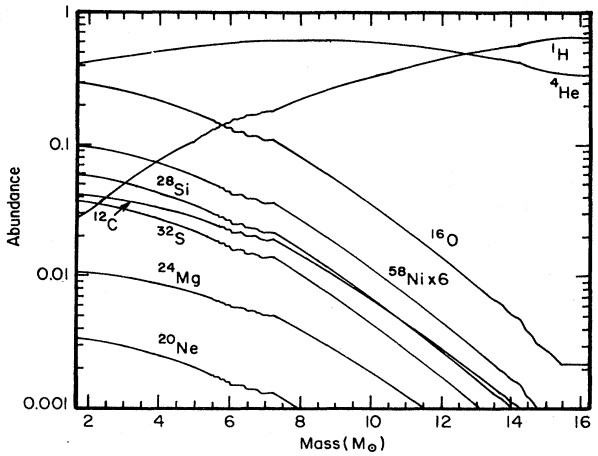

FIG. 21. Distribution of various elements in SN 1987A, after explosion. The abundance is the fraction of mass in each element. From Pinto and Woosley (1988a, 1988b).

that the heavy material is likely to be in clumps (see Sec. VII.J), Kumagai's analysis is the basis of the theory of Shigeyama and Nomoto, which we reported in Sec. VII.F. Kumagai *et al.* also predict that γ rays from ^{67}Co and ^{44}Ti will become appreciable 1200 days after explosion.

The energies of the observed γ rays agree with those observed in the laboratory, showing that indeed it is ^{56}Co which exists and decays in the supernova.

J. Mixing

The γ-ray observations clearly indicate a great deal of mixing of the radioactive ^{56}Co with other parts of the supernova, in fact a breakup of the Co shell into separate clumps. It is generally accepted that this mixing is due to Rayleigh-Taylor (RT) instability. This instability occurs when material of low density pushes denser material.

The shock wave in the supernova, whose first four seconds we have discussed in Sec. VI, will be slowed down as it has to pick up more and more material in the mantle and envelope. The outgoing material in the shock wave thus has to be decelerated. Within this material, there is a density discontinuity where the He mantle adjoins the H envelope. In the deceleration, the lighter H gas has to push the heavier He, the classical situation for RT instability.

[Contrary to prevailing opinion, I do not believe that the density discontinuity *causes* the "reverse shock." The deceleration takes place because the product ρr^3 increases going out. The main increase, from 7×10^{31} to 1.2×10^{33}, takes place continuously in the H envelope, from $m_r/M_\odot=7-11$ (see Fig. 22). In the Sedov theory, a shock wave continues at constant speed if $\rho r^3=$const because its velocity is

$$U\sim(p/\rho)^{1/2} \quad (7.28)$$

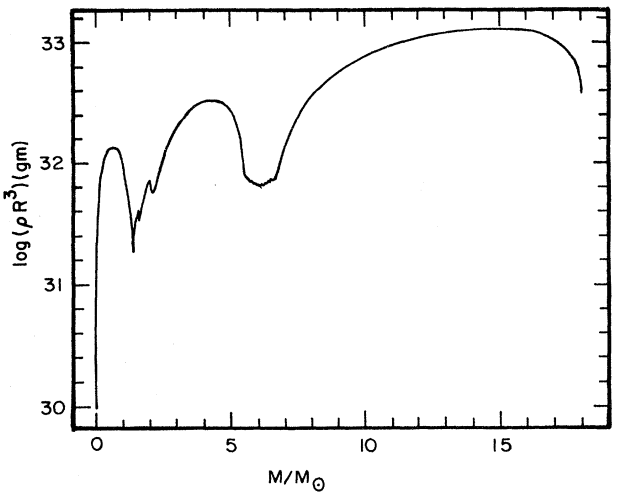

FIG. 22. Distribution of ρR^3 vs included mass in the presupernova model of a star of mass 18 $M_\odot$, according to Woosley (private communication).

and p is inversely proportional to the enclosed volume. But if ρr^3 increases, the shock has to slow down, and the material behind it likewise. This deceleration gradually sharpens into an ingoing shock.]

Ebisuzaki *et al.* (1989), using a linear approximation, showed that RT instability exists, both at the interface between heavier material (CO) and He, and especially at that between He mantle and H envelope. Ebisuzaki *et al.* show that the growth of the RT instability is rapid compared with the movement of the shock.

Hachisu *et al.* (1990) then investigated the large-scale (nonlinear) development of RT instability in a two-dimensional calculation. Similar calculations, with even better resolution, were carried out by Arnett, Fryxell, and Müller (1989), and Fryxell *et al.* (1990). Both groups found, in agreement with many previous calculations and laboratory experiments, that the heavy material moves out fast in fingers or curtains between slower-moving light material. At the top of the fingers, the material spreads out in a mushroom shape. The fingers are more or less equally spaced. These results are in accord (1) with the heavy material's penetrating deep into the H envelope and (2) with a clumpy structure of the heavy material. Both of these features are required by the γ-ray and x-ray observations (Sec. VII.I).

K. The deceptive pulsar

On 18 January 1989, Kristian, Pennypacker, Middleditch, *et al.* (1989) obtained evidence of a pulsar at the center of SN 1987A. The supernova was very opaque to radiation in the range of a few hundred megahertz in which pulsars are usually observed, but reasonably transparent in the red and infrared. So the observers used an interesting trick: they used a silicon photodiode sampling the light received from the supernova with a frequency of 5 kHz, and then made a Fourier analysis, by computer, of the received signal. The fluctuating part was only about 0.05 percent of the steady signal, but they were able to find in it a clear frequency of 1969 Hz, a period of 0.51 milliseconds. It was reasonable to interpret this as a signal from the pulsar.

One disturbing fact was that the signal never appeared again, in spite of much effort. But equally disturbing was the theoretical interpretation. The period was the shortest ever observed in a pulsar. How could such a large angular momentum exist in the neutron star, and how could that star hold together against the enormous centrifugal force? An extensive literature was devoted to this question, with many different suggestions. It was also very difficult to explain how such a large angular momentum could have existed in the progenitor. Finally, the kinetic energy of rotation of the neutron star would have been enormous, about one foe, stressing the energy budget of the supernova.

It has now turned out that the observation was an experimental error. Middleditch (1990) has announced that the guiding TV camera had a built-in irregularity which returned with a frequency of 1969 Hz. It was most difficult to discover this irregularity but it is now well established. As Middleditch points out, this error must not discourage experimentalists from publishing their results: It is not always possible to test the apparatus against all possible mistakes, and a nearby supernova occurs only once in a very long time.

Discovery of the neutron star must now wait until it contributes a major part of the total energy of the supernova. We may be close to that time; it would show in a leveling-out of the light curve. At present, there appears to be some controversy whether this has happened. If so, the luminosity is near 10^{38} ergs/s.

VIII. PRESUPERNOVA EVOLUTION

A. The Si fusion

In the core of the star, the nuclear reactions are, successively, the fusion of H, of He, C, Ne, and O. The last stage is the fusion of ^{28}Si. This takes place by the successive addition of α particles to the Si; the α particles are produced by thermal dissociation of Si. Temperatures of the order of 4×10^9 K$=$350 keV are needed for these processes. The end result of Si fusion is either ^{56}Ni or ^{54}Fe.

Si fusion proceeds in the center of the star where the temperature is highest. It creates an entropy maximum at the center which gives rise to convection (see Sec. V.J.). A convective core is formed that has uniform entropy and composition. As Weaver has suggested, the core extends out to a point where the preexisting entropy is higher than that in the convective core. As the reaction proceeds, the latter entropy increases, and the core grows in mass. This finally stops as the Si gets used up, so the core grows to a certain size, typically 0.8–1 $M_\odot$,

which takes a few days. (The condition for the extension of the core must be slightly modified to conform to the Ledoux condition (Sec. V.J), i.e., to take into account that the mean molecular weight in the core is slightly higher than in the unreacted Si outside).

When the growth has stopped, the core contracts slowly, under gravity, like a Kelvin-Helmholtz star. The gravitational energy released is emitted in the form of neutrinos. Much of this proceeds by electron capture, in a process such as

$$^{56}\mathrm{Ni}+\varepsilon^{-}\rightarrow{}^{56}\mathrm{Co}+\nu \tag{8.1}$$

$$^{55}\mathrm{Fe}+\varepsilon^{-}\rightarrow{}^{55}\mathrm{Mn}+\nu \tag{8.2}$$

and many others like it. Electron capture is favored in the Fe-Ni region because the binding energy per nucleon increases strongly with increasing number of neutrons in the nucleus. In the region of Si-S there is only a weak increase. The electron capture means a decrease of Y_e, and the neutrino emission tends to cool the star. Since there is no longer a source of energy at the center, convection stops: each material element evolves on its own. The center, having the highest density, evolves fastest.

Woosley, Pinto, and Weaver (1989) have carried out extensive evolution calculations, as have Nomoto and his collaborators. Woosley and Weaver use electron capture rates of Fuller (1982) and Fuller, Fowler, and Newman (1982a, 1982b). These seem reasonable but include only nuclei up to about $A=60$. Heavier nuclei are likely to contribute substantially (see Sec. VIII.C).

Woosley *et al.* (1989) find $Y_e\sim 0.47$ throughout the core when core burning ends. During the contraction, Y_e goes down to about 0.44 at the center and is somewhat higher at larger r. If we assume $\rho=10^8$, $Y_e=0.45$, and $T=4\times 10^9$ on average, the Chandrasekhar mass is about 1.7 $M_\odot$. It then decreases as the density goes up. But we shall see in Sec. VIII.B that the Chandrasekhar mass is not directly significant.

As the core contracts, the temperature just outside the core may increase enough to make the Si burn in a shell around the core. Since this makes the shell expand, it also decreases the core density. A second contraction of the core follows, with more neutrino cooling, and a second Si shell may burn. Either before or after that event, the core finally collapses. This starts roughly at a central density of a few times 10^9. This entire evolution depends sensitively on the evolution before the core Si burn, and on details of electron capture.

B. Mass of the iron core

According to the traditional assumption, the iron core will collapse when its mass exceeds the Chandrasekhar mass,

$$M_{\mathrm{ch}}/M_\odot=5.8Y_e^2F\ , \tag{8.3}$$

where approximately

$$F=\left[1+\left[\frac{S_e}{\pi Y_e}\right]^2\right]\left[1-\frac{3}{5}\left[\frac{12}{11}\right]^{1/3}\alpha\bar{Z}^{2/3}+\frac{p_{\mathrm{rad}}}{p_{\mathrm{mat}}}\right]\ . \tag{8.4}$$

S_e is the entropy of the electron gas (per nucleon in units of k_B), $\bar{Z}$ is the average charge of the nuclei, α is the fine-structure constant, and p_{rad},p_{mat} are the pressures of radiation and matter. All quantities are averages over the mass of the Fe core.

Aufderheide, Woosley, and Weaver (1990) have shown that the condition $M_{\mathrm{core}}>M_{\mathrm{Ch}}$ is not fulfilled in evolution computations. In particular, they consider two such computations by Woosley and Weaver (1988) for a star of 18 $M_\odot$, one (18A) carried out with the large cross section for the $^{12}\mathrm{C}+\alpha$ reactions obtained experimentally in 1982 and 1985 (Kettner *et al*; Redder *et al.*), the other (18B) with the smaller cross section of 1988 (Kremer *et al.*). In both of these calculations, the core contracts when its mass is far below the Chandrasekhar mass (which it should not do), and in model 18A it even collapses rapidly when this condition is still true.

Aufderheide *et al.* then observed that this behavior is not unexpected. The Chandrasekhar mass is derived with the assumption that the pressure at the surface of the star is zero, as is the case for a white dwarf. At the surface of the Fe core, however, the pressure is by no means zero, but it can be obtained in the evolution computation, as can the ratio of this pressure to that at the center p_e/p_c (subscript e for edge). The interior of the Fe core is very nearly a polytrope of $\gamma=4/3$, since the pressure of relativistic electrons dominates; its pressure distribution can therefore be described by a Lane-Emden function of index $n=3$. Aufderheide *et al.* propose to replace the Chandrasekhar mass by the mass of a Lane-Emden sphere, whose surface pressure has the same ratio to the central pressure as the p_e/p_c from the computation. In the Lane-Emden function of $n=3$, the enclosed mass depends only on the ratio p_e/p_c; they call this mass M_p. Evidently, this mass is less than the Chandrasekhar mass.

The prescription is successful: M_p very closely tracks the iron core mass until, at the end of the computation, M_p falls well below M_{core}. Then collapse occurs. The core mass then is 1.32 and 1.33 $M_\odot$, respectively, in problems 18A and 18B. Both core mass and M_p have stayed at essentially this value from the time the Si burn (in a shell) is finished. It appears, then, that 1.33 $M_\odot$ is the correct value of the core mass for these models.

Aufderheide, Woosley, and Weaver include a refinement: The factor F in Eq. (8.4) varies with r in the core. They are able to redefine the dependent variable in the Lane-Emden equation to take this variation into account and then preserve the feature that the enclosed mass depends only on p_e/p_c. They also give more accurate formulas for F than Eq. (8.4).

The final collapse occurs chiefly due to cooling of the core, i.e., decrease of S_e both at the center and at the edge.

C. Beta decays

Aufderheide, Brown, *et al.* (1990) have investigated the contribution of nuclei of mass number A between 60 and 70 to evolution just before supernova collapse. Isotopes of Co and Cu may contribute to electron capture.

They have also considered especially

$$^{63}\mathrm{Co}\rightarrow{}^{63}\mathrm{Ni}+e^{-}+\bar{\nu}\ . \tag{8.5}$$

For free atoms, the half-life of ^{63}Co is 26 sec and the energy release 3.6 MeV. Since this is a high energy, the decay rate will not be greatly reduced by Pauli blocking at densities like 10^8. Moreover, the abundance of ^{63}Co is quite high, according to an approximate calculation by Aufderheide, Brown, *et al.* The values $T_9=4$ and $Y_e=0.44$ are typical of the results of Woosley *et al.* in evolution computations. Taking the abundance for this condition, and assuming no blocking, the β decay of ^{63}Co will lead to an *increase* of Y_e at the rate

$$dY_e/dt=1.3\times10^{-6}\ \mathrm{s}^{-1}\ . \tag{8.6}$$

The contraction phase of the core is calculated to last about 4×10^4 s. Thus Y_e could increase by this process by 0.05, so the effect of the β decay (8.5) is sizable.

There will be dynamic equilibrium between the β decay of ^{63}Co and electron capture by other nuclei. (The statistical equilibrium between nuclei, as appropriate to the existing Y_e and temperature, is always maintained by strong nuclear forces.) In each electron capture and β decay, energy is lost to neutrinos that escape, so we have an urca process which will cool the material.

In addition to the decay (8.5), the β decay of ^{55}Fe to ^{55}Mn and of ^{53}Mn to ^{53}Cr will also contribute appreciably.

On this basis, Brown had hoped that the temperature at the beginning of collapse would be lowered compared to the value commonly used. However, at present, pending further calculations, it looks as if this decrease of temperature is not very great.

IX. THE PROTO-NEUTRON STAR

A. Heating

At collapse, the temperature in the homologous core of the supernova is about 10 MeV throughout. This rather low temperature is due to the low initial entropy, of <1 k_B per nucleon. The energy released by the gravitational collapse is stored mostly in degeneracy energy of electrons and neutrinos: The electron chemical potential μ_e at the center is of order 300 MeV and the neutrino chemical potential μ_ν about 200 MeV.

Neutrinos diffuse outward, driven by the gradient in neutrino density. An analytical description of this process was given by Burrows, Mazurek, and Lattimer (1981). In the following, we give a simplified derivation of their result.

They first point out that while only neutrinos diffuse, equilibrium between electron and neutrino number is immediately restored in the core because of the high matter density. Therefore neutrino diffusion changes the total lepton number X_L,

$$n_B\frac{dX_L}{dt}=-\mathrm{div}\mathbf{F}_n\ , \tag{9.1}$$

where n_B is the baryon density and $\mathbf{F}_n$ is the number flux of neutrinos; for a spherically symmetric distribution, $\mathbf{F}_n$ is in the radial direction and

$$F_n=-\frac{c\lambda_n}{3}\frac{\partial n_\nu}{\partial r}\ , \tag{9.2}$$

where λ_n is (a suitable average of) the neutrino mean free path, and n_ν is the neutrino density. The energy flux is

$$F_\varepsilon=-\frac{c\lambda_\varepsilon}{3}\frac{\partial U_\nu}{\partial r}\ , \tag{9.3}$$

where U_ν is the energy density of the neutrinos. The total energy per baryon, E_T, changes like this:

$$n_B\frac{dE_T}{dt}=-\mathrm{div}\mathbf{F}_\varepsilon\ . \tag{9.4}$$

In the homologous core, the neutrinos are degenerate, therefore only neutrinos near the Fermi energy can diffuse and (approximately)

$$F_\varepsilon=\mu_\nu F_n \tag{9.5}$$

$$\lambda_\varepsilon=\lambda_n\ . \tag{9.6}$$

The change of entropy of a given mass element is

$$kT\frac{dS}{dt}=\frac{dE_T}{dt}-\mu_\nu\frac{dX_L}{dt}\ , \tag{9.7}$$

where we have omitted the PdV term because the homologous core quickly settles down to a hydrostatic condition, $dV=0$, as shown both by analytic arguments (Brown *et al.*, 1982) and by explicit computation. Inserting Eqs. (9.1) and (9.4), we have

$$n_BkT\frac{dS}{dt}=-\mathrm{div}(\mu_\nu\mathbf{F}_n)+\mu_\nu\mathrm{div}\mathbf{F}_n \tag{9.8}$$

$$=-\mathbf{F}_r\cdot\nabla\mu_\nu\ . \tag{9.9}$$

We now insert Eq. (9.2) and note that

$$n_\nu=B\mu_\nu^3 \tag{9.10}$$

where B is a constant; then

$$n_BkT\frac{dS}{dt}=c\lambda_n\mu_\nu^2B\left[\frac{\partial\mu_\nu}{\partial r}\right]^2\ . \tag{9.11}$$

Equation (9.11) is a most interesting result; it shows that the entropy increases everywhere due to neutrino diffusion. Burrows *et al.* point out that this is analogous to the resistive (Joule) heating of an electric conductor. They further point out that the rate of increase of the entropy per baryon is proportional to n_B^{-2}, since the mean

free path of neutrinos (for given energy) is inversely proportional to the density, n_B. Thus the energy, which initially resides in the inner part of the core as Fermi energy, is transported to the outer part as heat, and preferentially to low-density regions. In computations, the temperature of the outer core rises to about 40 MeV.

The argument, as here reported, holds strictly only for degenerate neutrinos, $\mu_\nu > \pi T$, which means in practice $\rho > 3\times 10^{13}$. At lower material density, both temperature and μ_ν must be taken into account. This has been done by Cooperstein, van den Horn, and Baron (1986, 1987a, 1987b). The qualitative results, however, remain the same. Diffusion theory, as used in Eqs. (9.2) and (9.3), remains valid nearly to the neutrino sphere, from which the neutrinos then emerge essentially as a free stream.

The scattering mean free path of neutrinos in a gas of nucleons is

$$\lambda_n = \frac{1.0\times 10^{20}}{\rho \varepsilon_\nu^2} , \tag{9.12}$$

where ε_ν is the neutrino energy in MeV. If the nucleons are in nuclei, the mean free path is decreased by the factor in brackets in Eq. (2.30), but only as long as the scattering is coherent. But when the neutrino energy is high, as it is in the core, and the nuclear mass A is large, the neutrino wavelength is less than the nuclear radius, and destructive interference occurs. The effect of this is discussed in detail by Burrows and Lattimer (1986). Typically, inside the homologous core, $\varepsilon_\nu > 100$ MeV and $A > 300$. In this case, the coherent scattering is small; in Eq. (2.30) the term $N^2/6A$ is to be replaced by less than 0.4. Then a nucleus acts essentially like an assembly of nucleons; neutrinos are scattered quasielastically by individual nucleons. Thus, as far as neutrino scattering is concerned, all regions inside the neutrino sphere act essentially alike—the dense pack, which consists of nuclear matter, the outer part of the homologous core, which has heavy nuclei, and the hot shock, in which the nucleons are free, all act like assemblies of nucleons.

Neutrino capture should also be considered,

$$\nu + n \rightarrow e^- + p \tag{9.13}$$

(n=neutron, p=proton); it depends on the occupation of electron states, i.e., on μ_e and T.

The neutrino current carries both lepton number and energy. When it leaves the dense pack (i.e., the nuclear matter region), it consists of ν_e having energies of about 150 MeV. As it approaches the neutrino sphere, the average neutrino energy is of the order of 20 MeV (i.e., $4T$), and all flavors of neutrinos are about equally represented, ν_e, $\bar{\nu}_e$, ν_μ, $\bar{\nu}_\mu$, ν_τ, and $\bar{\nu}_\tau$. Since the energy flux is nearly continuous, some seven neutrinos emerge for every one emitted by the dense pack. However, the net lepton flow is just one unit, so schematically we may say there are two ν_e and one of every other flavor per neutrino emitted by the dense pack. (A more accurate distribution is given below in connection with Fig. 28.)

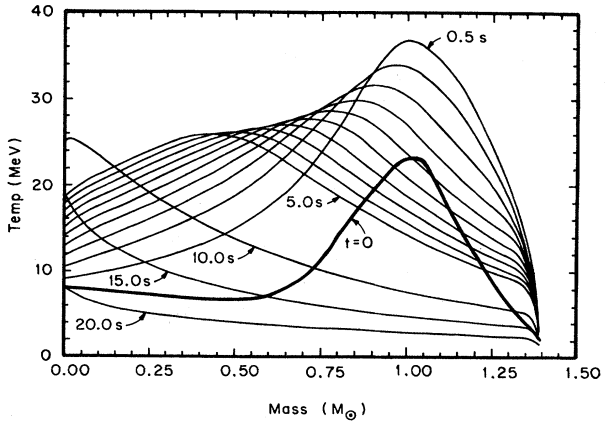

FIG. 23. Temperature distribution in a proto–neutron star as a function of time, according to Burrows and Lattimer (1986).

B. Evolution up to 20 seconds

Burrows and Lattimer (1986) have followed the evolution of temperature, density, lepton number, and neutrino diffusion in a proto–neutron star of mass 1.4 $M_\odot$ for 20 seconds. Because of the long time involved, they did not use direct integration of hydrodynamic and diffusion equation, but rather a relaxation technique due to Henyey *et al.* (1964). Their equation of state is of the standard form of Baron, Cooperstein, and Kahana, Eq. (5.43); it is rather stiff, using $K_0 = 220$ MeV and $\gamma = 3$. They include the corrections due to general relativity. They tacitly assume that there is essentially no material outside the proto-neutron star. This is likely to be right from about 0.5 seconds after collapse on, either because of the thinning of material (Sec. VI.E), or even more after the radiation bubble forms (Sec. VI).

The evolution of temperature is given in Fig. 23, as a function of included mass and time. Figure 24 gives similar information in terms of entropy. Figure 25 gives the lepton number in terms of the same quantities.

From Fig. 24 it can be seen that initially the entropy

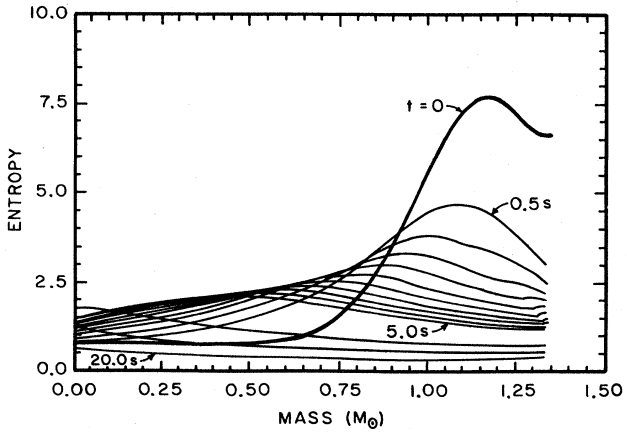

FIG. 24. Entropy distribution in a proto–neutron star as a function of time, according to Burrows and Lattimer (1986).

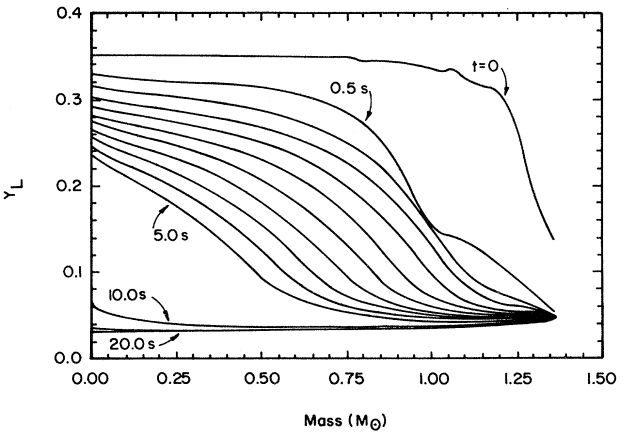

FIG. 25. Distribution of lepton fraction Y_L in a proto–neutron star as a function of time, according to Burrows and Lattimer (1986).

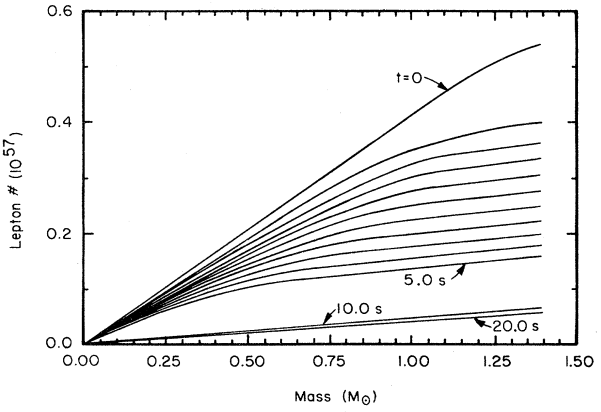

FIG. 26. Total number of leptons included in a given mass, as a function of time, according to Burrows and Lattimer (1986).

has a high maximum, about 8, rather far out, at about $M=1.18$. This is due to the shock's having gone through the core and is in accord with our discussions in Sec. V. The temperature also has a maximum far out, and this maximum becomes very high after 0.5 s, due to the "Joule heating" discussed in Sec. IX.A. Since neutrino energy density is roughly proportional to T^4, the neutrinos now diffuse inward as well as outward. Therefore the temperature and entropy maximum move inward as well as becoming lower. Some time before 10 seconds, the maximum arrives at the center and is now about 25 MeV. It then decreases in the next 10 seconds, getting down to the value of 10 MeV which it had at collapse; the entropy behaves similarly.

The density stays fairly constant at the center, somewhat under 10^{15} g cm^{-3}. At the surface, it increases slowly with time, reaching about 10^{14} after 1 s. The radius, in the meantime, decreases to 12 km (see Fig. 5 in Burrows and Lattimer, 1986). This density distribution corresponds to a Lane-Emden distribution; it should be supplemented by a barometric decrease in density, as discussed in Sec. VI.G; the scale height is of the order of 0.5 km.

The lepton fraction Y_L, Fig. 25, goes to a very small number, about 0.05, at the surface. This result is contingent on the assumption that there is very low density "outside"; see the beginning of this section. At very early times, such as 10–100 ms, when there is a shock outside, Y_L at the surface is close to its value in the presupernova, i.e., about 0.5. It then decreases rapidly due to electron capture, thanks to the high surface density. $Y_L = Y_e = 0.05$ is an equilibrium value.

The Y_L at the center decreases only very slowly, from 0.35 to 0.23 in 5 seconds. This is because diffusion is very slow at the high central density. But, according to Burrows and Lattimer, the next 5 seconds lead to effective deleptonization. Figure 26 gives the total number of leptons inside a given mass M_r: At $r=0$, this is almost proportional to M_r. At $t=0.5$ s, nearly all leptons outside $M_r=1.0$ have been lost. But it takes 5 s before half the leptons inside $M_r=0.5$ are lost; this might be called the deleptonization time of the core.

In another paper, Burrows and Lattimer (1988) extend their theory. They point out that (at short times) the lepton fraction calculated by various authors varies widely, at does the entropy distribution. They calculate the average energy of the emerging neutrinos (their Fig. 12). This has also been done by Wilson and Mayle (1989) up to 3.6 s, and by Bruenn (1990) up to 0.5 s. In Fig. 27, we show Bruenn's result for the various species of neutrinos. The average energy increases slowly with time and is about 15 MeV for $\bar{\nu}_e$, in good agreement with the observations at Kamioka for SN 1987A.

In their paper of 1988, Burrows and Lattimer point out the possibility of convection and its possible beneficial effect on neutrino emission. Their Fig. 12 shows this effect: the average neutrino energy is about 10% higher if convection operates. This will be discussed further in Sec. IX.C.

C. Convection

At some places and some times, the condition for convection in the supernova is fulfilled. We showed in Sec. V.L that convection is not useful for restarting the prompt shock. But Arnett (1986) has suggested that convection may increase the flux of neutrinos for the delayed shock (Sec. VI), and Burrows and Lattimer (1988) have investigated this in more detail.

For quantitative results, I am using the calculations by Wilson and Mayle (1989). In order to affect neutrino emission, the convection has to be *inside* the neutrino sphere. At late times, when the delayed shock operates, the neutrino sphere is at the surface of the proto–neutron star. Outside of this, there is the bubble, which has very high entropy, and outside of that are the ejecta: here the entropy decreased rapidly with r, so that conditions are favorable for convection (Sec. VI.J), but since this is far outside the neutrino sphere, it is irrelevant for affecting

TABLE IX. Regions of convective instability, according to computation by Wilson and Mayle (1989).

Time (sec)	R (km)	M_r ($M_\odot$)	S	Y_L	$\sqrt{p/\rho}$ (10^4 km/s)	ΔS	ΔY_L
0.888	10.07	1.138	4.11	0.209	5.7	−0.07	−0.116
	14.43	1.548	4.04	0.093			
1.323	7.98	0.860	2.72	0.233	7.5	+0.01	−0.065
	9.71	1.198	2.73	0.168			
	10.63	1.341	3.77	0.163	5.1	−0.09	−0.075
	12.84	1.548	3.68	0.088			
1.864	8.10	0.993	2.49	0.207	6.9	−0.08	−0.084
	10.16	1.419	2.41	0.123			
	10.51	1.474	3.57	0.144	4.7	+0.10	−0.062
	11.82	1.575	3.67	0.082			
2.297	7.23	0.860	2.21	0.219	6.6	−0.30	−0.163
	10.35	1.548	1.91	0.056			
3.644	6.80	0.782	1.98	0.207	6.7	−0.72	−0.181
	10.30	1.605	1.26	0.026			

the neutrino emission.

We must look for conditions *inside* the proto–neutron star, which is the region Burrows and Lattimer are concerned with. There is always a region in which the *lepton fraction* Y_L decreases rapidly, namely the region originally traversed by the prompt shock. Burrows and Lattimer call it the mantle; it extends typically from $M_r=0.9$ to 1.5 or $1.6M_\odot$ according to Wilson and Mayle. But at early times, up to about 1/2 seconds, the decrease of Y_L is more than compensated by a rapid increase of S, as Lattimer and Mazurek (1981) showed and as Burrows and Lattimer point out. As we showed in Eq. (95), the condition for convection is of the form

$$\frac{dS}{dr}+a\frac{dY_L}{dr}<0\ , \tag{9.14}$$

where a depends on pressure and entropy. In the example discussed in Sec. V.L, $a=7$, and I shall assume that a is generally of this order.

As discussed in Sec. IX.B, the maximum of S, which is originally near the surface of the proto–neutron star, gradually moves inward: By $t=0.6$ s there is a region in which the Ledoux condition (9.14) is fulfilled. Table IX shows regions of convective instability for various times. In some of these, entropy decreases as well as Y_L, in others, the increase of S is so slight that the Ledoux criterion (9.14) is obviously fulfilled. At $t=1.323$ and 1.864 s there are two separate convective regions; in between, the entropy goes up steeply, so that the Ledoux criterion (9.14) is not fulfilled. Outside the regions listed in Table IX, the material is convectively stable.

In particular, the inner core, up to about $M_r=0.9$, does not have convection. Thus the very slow neutron diffusion in this inner core cannot be substantially accelerated. The transport of neutrinos therefore has to be by diffusion up to M about 0.9, then convection to about 1.5, then diffusion again.

The speed of convection is some fraction of the sound speed, as discussed in Sec. V.J, the fraction depending on the change of entropy and Y_L, ΔS, and ΔY_L. In Table IX we give $\sqrt{p/\rho}$ which is close to the sound speed. It is generally about 6×10^4 km/s. The distance of convection is of the order of 3 km. So, if convection went with sound velocity, it would take less than 10^{-4} seconds. Even if the convection velocity is a small fraction of sound velocity, it will still take less than a millisecond, and is therefore practically instantaneous compared with diffusion.

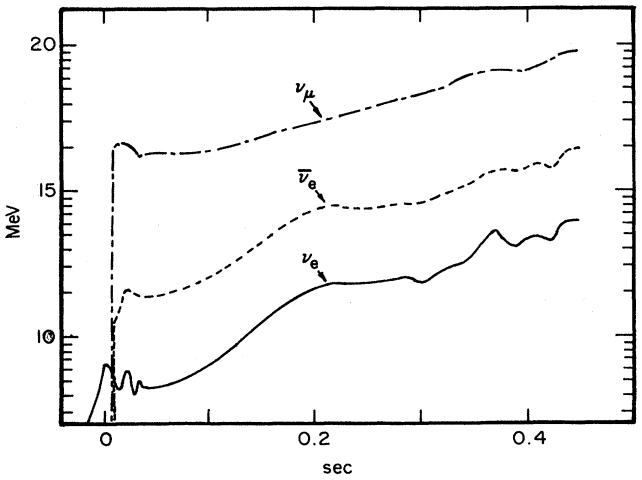

FIG. 27. Mean energy of emitted neutrinos of various types in MeV, vs time (Bruenn, 1990).

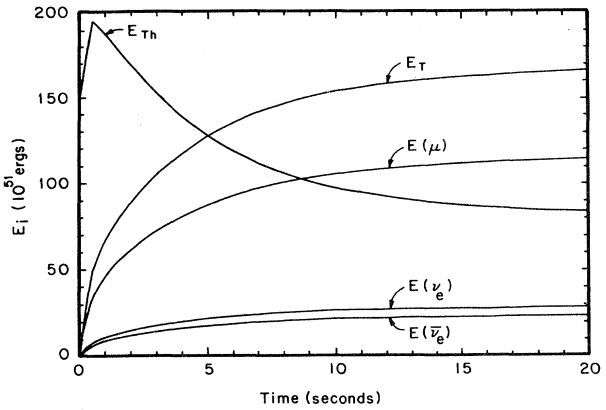

FIG. 28. Total energy emitted in neutrinos of various types, up to 20 seconds. E_T = total of all types of neutrinos; E_{Th} = thermal energy in neutron star. From Burrows and Lattimer (1986).

Convection brings to the surface some material that has higher Y_L and, after 2 s, also higher S. Both should be helpful in increasing the neutrino supply at the neutrino sphere. A much more detailed calculation, however, would be needed to determine the quantitative effect. And, as Burrows and Lattimer point out, the result will depend on the model used.

Burrows and Lattimer themselves make an estimate which is shown in their Fig. 12. In our Fig. 28, the total energy emitted in neutrinos, with and without convection, is shown. It is about 30% higher in the first two seconds when convection is included. The discussion above shows that this quantitative result is strongly model dependent. In Fig. 29 we show the result of Bruenn (1990) for the same quantity, without convection. Bruenn's result, especially for $\bar{\nu}_e$, is considerably higher than that of Burrows and Lattimer.

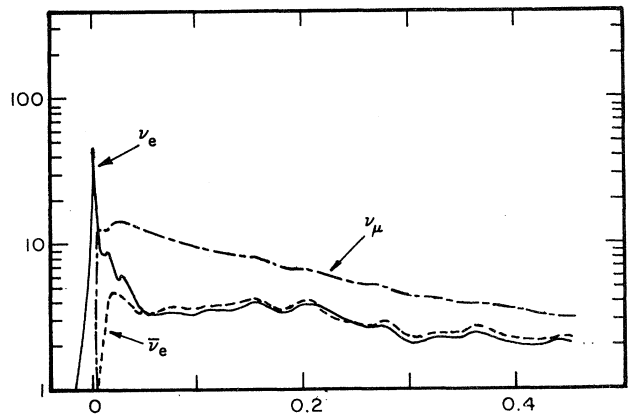

FIG. 29. Luminosity in neutrinos of various types, in units of 10^{52} ergs/s, up to 0.5 seconds (Bruenn, 1990).

D. Conversion of neutrinos

Observation of neutrinos from the sun has given results that are only 1/4 to 1/2 of the expected number. The most likely (though not universally accepted) explanation is that of Mikheyev and Smirnov (1987), namely, that electron neutrinos get converted into μ (or possibly τ) neutrinos while escaping [the MSW (Mikheyev-Smirnov-Wolfenstein) effect]. μ and τ neutrinos of a few MeV energy are unobservable by presently existing experimental equipment. (See also Bethe, 1986, 1989). Does such conversion have any influence on the supernova?

The first point to make is that the MSW conversion of neutrinos of a few MeV takes place at solar densities, 100 g cm^{-3} or less. This means that it is irrelevant for the mechanism of the supernova, which takes place at densities from 10^5 to 10^{14} g cm^{-3}. (The energy of SN neutrinos, 5 to 100 MeV, is somewhat higher than that of solar neutrinos, 1 to 15 MeV, and the critical density for conversion goes as $1/E$, and is thus somewhat lower for supernova neutrinos than for solar ones.)

However, if the MSW theory is correct, supernova neutrinos will be converted on their way out from the core to interstellar space. Here the second point comes in: antineutrinos are not converted (see Bethe, 1986), and it is electron antineutrons which are (at least primarily) detected in the supernova neutrino experiments. The difference between ν_e and $\bar{\nu}_e$ arises from the fact that ordinary matter (at density 100 or less) contains electrons but no positrons; ν_e can exchange with e^- in the MSW process but $\bar{\nu}_e$ could only exchange with e^+.

If, for some future supernova, many more neutrinos can be observed than for SN 1987A, it is likely that some of them will be ν_e rather than $\bar{\nu}_e$. But even then, not much will be changed by the MSW conversion. True, the ν_e produced in the core will be converted into ν_μ and vice versa (I disregard ν_τ in this paragraph). But we have seen that ν_e and ν_μ are produced in roughly equal numbers. Only if the time sequence can be measured accurately, could it be significant that at *early* times, $t \ll 1$ sec, many

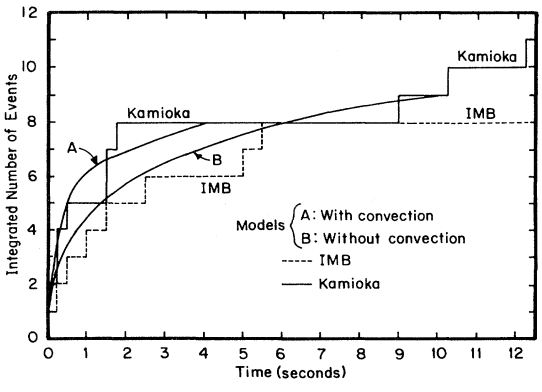

FIG. 30. Neutrinos from SN 1987A. Solid curves: Predicted number of neutrinos vs time, according to Burrows and Lattimer, 1987 (arbitrary units), compared with the observed neutrinos at Kamiokande II and IMB (dashed step functions).

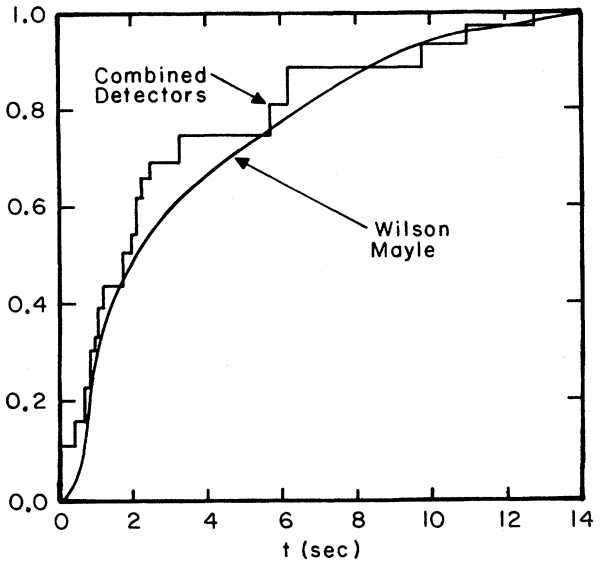

FIG. 31. Neutrinos from SN 1987A. Curve is the predicted number of neutrinos according to Wilson and Mayle (arbitrary units). Step function is the observed number, combining the results of the two laboratories.

more ν_e will be produced than ν_μ. If there is no MSW, this would show in the record. Whether the MSW theory is correct will probably be determined by solar neutrino experiments in 1990 or 1991.

E. Comparison with observations

Burrows and Lattimer (1987) have calculated the emission of neutrinos expected for SN 1987A as a function of time, both with and without convection. The result is shown in Fig. 30 and compared with the observations in Kamiokande II and IMB. The agreement is satisfactory, both with and without convection. Wilson and Mayle (Fig. 31) have compared their calculations with a combination of the two observations, and also found satisfactory agreement. Thus it appears that the diffusion of neutrinos out of the proto–neutron star is satisfactorily explained.

ACKNOWLEDGMENTS

Many people have contributed to this paper. I thank in particular my collaborators for twelve years, Gerald Brown, Jerry Cooperstein, Edward Baron, and more recently Pierre Pizzochero. Stanford Woosley has given me much basic advice. James Wilson and Ronald Mayle have freely sent me outputs from their computers, as have Cooperstein and Baron. Cooperstein and Stirling Colgate have carefully reviewed different parts of this paper. I have also used many preprints that were sent to me. To all these persons go my thanks. This work was supported in part by the National Science Foundation.

REFERENCES

Aichelin, J., A. Rosenhauer, G. Peilert, H. Stöcker, and W. Greiner, 1987, Phys. Rev. Lett. **58**, 1926.
Ainsworth, T. L., E. Baron, G. E. Brown, J. Cooperstein, and M. Prakash, 1987, Nucl. Phys. A **464**, 740.
Ainsworth, T. L., G. E. Brown, M. Prakash, and W. Weise, 1988, Phys. Lett. B **200**, 413.
Andreani, P., R. Ferlet, and A. Vidal-Madjar, 1987, Nature **326**, 770.
Arnett, W. D., 1966, Can. J. Phys. **44**, 2553.
Arnett, W. D., 1967, Can. J. Phys. **45**, 1621.
Arnett, W. D., 1968a, Astrophys. J. **153**, 341.
Arnett, W. D., 1968b, Nature **219**, 1344.
Arnett, W. D., 1969, Astrophys. Space Sci. **5**, 180.
Arnett, W. D., 1971, Astrophys. J. **169**, 113.
Arnett, W. D., 1972, Astrophys. J. **176**, 681 (Part 1); **176**, 699 (Part II).
Arnett, W. D., 1977, Astrophys. J .**218**, 815.
Arnett, W. D., 1977b, Astrophys. J. Suppl. Ser. **35**, 145.
Arnett, W. D., 1982, Astrophys. J. **253**, 785.
Arnett, W. D., 1983, Astrophys. J. **263**, L55.
Arnett, W. D., 1986, Bull. Am. Astron. Soc. **17**, 908.
Arnett, W. D., 1987a, Astrophys. J. **319**, 136.
Arnett, W. D., 1987b, Bull. Am. Astron. Soc. **19**, 1072.
Arnett, W. D., 1988, in *Supernova 1987A in the Large Magellanic Cloud,* edited by M. Kafatos and A. G. Michalitsianos (Cambrdige University, Cambridge, England), p. 301.
Arnett, W. D., 1989, Astrophys. J. **343**, 834.
Arnett, W. D., J. N. Bahcall, R. P. Kirshner, and S. E. Woosley, 1989, Annu. Rev. Astron. Astrophys. **27**, 629.
Arnett, W. D., B. Fryxell, and E. Müller, 1989, Astrophys. J. **341**, L63.
Arnett, W. D., and A. Fu, 1989, Astrophys. J. **340**, 396.
Arnett, W. D., and J. L. Rosner, 1987, Phys. Rev. Lett. **58**, 1906.
Aufderheide, M. B., G. E. Brown, T. T. S. Kuo, D. B. Stout, and P. Vogel, 1990, Astrophys. J., in press.
Aufderheide, M. B., S. E. Woosley, and T. A. Weaver, 1990, unpublished.
Baade, W., F. Zwicky, 1934, Proc. Natl. Acad. Sci., USA **20**, 254.
Bahcall, J. N., and S. L. Glashow, 1987, Nature **326**, 476.
Bahcall, J. N., T. Piran, W. H. Press, and D. N. Spergel, 1987, Nature **327**, 682.
Bahcall, J. N., D. N. Spergel, and W. H. Press, 1988, in *Supernova 1987A in the Large Magellanic Cloud,* edited by M. Kafatos and A. G. Michalitsianos (Cambridge University, Cambridge, England), p. 172.
Barkat, Z., and J. C. Wheeler, 1988, Astrophys. J. **332**, 247.
Baron, E. A., and J. Cooperstein, 1988, unpublished.
Baron, E. A., and J. Cooperstein, 1990, Astrophys. J. **353**, 597.
Baron, E. A., J. Cooperstein, and S. Kahana, 1985a, Phys. Rev. Lett. **55**, 126.
Baron, E. A., J. Cooperstein, and S. Kahana, 1985b, Nucl. Phys. A **440**, 744.
Baron, E., J. Cooperstein, and S. Kahana, 1987, Astrophys. J. **320**, 300.
Baym, G., H. A. Bethe, and C. J. Pethick, 1971, Nucl. Phys. A **175**, 225.
Beaudet, G., V. Petrosian, and E. E. Salpeter, 1967, Astrophys. J. **150**, 979.
Bethe, H. A., 1986, Phys. Rev. Lett. **56**, 1305.

Bethe, H. A., 1988, Annu. Rev. Nucl. Part. Sci. **38**, 1.
Bethe, H. A., 1989, Phys. Rev. Lett. **63**, 837.
Bethe, H. A., J. H. Applegate, and G. E. Brown, 1980, Astrophys. J. **241**, 464.
Bethe, H. A., and G. E. Brown, 1989, unpublished.
Bethe, H. A., G. E. Brown, J. Applegate, and J. M. Lattimer, 1979, Nucl. Phys. A **324**, 487.
Bethe, H. A., G. E. Brown, and J. Cooperstein, 1987, Astrophys. J. **320**, 201.
Bethe, H. A., and M. B. Johnson, 1974, Nucl. Phys. A **230**, 1.
Bethe, H. A., and P. Pizzochero, 1990, Astrophys. J. **350**, L33.
Bethe, H. A., and J. R. Wilson, 1985, Astrophys. J. **295**, 14.
Bionta, R. M., *et al.*, 1987, Phys. Rev. Lett. **58**, 1494.
Blanco, V. M., *et al.*, 1987, Astrophys. J. **320**, 589.
Blaizot, J. P., 1980, Phys. Rep. **64**, 171.
Blaizot, J. P., D. Gogny, and B. Grammaticos, 1976, Nucl. Phys. A **265**, 315.
Bludman, S. A., 1988, Phys. Rep. **163**, 47.
Bohigas, O., H. Krivine, and T. Treiner, 1980, Nucl. Phys. A **336**, 155.
Böhm-Vitense, E., 1958, Z. Astrophys. **46**, 108.
Bohr, A., and B. R. Mottelson, 1969, *Nuclear Structure* (Benjamin, New York/Amsterdam), Vol. I, p. 183.
Bonche, P., and D. Vautherin, 1981, Nucl. Phys. A **372**, 476.
Bonche, P., and D. Vautherin, 1982, Astron. Astrophys. **112**, 268.
Bowers, R. L., and J. R. Wilson, 1982a, Astrophys. J. Suppl. **50**, 115.
Bowers, R. L., and J. R. Wilson, 1982b, Astrophys. J. **263**, 366.
Branch, D., 1986, Astrophys. J. Lett. **320**, L121.
Bratton, C. B., *et al.*, 1988, Phys. Rev. D **37**, 3361.
Brown, G. E., 1971, Rev. Mod. Phys. **43**, 1.
Brown, G. E., 1988a, Phys. Rep. **163**, 167.
Brown, G. E., 1988b, Nucl. Phys. A **488**, 689.
Brown, G. E., 1988c, Z. Phys. C **38**, 291.
Brown, G. E., H. A. Bethe, and G. Baym, 1982, Nucl. Phys. A **375**, 481.
Brown, G. E., H. Müther, and M. Prakash, 1990, Nucl. Phys. **506**, 565.
Brown, G. E., and E. O. Osnes, 1985, Phys. Lett. B **159**, 223.
Brown, G. E., and M. Rho, 1981, Nucl. Phys. A **372**, 397.
Brown, G. E., and P. Siemens, 1987, SUNY Stony Brook preprint.
Bruenn, S. W., 1985, Astrophys. J. Suppl. **58**, 771.
Bruenn, S. W., 1988, Astrophys. Space Sci. **143**, 15.
Bruenn, S. W., 1989a, Astrophys. J. **340**, 955.
Bruenn, S. W., 1989b, Astrophys. J. **341**, 385.
Bruenn, S. W., 1990, private communication.
Burrows, A., 1987, Astrophys. J. Lett. **328**, L51.
Burrows, A., 1988, Astrophys. J. **334**, 891.
Burrows, A., and J. M. Lattimer, 1985, Astrophys. J. **299**, L19.
Burrows, A., and J. M. Lattimer, 1986, Astrophys. J. **307**, 178.
Burrows, A., and J. M. Lattimer, 1987, Astrophys. J. Lett. **318**, L63.
Burrows, A., and J. M. Lattimer, 1988, Phys. Rep. **163**, 51.
Burrows, A., T. J. Mazurek, and J. M. Lattimer, 1981, Astrophys. J. **251**, 325.
Casatella, A., *et al.*, 1987, Astron. Astrophys. **177**, L29.
Catchpole, R. M., *et al.*, 1988, Mon. Not. R. Astron. Soc. **229**, 15P.
Celenza, J. S., and C. M. Shakin, 1986, *Relativistic Nuclear Physics* (World Scientific, Singapore).
Clark, D. H., and F. R. Stephenson, 1977, *The Historical Supernovae* (Pergamon, Oxford).
Colgate, S. A., 1971, Astrophys. J. **163**, 221.
Colgate, S. A., 1989, Nature **341**, 489.
Colgate, S. A., and M. H. Johnson, 1960, Phys. Rev. Lett. **5**, 235.
Colgate, S. A., and C. McKee, 1969, Astrophys. J. **157**, 623.
Colgate, S. A., and R. H. White, 1966, Astrophys. J. **143**, 626.
Cooperstein, J., 1985, Nucl. Phys. A **438**, 722.
Cooperstein, J., 1988a, Phys. Rev. C **37**, 786.
Cooperstin, J., 1988b, Phys. Rep. **163**, 95.
Cooperstein, J., and E. A. Baron, 1990, in *Supernovae,* edited by A. Petschek (Springer, Berlin), p. 213.
Cooperstein, J., H. A. Bethe, and G. E. Brown, 1984, Nucl. Phys. A **429**, 527.
Cooperstein, J., L. J. van den Horn, and E. A. Baron, 1986, Astrophys. J. **309**, 653; **315**, 729(E).
Cooperstein, J., L. J. van den Horn, and E. A. Baron, 1987, Astrophys. J. Lett. **321**, L129.
Cooperstein, J., and J. Wambach, 1984, Nucl. Phys. A **420**, 591.
de Rujula, A., 1987, Phys. Lett. B **193**, 514.
Dicus, D. A., 1972, Phys. Rev. D **6**, 941.
Dotani, T., *et al.*, 1987, Nature **330**, 230.
Ebisuzaki, T., T. Shigeyama, and K. Nomoto, 1989, Astrophys. J. **344**, L65.
Ejiri, H., 1982, Phys. Rev. C **26**, 217.
Elias, J. H., B. Gregory, M. M. Phillips, R. E. Williams, J. R. Graham, W. P. S. Meikle, R. D. Schwartz, and B. Wilking, 1988, Astrophys. J. **331**, L9.
Elias, J. H., K. Mathews, G. Neugebauer, S. E. Pearson, 1985, preprint.
Fowler, W. A., and F. Hoyle, 1964, Astrophys. J. Suppl. **9**, 201.
Freedman, D. Z., 1974, Phys. Rev. D **9**, 1389.
Friedman, B., and V. R. Pandharipande, 1981, Nucl. Phys. A **361**, 502.
Friman, B. L., and A. K. Dhar, 1979, Phys. Lett. B **85**, 1.
Fryxell, B., E. Müller, and W. D. Arnett, 1990, Astrophys. J, in press.
Fuller, G. M., 1982, Astrophys. J. **252**, 741.
Fuller, G. M., W. A. Fowler, M. J. Newman, 1982a, Astrophys. J. Suppl. **48**, 279.
Fuller, G. M., W. A. Fowler, M. J. Newman, 1982b, Astrophys. J. **252**, 715.
Gale, C., G. Bertsch, and S. Das Gupta, 1987, Phys. Rev. C **35**, 1666.
Gilmozzi, R., *et al.*, 1987, Nature **328**, 318.
Gogny, D., 1975, in *Nuclear Self-Consistent Fields,* edited by G. Ripka and M. Porneuf (North-Holland, Amsterdam), p. 333.
Goldreich, P., and S. V. Weber, 1980, Astrophys. J. **238**, 991.
Goodman, S. A., A. Dar, and S. Nussinov, 1987, Astrophys. J. **314**, L7.
Hachisu *et al.*, 1990.
Hamuy, M., *et al.*, 1988, Astron. J. **95**, 63.
Harris, J. W., *et al.*, 1985, Phys. Lett. B **153**, 377.
Helfand, D. J., and R. H. Becker, 1984, Nature **307**, 215.
Henyey, L. G., J. E. Forbes, and N. L. Gould, 1964, Astrophys. J. **139**, 306.
Hillebrandt, W., 1982a, in *Supernovae: A Survey of Current Research,* edited by M. J. Rees and R. J. Stoneham (Reidel, Dordrecht), p. 123.
Hillebrandt, W., 1982b, Astron. Astrophys. **110**, L3.
Hillebrandt, W., 1984, Ann N.Y. Acade. Sci. **422**, 197.
Hillebrandt, W., K. Nomoto, and R. G. Wolff, 1984, Astron. Astrophys. **133**, 175.
Hirata, K. S., *et al.*, 1987, Phys. Rev. Lett. **58**, 1490.
Hirata, K. S., *et al.*, 1988, Phys. Rev. D **38**, 448.

Horowitz, C. J., and B. D. Serot, 1987, Nucl. Phys. A **464**, 613.
Hoyle, F., and W. A. Fowler, 1960, Astrophys. J. **132**, 565.
Jackson, A. D., 1983, Annu. Rev. Nucl. Part. Sci. **33**, 105.
Jackson, A. D., M. Rho, and E. Krotscheck, 1985, Nucl. Phys. A **407**, 495.
Jaminon, M., C. Mahaux, and P. Rochus, 1985, Nucl. Phys. A **365**, 371.
Johnson, C. H., D. J. Horen, and C. Mahaux, 1987, Phys. Rev. C **36**, 2252.
Kettner, K. U., H. W. Becker, L. Buchmann, J. Görres, H. Kräwinkel, C. Rolfs, P. Schmalbrock, H. P. Trautvetter, and A. Vlieks, 1982, Z. Phys. A **308**, 73.
Kirshner, R. P., G. Sonneborn, D. M. Crenshaw, and G. E. Nassiopoulos, 1987, Astrophys. J. **320**, 602.
Kremer, R. M., C. A. Barnes, K. H. Chang, H. C. Evans, B. W. Filippone, K. H. Hahn, and L. W. Mitchell, 1988, Phys. Rev. Lett. **60**, 1475.
Kristian, J., *et al.*, 1989, Nature **338**, 234.
Kumagai, S., *et al.*, 1989, Astrophys. J. **345**, 412.
Lamb, D. Q., and C. J. Pethick, 1976, Astrophys. J. **209**, L77.
Lamb, D. Q., J. M. Lattimer, C. J. Pethick, and D. G. Ravenhall, 1978, Phys. Rev. Lett. **41**, 1623.
Lamb, D. Q., J. M. Lattimer, C. J. Pethick, and D. G. Ravenhall, 1981, Nucl. Phys. A **360**, 459.
Landau, L. D., 1956, Zh. Eksp. Teor. Fiz. **30**, 1058 [Sov. Phys. JETP **3**, 920 (1956)].
Landau, L. D., 1957, Zh. Eksp. Teor. Fiz. **32**, 59 [Sov. Phys. JETP **5**, 101 (1957)].
Landau, L. D., 1958, Zh. Eksp. Teor. Fiz. **35**, 97 [Sov. Phys. JETP **8**, 70 (1958)].
Lattimer, J. M., and J. Cooperstein, 1988, Phys. Rev. Lett. **61**, 23.
Lattimer, J. M., and T. J. Mazurek, 1981, Astrophys. J. **246**, 945.
Lattimer, J. M., C. J. Pethick, D. G. Ravenhall, and D. Q. Lamb, 1985, Nucl. Phys. A **432**, 646.
Lee, T. D., and M. Margulies, 1975, Phys. Rev. D **11**, 1591.
Lee, T. D., and G. C. Wick, 1974, Phys. Rev. D **9**, 2291.
Machleidt, R., K. Holinde, and C. Elster, 1987, Phys. Rep. **149**, 1.
Mahaux, C., and R. Sartor, 1987, Nucl. Phys. A **475**, 247.
Marschall, L. A., 1988, *The Supernova Story* (Plenum, New York/London).
Mayle, R., and J. R. Wilson, 1988, Astrophys. J. **334**, 909.
Mazurek, T., 1975, Astrophys. Space Sci. **35**, 117.
Mazurek, T. J., 1976, Astrophys. J. **207**, L87.
Menzies, J. W., *et al.*, 1987, Mon. Not. R. Astron. Soc. **227**, 39P.
Migdal, A. B., 1967, *Theory of Finite Fermi Systems and Applications to Atomic Nuclei* (Interscience, New York).
Mikheyev, S. P., and A. Yu. Smirnov, 1987, Sov. Phys. Usp. **30**, 759.
Molitoris, J. J., D. Hahn, and H. Stöcker, 1985, Nucl. Phys. A **447**, 13.
Molitoris, J. J., and H. Stöcker, 1985, Phys. Rev. C **32**, 346.
Murdin, P., and L. Murdin, 1985, *Supernovae* (Cambridge University, Cambridge, England).
Myra, E. S., S. A. Bludman, Y. Hoffman, I. Lichtenstadt, N. Sack, and K. A. Van Riper, 1987, Astrophys. J. **318**, 744.
Myra, E. S., and S. A. Bludman, 1989, Astrophys. J. **340**, 384.
Nomoto, K., 1984, Astrophys. J. **277**, 791.
Nomoto, K., and M. Hashimoto, 1988, Phys. Rep. **163**, 13.
Nomoto, K., and T. Shigeyama, 1988, in *Supernova 1987A in the Large Magellanic Cloud,* edited by M. Kafatos and A. Michalitsianos (Cambridge University Press, Cambridge, England).
Pandharipande, V. R., 1973, Nucl. Phys. A **217**, 1.
Phillips, M., 1988, in *Supernova 1987A in the Large Magellanic Cloud,* edited by M. Kafatos and A. Michalitsianos (Cambridge University Press, Cambridge, England), p. 16.
Pines, D., K. F. Quader, and J. Wambach, 1988, Nucl. Phys. A **477**, 365.
Pinto, P. A., and S. E. Woosley, 1988a, Nature **333**, 534.
Pinto, P. A., and S. E. Woosley, 1988b, Astrophys. J. **329**, 820.
Pizzochero, P., 1990, Astrophys. J. **354**, 333.
Ravenhall, D. G., C. D. Bennett, and C. J. Pethick, 1972, Phys. Rev. Lett. **28**, 978.
Ravenhall, D. G., C. J. Pethick, and J. R. Wilson, 1983, Phys. Rev. Lett. **50**, 2066.
Redder, A., *et al.*, 1985, Phys. Rev. Lett. **55**, 1262.
Reid, R. V., 1968, Ann. Phys. (N.Y.) **50**, 411.
Renfordt, R. E., *et al.*, 1984, Phys. Rev. Lett. **53**, 763.
Richtmyer, R. D., and K. W. Morton, 1957, *Difference Methods for Initial-Value Problems* (Interscience, New York).
Saio, H., M. Kato, and K. Nomoto, 1988a, Astrophys. J. **331**, 388.
Saio, H., K. Nomoto, and M. Kato, 1988b, Nature **334**, 508.
Sato, K., 1975, Prog. Theor. Phys. **54**, 1352.
Serot, B. D., J. D. Walecka, 1985, Adv. Nucl. Phys. **16**, 1.
Shelton, I., O. Duhalde, and A. Jones, 1987, Int. Astron. Union Circular 4316.
Shigeyama, T., and K. Nomoto, 1990, Astrophys. J., in press.
Shigeyama, T., K. Nomoto, and M. Hashimoto, 1988, Astron. Astrophys. **196**, 411.
Sonneborn, G., B. Altner, and R. P. Kirshner, 1987, Astrophys. J. **323**, L35.
Soyeur, M., and G. E. Brown, 1979, Nucl. Phys. A **324**, 464.
Spergel, D. N., and J. N. Bahcall, 1988, Phys. Lett. B **200**, 366.
Spergel, D. N., T. Piran, A. Loeb, J. Goodman, and J. N. Bahcall, 1987, Science **237**, 1471.
Stock, R., *et al.*, 1982, Phys. Rev. Lett. **49**, 1236.
Sunyaev, R. A., *et al.*, 1987a, Pis'ma Astron. Zh. **13**, 1027.
Sunyaev, R. A., *et al.*, 1987b, Nature **330**, 227.
Tanaka, Y., 1988, in *Physics of Neutron Stars and Black Holes,* edited by Y. Tanaka (Universal Academic, Tokyo), p. 431.
ter Haar, B., and R. Malfliet, 1986a, Phys. Rev. Lett. **56**, 1237.
ter Haar, B., and R. Malfliet, 1986b, Phys. Lett. B **172**, 10.
Thielemann, F. K., M. Hashimoto, and K. Nomoto, 1990, Astrophys. J. **349**, 222.
Truran, J. W., and A. Weiss, 1987, Lect. Notes Phys. **287**, 293.
Tubbs, D. L., and D. N. Schramm, 1975, Astrophys. J. **201**, 467.
Walborn, N. R., B. M. Lasker, V. G. Taidler, and Y. H. Chu, 1987, Astrophys. J. **321**, L41.
Wallace, S. J., 1987, Annu. Rev. Nucl. Part. Sci. **37**, 267.
Weaver, T. A., 1980, Ann. N.Y. Acad. Sci. **366**, 335.
Weinberg, S., 1967, Phys. Rev. Lett. **19**, 1264.
Whelan, J. C., and I. Iben, 1973, Astrophys. J. **186**, 1007.
Wilson, J. R., 1971, Astrophys. J. **163**, 209.
Wilson, J. R., 1985, in *Numerical Astrophysics,* edited by J. M. Centrella, J. M. LeBlanc, and R. L. Bowers (Jones & Bartlett, Boston), p. 422.
Wilson, J. R., and R. Mayle, 1988, in *Proceedings of the Fifth Marcel Grossmann Meeting on General Relativity,* edited by D. G. Blair and M. J. Buckingham (World Scientific, Singapore).
Wilson, J. R., and R. Mayle, 1989, Conference on Nuclear Equation of State, Peniscola, Spain (unpublished).
Woosley, S. E., 1988, Astrophys. J. **330**, 218.
Woosley, S. E., P. A. Pinto, and L. Ensman, 1988, Astrophys. J.

324, 466.
Woosley, S. E., P. A. Pinto, and T. A. Weaver, 1989, in *Proceedings of the Astronomical Society of Australia.*
Woosley, S. E., and T. A. Weaver, 1986, Annu. Rev. Astron. Astrophys. **24**, 205.
Woosley, S. E., and T. A. Weaver, 1988, Phys. Rep. **163**, 79.
Yahil, A., 1983, Astrophys. J. **265**, 1047.
Yahil, A., 1985, Astrophys. J. **288**, 644.
Yahil, A., and J. M. Lattimer, 1982, in *Supernovae: A Survey of Current Research,* edited by M. J. Rees and R. S. Stoneham (Reidel, Dordrecht), p. 53.